Masterarbeit im Fach Physik zum Erlangen des Grades
Master of Science (M. Sc.)

A Closer Look at Reactions in the Miller-Urey-Experiment using Coupled Gas Chromatography - Mass Spectrometry

Vorgelegt von: Thorben H. Mense

Matrikelnummer: 2409781
Universität Bielefeld
Fakultät für Physik

Betreuer: Dr. Petra Lutter
Fakultät für Biologie
Prof. Dr. Dominik Schwarz (Erstgutachter)
Fakultät für Physik
Prof. Dr. Dario Anselmetti (Zweitgutachter)
Fakultät für Physik

Bielefeld, Dezember 2019

Erklärung

Hiermit erkläre ich, dass ich die vorliegende Masterarbeit selbstständig verfasst und gelieferte Datensätze, Zeichnungen, Skizzen und grafische Darstellungen selbstständig erstellt habe. Ich habe keine anderen Quellen als die angegebenen benutzt und habe die Stellen der Arbeit, die anderen Werken entnommen sind – einschließlich verwendeter Tabellen und Abbildungen – in jedem einzelnen Fall unter Angabe der Quelle als Entlehnung kenntlich gemacht. Diese Arbeit wurde weder vollständig noch teilweise einer anderen Fakultät zur Erlangung eines akademischen Grades vorgelegt.

Bielefeld, 19.12.2019

Thorben H. Mense

Danksagung

Der interdisziplinäre Charakter dieser Arbeit erforderte die Zusammenarbeit mit einer ganzen Reihe von Menschen, ohne die das Schreiben nicht denkbar gewesen wäre.

Zuerst möchte ich mich bei den Veranstaltern des Astrobiologie-Seminars, meinem erweiterten Betreuungsteam bedanken: Dr. Hanna Bednarz, Prof. Dr. Veronica Dodero, Dr. Petra Lutter, Prof. Dr. Karsten Niehaus und Prof. Dr. Dominik Schwarz haben mich der Astrobiologie näher gebracht und bei Fragen stets unterstützt.

Für die Bereitschaft die Rolle des Zweitgutachters zu übernehmen danke ich Prof. Dr. Dario Anselmetti.

Dem CeBiTec insbesondere Dr. Stefan Weidner und Marga Ferrari danke ich für die Möglichkeit die nötigen Räumlichkeiten und Geräte zu nutzen.

Victoria Gödde und Dr. Marcus Persicke, danke ich für die Unterstützung mit der GCMS Analyse.

Dr. Karsten Rott und der D2 Arbeitsgruppe danke ich für die Unterstützung mit den REM Aufnahmen.

Darüber hinaus danke ich Julia Voß, die ebenfalls viele meiner Fragen beantworten konnte.

Nikolaj Koralewicz danke ich dafür, dass er als Parfümeur sein Wissen über die Chemie von Duftstoffen mit mir geteilt hat.

Auch den Kommilitonen in der theoretischen Physik danke ich für die gute Arbeitsatmosphäre und die Erfahrung unter Theoretikern eine experimentelle Arbeit zu schreiben. Insbesondere Pascal Kreling, Dennis Maseizik, Marius Neumann und Hendrik Roch danke ich für das Lesen der Arbeit und die Anregungen zu Korrekturen.

Nicht unerwähnt lässen möchte ich natürlich meine Familie, Freunde und besonders Rebekka, die mir eine große moralische Unterstüzung waren. Danke!

Contents

Introduction

> "If you want to make an apple pie from scratch, you must first invent the Universe." - Carl Sagan [Sagan, 1980]

The origin of life is one of the core questions astrobiology tries to solve. Only with a robust understanding what life is and how it can occur on other planets we might be able to find it or its traces.

Many theories have been proposed to answer this question. Some place the origin of the cell at the beginning of life [Oparin, 1924], some the replicating power of nucleic acids [Eigen, 1971] and others see clay crystals as the starting point of the origin of life [Cairns-Smith, 1966]. What all of these theories have in common is their modus operandi. All build life from simple building blocks. The production of these building blocks, the organic monomers, can thus be seen as the first obstacle the origin of life has to take.

The first option to study the prebiotic production of organic monomers in a laboratory, came with the experimental setup Stanley L. Miller described in his article "A Production of Amino Acids Under Possible Primitive Earth Conditions" [Miller et al., 1953]. In this article Miller describes a method to produce amino acids from a simulated primordial atmosphere by spark-discharge, ushering in the modern era of experimental study of prebiotic chemistry. The experiment, which became known as the Miller-Urey experiment, holds a special position in the scientific study of the the origin of life, as it is not designed to test a specific hypothesis or reaction, but merely provides conditions that might reasonably represent the early Earth [McCollom, 2013].

In the years since the publication of the original Miller-Urey experiments, laboratory investigations of prebiotic chemistry and early chemical evolution have been a major contributor to the progress towards a solution to the puzzle of life's origin. As a large variety of different reactions can occur in Miller-like experiments they allow testing the early stages of chemical evolution.

The aim of this project was to have a closer look at the reactions in the Miller-Urey experiment and study the effects of different atmospheres and of the abundance of montmorillonite clay as a catalyst to get a better understanding for the importance

of mineral surfaces during prebiotic chemistry. For this a strong emphasis is put on the reaction pathways of the Stecker synthesis, which leads to the production of amino acids and hydroxy acids, and the formose reaction, which leads to the production of sugars. Taking these two reaction pathways as proxies for all reactions occurring in a Miller-Urey-like experiment allows us to phrase a set of concrete research questions which will be answered over the course of this thesis:

1. Can we produce amino acids from an atmosphere with equal parts of nitrogen and methane using a Miller-Urey-like experimental setup? What are the yields and how do they compare to the original Miller-Urey experiment?
2. What is the effect of using montmorillonite clay as catalyst in the experiment and how can this effect be assessed for the Strecker synthesis and the formose reaction?
3. Does the abundance of nitrogen in the experiment hamper the production of sugars in the formose reaction?
4. Can the production of ribose in the experiment be observed?
5. Which improvements can be made to the GC-MS analysis to increase the accuracy of the analysis?

To answer these questions I will give a theoretical background in the first three chapters of this thesis, while the last three chapters are focused on the experimental work. In the first chapter theories on the origin of life on earth are discussed, with a short historical introduction followed by the presentation of modern theories about the origin of life and the origin of the building blocks of life. The second chapter is centred around the Miller-Urey experiment and the reactions which occur in it to produce amino acids, sugars and nucleobases. The intricacies of coupled gas chromatography-mass spectrometry (GC-MS) analysis are discussed in chapter three together with options to increase the performance of GC-MS. In the fourth chapter the experimental setup and the method and protocols used during this thesis are explained. Chapter five contains the results of the experiment and their discussion, starting with general observations and the first GC-MS analysis, going over the discovery of boric acid in our samples and finishing with the results of the improved GC-MS analysis. In the last chapter a conclusion is drawn from the findings and an outlook on the potential future of research is given.

Using the experiments described in this thesis I was able to produce amino acids, hydroxy acids, sugars and other organic molecules from atmospheres containing nitrogen, methane and water. Coupled gas chromatography-mass spectrometry was used to analyse the produced samples. A new analytical routine with an improved derivatisation and a new instrument method was established to allow for a more accurate analysis.

During early stages of the analysis the abundance of boric acid in the samples was observed and the borosilicate glassware could be identified as its source. The dissolution of the boric acid from the glassware was investigated with additional dissolution runs and allowed to use the boric acid in the step of quantitation due to its very consistent behaviour. This together with the increased GC-MS methodology allowed for a qualitative and quantitative analysis of the samples. The production of of amino acids was observed in the experimental runs with a mixed methane and nitrogen atmosphere, although only at low yields when compared to the original Miller-Urey experiment. Even though all intermediates of the sugar producing formose reaction were found in the samples no ribose could be found, possibly due to the abundance of boric acid. Results showed that the production of sugars benefited from the presence of nitrogen in the experiments instead of being hampered by it. The effect of montmorillonite clay was assessed by comparing the ratios of reaction products, showing the selective catalysis properties of the clay.

Chapter 1

1 Theories on the Origin of Life on Earth

How, where and why did life originate? Questions of this kind are probably older than science itself and for a long time in history the answers to those questions were dependent on the culture and religion of the time. The Greek philosopher Aristotle (384-322 BC) stated that any dry body becoming moist and any wet body becoming dry would give rise to animals, while the well known doctor and alchemist Jan Baptist van Helmont (1580-1644) even gave a recipe for the artificial production of mice by placing damp grain and dirty rags in a covered vessel [van Helmont and Knorr von Rosenroth, 1683, Oparin, 1924]. Theories of this kind are called theories of spontaneous generation and were very popular at their respective times. This changed with the results of Louis Pasteur (1822-1895), who was able to show beyond doubt that the spontaneous generation of microbes in organic media does not occur [Oparin, 1924, Lazcano, 2011].

With spontaneous generation ruled out as the origin of life another theory became fashionable: Panspermia. The theory of Panspermia describes an extraterrestrial origin of life and goes back to a review article by Hermann Richter (1808-1876) covering the Darwinian theory of evolution [Richter, 1865]. In this article Richter concluded that the Darwinian evolution needed a starting point and suggested that this common ancestor was of extraterrestrial origin. He assumed that microorganisms could be transported through space and "infect" a planet with life [Kamminga, 1982]. The small particles, which are carrying the germs of microorganisms, he titled "cosmozoa". He further refined this theory, proposing a mechanism with which microorganisms can be transported into space by gas exchange between Earth atmosphere and the interplanetary medium (he called it "Weltluft" or "Weltatmosphäre", translating to atmosphere of the worlds) [Richter, 1870]. While Richter did not specify how microorganisms were supposed to survive the harsh conditions of space, his theory removed the need for spontaneous generation, accommodated the Darwinian theory of evolution, got along without supernatural agencies and retained the idea of life being unique, by declaring that all organisms have to descend from other living beings [Kamminga, 1982]. These properties made his theory very compelling and thus it was picked up by influential

scientists like William Thomson, 1st Baron Kelvin (1824-1907), Hermann von Helmholtz (1821-1894) and Svante Arrhenius (1859-1927). In 1908 Arrhenius coined the term panspermia with his book "World in the Making", in which he presented a new version of the theory of cosmozoa. He assumed life in the Universe to be eternal, being transported to every suitable planet and thus stated that "it is useless to inquire its origin" [Arrhenius, 1908, p. 218]. To strengthen his statements Arrhenius cited cryogenic experiments carried out at the Jenner Institute in London which showed that bacteria can be stored in liquid hydrogen at temperatures of -252°C without loosing their germinating power and thus should be able to survive the temperature of space [Kamminga, 1982].

After the death of Arrhenius panspermia appeared to disappear as a theory. One reason for this disappearance might have been the work done by Alexander Ivanovich Oparin (1894-1980) creating the first modern theory on the origin of life with his book "The Origin of Life" published in 1924 in Russia. Although Oparin did not dismiss the theory of panspermia in general, he pointed out that panspermia can only explain the emergence of life on Earth not the origin of life in general and criticised the impassable barrier between living and dead matter created by such theories [Oparin, 1924]. In the time after Oparin's initial publication the idea that life had to start somewhere and thus a theory about its origin needed to be developed became widely accepted. The theory of panspermia thus changed from a theory about the origin of life to a pure theory about the transportation of life and organic compounds through the Universe, which is backed by recent results on the exchange of solid material among the different bodies in the solar system, the assumption of more benign environments in some of the other planets during the early stages of the planetary system and the surprising resistance of a number of species to the conditions of space [Lazcano, 2011].

1.1 Modern Theories

Since Oparin many different theories about the origin of life have been proposed, making it difficult to cover all of them individually. To cope with this problem Freeman Dyson (*1923) suggested to group theories of the same type together and name them by their most famous advocates: Oparin, Eigen and Cairns-Smith [Dyson, 1985].

1.1.1 Oparin - Cells first

The Oparin theory was described first by the books Oparin published in 1924 and 1936 [Oparin, 1924, Oparin et al., 1957]. He suggested the production of organic substances

from a reducing, primordial Earth atmosphere. Some of these organic molecules then form coacervate droplets in which other substances can accumulate and form simple self sustaining metabolic cycles. Enzymes emerge as catalysts of these metabolic cycles, organising the random population of molecules. These so formed coacervate protocells form the precursors of the first heterotrophic[1] microbes [Dyson, 1985]. Replication of these protocells took place by division of the coacervate droplets due to external forces [Oparin, 1968]. In this theory genetic material only formed much later as an convenient information carrier [Lazcano, 2011]. Though the original theory by Oparin was later confuted in some parts, it has done benchmark contributions to the research on the origin of life. It established the hypothesis that heterothrophs and anaerobic fermentation were primordial, proposed a reducing atmosphere for the prebiotic synthesis of organic compounds, postulated the transition from heterotrophy to autotrophy and addressed all these concepts with considerable detail [Miller et al., 1997].

Numerous theories build upon this initial work and with the distinct order of events as synoptic feature. This order sets the origin of cells at the starting point of the evolution of life, right after the origin of organic monomers. Coacervates, however, are no longer considered as a plausible model for these first cells, as they lack features found in modern cells, like bilayer membranes [Lazcano, 2010]. Self-assembled vesicles of fatty acids are currently accepted as a plausible candidate of the first cells [Chen and Walde, 2010]. Other suggestions are inorganic microcompartments in alkaline vents [Martin et al., 2014] or membraneless polyester microdroplets formed from hydroxy acid polymers, like they are currently investigated by Jia and Chandru [Jia et al., 2019].

1.1.2 Eigen - RNA first

The Eigen theory, named after Manfred Eigen (1927-2019), reverses the order of events. It has self-replicating ribonucleic acid chains (RNA) at the beginning, enzymes appearing to build with the RNA a primitive form of the modern genetic transcription apparatus soon afterwards, and cells appearing later to give the apparatus physical cohesion [Dyson, 1985].

Eigen stated that in nature only simple polymerisation reactions can occur. The larger functional chain molecules, which are required for life, could thus only be produced in autocatalytic processes, limiting their length due to the so called error catastrophe [Eigen, 1971]. RNA chains can be considered as a good example for this.

[1] A heterotroph is an organism that requires the presence of reduced organic compounds to produce energy in contrast to autotrophs, which are capable of biosynthesis of all cell material from carbon dioxide as only carbon source [Gargaud et al., 2011].

In a system without a specialised replicase or error correction, mutations occur with a very high probability. In order to decrease the mutation probability a more complex replication mechanism is needed. To code this mechanism more information meaning a longer RNA chain is required, which again increases the mutation rate and thus again needs a better replication mechanism - a vicious circle called Eigen's Paradox [Eigen and Schuster, 1982]. To solve this issue Eigen introduced the concept of hypercycles, which are cycles of connected autocatalytic reactions called subcycles. The subcycles are coupled, depend on each other and show cooperative behaviour. Even if the amount of information in a single subcycle is limited by the error catastrophe, the whole hypercycle can store much more information, allowing for more complex reactions to occur [Szostak et al., 2016].

This concept leads to a prebiotic evolution of life in which replicating systems occur prior to metabolic systems. Such replicating, non-metabolic systems do exist, as has been shown by Sol Spiegelman (1914-1983), Leslie Orgel (1927-2007) and Gerald Joyce (*1956) [Pross, 2004]. Especially the discovery of ribozymes, RNA chains with enzymatic properties, strengthened the Eigen theory on the origin of life. Highly efficient, self-replicating ribozymes were produced by Robertson and Joyce using in vitro evolution, leading to much faster replication rates while lowering the needed concentration of the nucleic acid monomers for the replication to occur [Robertson and Joyce, 2014]. Vaida et al. showed the spontaneous organisations of networks by cooperative working RNA replicators, forming a hypercycle like system of ribozymes [Vaidya et al., 2012]. It can be concluded that the Eigen theory with its RNA world was very popular in the past and still is today.

1.1.3 Cairns-Smith - Clay first

According to the Cairns-Smith theory, proposed by Alexander Graham Cairns-Smith (1931-2016), naturally occurring microscopic crystals of minerals contained in common clay served as genetic material before the emergence of nucleic acids. The Cairns-Smith theory thus has clay first, enzymes second, cells third and genes fourth [Dyson, 1985]. This order of events makes the theory a two step theory, with a genetic metamorphosis occurring after the emergence of nucleic acids. This metamorphosis step marks the so called secondary origin of life [Cairns-Smith, 1966].

The genetic information is stored in the form of crystal growth defects, aperiodic cation distributions or random layer stacking analogous to the nucleotide sequences found in RNA or DNA. Replication of the clay minerals is done by cleaving, with more stable sequences evolving at the expense of less favourable sequences through a selective process of growth and dissolution. By this process the clay crystals pro-

vide a scaffolding for the evolution of organic molecules to the modern biochemistry [Hazen and Sverjensky, 2010].

The Cairns-Smith theory of life was first tested experimentally in 2007 by Bullard et al. using a model crystalline system of potassium hydrogen phthalate. In this experiment the inheritance of imperfection patterns from "mother" to "daughter" crystals was indeed observed, but the replication of the imperfection pattern was not ideal, with new imperfections being included during crystal growth even though greatest care was taken to keep the system as ideal as possible [Bullard et al., 2007].

While the theory of clay as genetic material might have it flaws, the idea of life evolving in two steps, with a genetic takeover as soon as RNA or DNA occurs, has to be taken into consideration when talking about the origin of life [Dyson, 1985].

1.2 The Origin of Organic Monomers

What all theories presented in section 1.1 have in common is the need for readily available organic monomers, simple organic molecules which form the building blocks of the larger chain molecules needed for life.

1.2.1 Primordial Atmosphere

As briefly mentioned in subsection 1.1.1, Oparin suggested in his work, that these organic monomers are formed from a reducing primordial atmosphere. This view was shared by John Burdon Sanderson Haldane [Haldane, 1929], John Desmond Bernal [Bernal, 1949] and later by Harold Urey [Urey, 1952]. A true breakthrough in this field was the work done by Stanley Miller, a student of Urey. In his article "A Production of Amino Acids Under Possible Primitive Earth Conditions" [Miller et al., 1953] he describes a method to produce amino acids using electric discharges in a primordial atmosphere. The experiment, which became known as the Miller-Urey-Experiment, was repeated in many different configurations with different gases, energy sources or both. The production of amino acids, sugars and carbon acid has been reported for many of them, as long as sources of nitrogen, carbon and hydrogen were available in the atmosphere [Miller and Orgel, 1974, Gishlick, 2002]. In specialised setups even the production of nucleobases is possible [Ferus et al., 2017]. One of the key points of discussion about this theory is the primordial atmosphere. The atmospheres suggested by Oparin, Haldane and Urey were strongly reducing with methane (CH_4), ammonia (NH_3) and hydrogen (H_2) as main constituents [Bernal, 1949, Urey, 1952].

More recent models of the primordial atmosphere favour a more neutral composition, with nitrogen ($\mathrm{N_2}$) and carbon dioxide ($\mathrm{CO_2}$) dominating the gaseous phase [Kasting, 1993]. This changing view of the atmosphere caused heavy debates about the plausibility of atmospheric processes as source of prebiotic, organic monomers. While early results from experiments with less reducing atmospheres showed only very low yields of organic monomers, later experiments succeeded in producing quantities comparable to the original experiments, when using calcium carbonate ($\mathrm{CaCO_3}$) as buffer in the aqueous phase of experiments. As $\mathrm{CaCO_3}$ is readily available in the oceans of today's Earth it can be assumed to be abundant in primordial oceans as well. This keeps the production of organic monomers from the primordial atmosphere a plausible option, no matter of the oxidation state of the atmosphere [McCollom, 2013].

1.2.2 Hydrothermal Vents

Another option for the origin for the production of organic monomers are hydrothermal vents [Martin et al., 2014]. Thermodynamic calculations suggest the abundance of compounds such as formaldehyde (HCHO) and hydrogen cyanide (HCN) in hydrothermal systems, even though they have not been measured directly [McCollom, 2013]. Experiments with solutions of HCHO, HCN and $\mathrm{NH_3}$ at concentrations around $0.2\frac{\mathrm{mol}}{\mathrm{L}}$ under hydrothermal conditions (high temperature and pressure) yielded millimolar concentrations of glycine. However, it is very unlikely that the initial concentrations used in these experiments can be found in hydrothermal vents. Using more reasonable conditions the yield of amino acids under hydrothermal condition decreases dramatically [Aubrey et al., 2009]. The situation is similar for organic bases and sugars: The production of them under hydrothermal conditions is plausible, but the needed concentrations of formaldehyde and hydrogen cyanide are probably not reached in hydrothermal vents [LaRowe and Regnier, 2008].

1.2.3 Comets and Meteorites

Similar to the theory of panspermia one can think about the origin of organic molecules on Earth as extraterrestrial, which is then called molecular panspermia. In 1974 $\textsc{Nalin Chandra Wickramasinghe}$ $(*1939)$ suggested organic polymers as one of the main components of interstellar dust. He argued that formaldehyde, which has been detected in interstellar clouds, is able to condense on silicate grains and form polyoxymethylene [Wickramasinghe, 1974]. In 2011 the production of amino acids from interstellar ice analogues by ultraviolet irradiation was shown, further cementing the possibility of organic monomer production in space [de Marcellus et al., 2011]. Using circularised

light this experiment can produce an enantiomeric excess which can even be stable under the radiation conditions comets and meteorites face [Iglesias-Groth et al., 2010]. Recently traces of sugars like Ribose, Arabinose, Xylose and Lyxose were found in carbonaceous meteorites, indicating a possible extraterrestrial, sugar production mechanism [Furukawa et al., 2019]. These findings indicate that organic chemistry can occur in space, even able to form complex bio-molecules.

Deposition of the extraterrestrially formed organic monomers on Earth is another question to be answered. Traces of bio-molecules in carbonaceous chondrites show that extraterrestrial organic monomers can survive the intense heat of reentry and impact, if enclosed in rocky media. When it comes to more icy bodies like comets this is certainly not the case. ZAHNLE and GRINSPOON suggest based on geological data, that Earth can sweep up comet dust of an incoming comet, while any organic monomers conveyed by the impactor itself would be destroyed [Zahnle and Grinspoon, 1990]. Measurements of glycine, methylamine and ethylamine from the Rosetta spacecraft show that the coma of comets indeed contains significant amounts of organic molecules [Altwegg et al., 2016]. Assuming a production of organic monomers for the atmosphere like described in section 1.2.1, these mechanisms would have rivalled or exceeded terrestrial organic synthesis in the case of an early carbon dioxide-rich terrestrial atmosphere, while in an early reducing (methane-rich) atmosphere, the exogenous sources would have been quantitatively unimportant compared to atmospheric production [Chyba and Sagan, 1997].

2 Chapter 2
Reactions in the Miller-Urey Experiment

When investigating the origin of life, one will inevitably read about the Miller-Urey-Experiment. This experiment, first conducted by Stanley Miller (1930-2007) under the supervision of Harold Urey (1893-1981) in 1953, is used to test the production of organic monomers from a simulated primordial atmosphere discussed in section 1.2.1. The first observations were about the production of amino acids in the experiment, but over the years many of the basic building blocks of the origin of life as we know it have been synthesised from simple ingredients. This includes besides amino acids, sugars, nucleobases and membrane forming lipids [McCollom, 2013].

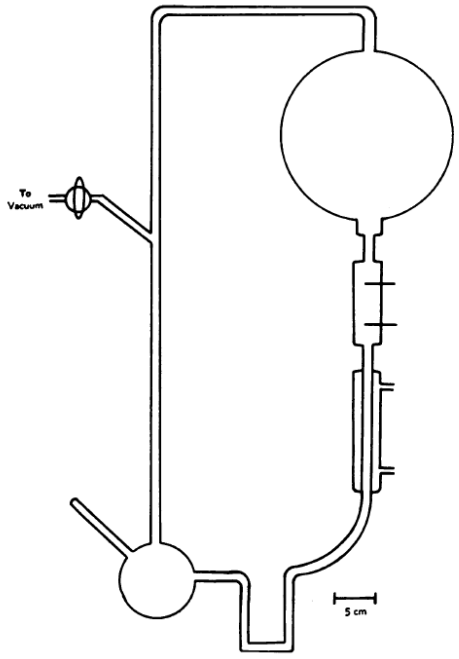

Figure 2.1: A drawing of the apparatus used by Miller in 1953 for his experiments [Miller et al., 1953]. The boiling flask is situated bottom left and the electric discharges occur between the electrodes mid right.

2.1 Setup of the Original Experiment

The original setup used by MILLER consisted of a one piece glass apparatus (see figure 2.1). To conduct the experiment purified water is added to the boiling flask and the apparatus is filled with an atmosphere consisting of methane, ammonia and hydrogen. The water is then boiled and the resulting vapour mixes with the atmosphere, circulates past the electrodes, which produce electric discharges under high voltage, is then condensed in a cooler and flows back to the initial flask via a U-tube. Using this setup a diverse bunch of organic molecules can be produced.

2.2 The Strecker Synthesis - Amino Acid Formation

There is strong evidence that the synthesis of amino acids in the Miller-Urey experiment occurs through a variation of the Strecker synthesis [McCollom, 2013]. In this reaction aldehydes react with ammonia and hydrogen cyanide under aqueous conditions to form amino nitriles, which are subsequently hydrolysed to amino acids. The reaction takes place in three separate steps:

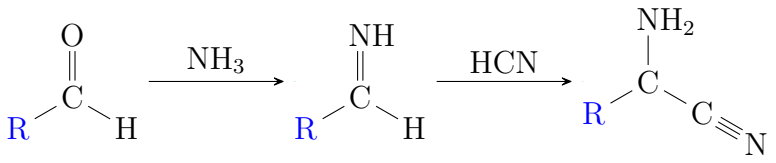

(2.1)

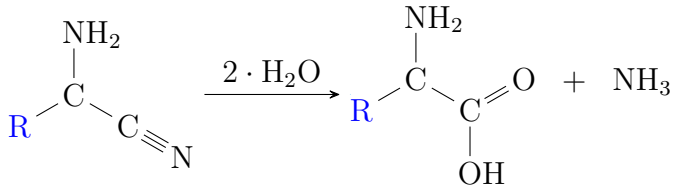

(2.2)

In the first step ammonia gets added to aldehyde forming an imine, with R representing the hydro carbon side chain of the aldehyde. This imine is then converted to an aminonitrile by addition of hydrogen cyanide in the second step. In the last step hydrolysis of the amino nitrile to the amino acid takes place, with ammonia as a side product [Miller and Orgel, 1974].

Another pathway of the Strecker synthesis leads to the production of hydroxy acids

from aldehydes and hydrogen cyanide. This reaction path has only two steps:

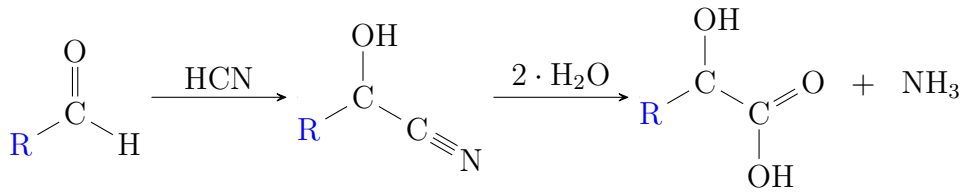

(2.3)

In this case the hydrogen cyanide is added directly to the aldehyde in the first step forming a hydroxy nitrile. Then this hydroxynitrile undergoes hydrolysis forming the hydroxy acid and releasing ammonia as a side product [Miller and Orgel, 1974].

Since amino nitriles and hydroxy nitriles can interconvert one has to consider the kinetics of the following equilibrium reaction:

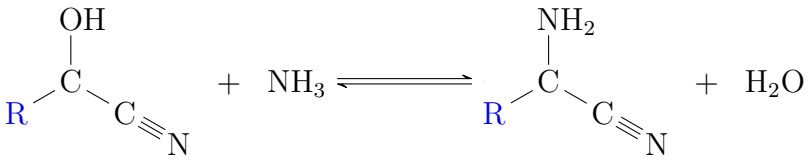

(2.4)

This leads to the product ratio

$$\frac{[\text{hydroxy acid}]}{[\text{amino acid}]} = \frac{k_{1HN}K_{HN}}{k_{1AN}K_{AN}} \cdot \frac{1}{[\text{ammonia}]} \tag{2.5}$$

after hydrolysis, where the brackets mark the concentration of a substance, K_{HN} and K_{AN} are the equilibrium constants for hydroxy nitriles and amino nitriles and k_{1HN} and k_{1AN} are the rate constants for the hydrolysis of the corresponding nitrile[1][Miller and Orgel, 1974, Miller and Van Trump, 1981]. The amount of available ammonia thus has a strong impact on the yield of amino acids. Due to the conversion of hydrogen cyanide to ammonia during the hydroxy acid pathway, at least a small amount of amino acids will always be produced.

In the Miller-Urey experiment the production of the raw materials (aldehydes, hydrogen cyanide and ammonia) occurs in the gaseous atmosphere by electric discharges or other methods of ionisation or radicalisation. The reaction itself happens in the aqueous phase, either in the boiling flask or in small drops of condensed water [McCollom, 2013].

2.3 The Formose Reaction - Ribose Formation

The formose reaction produces sugars from formaldehyde and is thought to be the main mechanism of sugar production in the Miller-Urey experiment. Sugars are especially

[1]The values of these constants depend on the pH and temperature and can be looked up for individual use cases in the literature, but will not be given here.

important for life, as they form the backbone of many organic molecules like RNA, where one of the main components is ribose [Joyce, 1989].

In the Miller-Urey experiment formaldehyde is produced from the atmosphere by electric discharges and dissolves in the aqueous phase of the experiment, where the formose reaction takes place [Miller and Orgel, 1974].

The first step of the reaction is the condensation of two molecules of formaldehyde to glycolaldehyde:

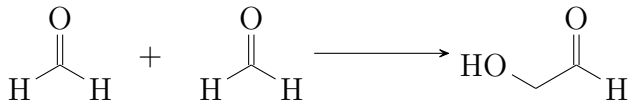

(2.6)

This step is fairly slow and poses the main bottleneck of the production. As soon as the first glycolaldehyde is produced the reaction gains in speed, as in the process of the reaction more and more glycolaldehyde is produced to which formaldehyde can be directly added. This behaviour is called autocatalytic.

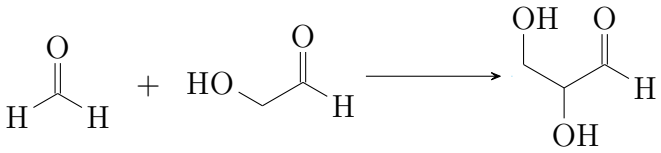

(2.7)

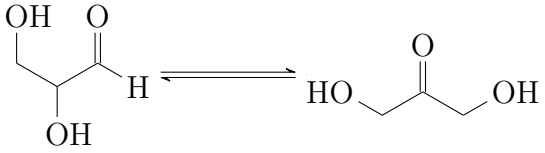

(2.8)

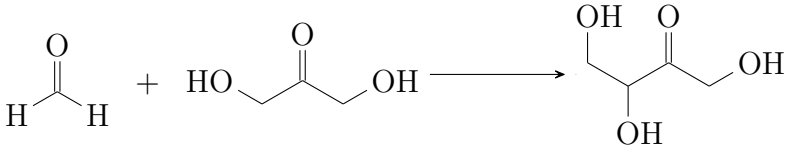

(2.9)

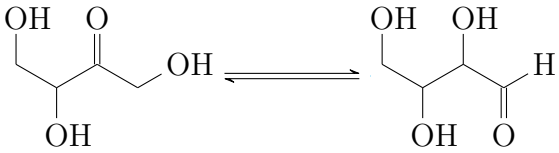

(2.10)

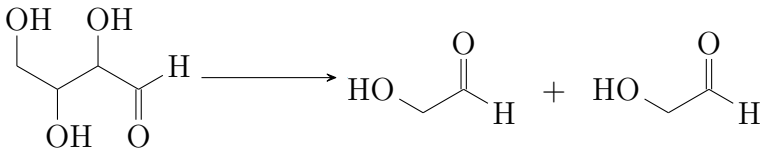

(2.11)

Reaction (2.7) is an aldol condensation reaction in which another formaldehyde is added to the glycolaldehyde to form glyceraldehyde. It is then followed by (2.8), an isomerisation reaction converting the glyceraldehyde to dihydroxyacetone. With another aldol condensation (2.9) ketotetrose is formed, which can be converted via another isomerisation reaction (2.10) to aldotetrose. This aldotetrose can then be split in the reverse aldol reaction (2.11) to two molecules of glycolaldehyde, closing the cycle again [Breslow, 1959, Miller and Orgel, 1974].

From this reaction cycle larger sugars can emerge when the intermediates of the cycle react with each other. For example the aldol condensation reaction

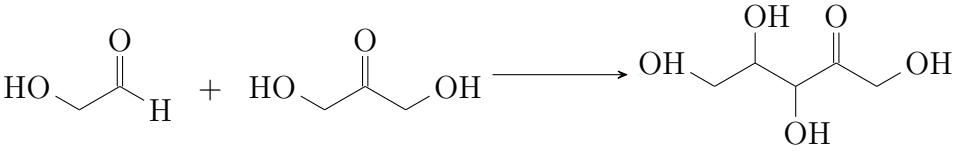

(2.12)

produces ribulose from glycolaldehyde and dihydroxyacetone. The ribulose can then be converted to ribose by an isomerisation reaction,

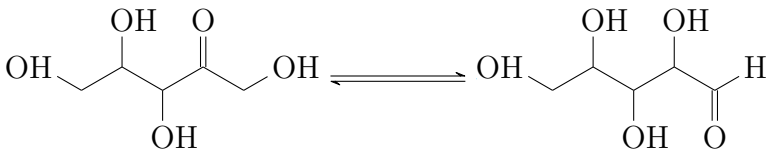

(2.13)

which gives us the pathway leading to the sugar forming the backbone of RNA [Joyce, 1989].

2.4 Nucleobase Formation

The production of nucleobases is one of the more complex processes which can occur in the Miller-Urey experiment. Early studies done by Joyce in 1989 showed that only the prebiotic production of the purine bases is possible while the production of pyrimidines only occurred when using reaction pathways not suitable for prebiotic synthesis [Joyce, 1989]. More recent work done by Ferus et al. appears to have overcome this problem with all RNA nucleobases being produced in a Miller-like experiment [Ferus et al., 2017].

As shown in figure 2.2, the pathway suggested by Joyce starts with hydrogen cyanide, which undergoes a tetramerisation reaction to produce diaminomaleonitrile (DAMN). The DAMN then reacts with either formamidine or ultraviolet light to produce 4-aminoimidazole-5-carbonitrile (ACN), which can be converted to various purines [Joyce, 1989].

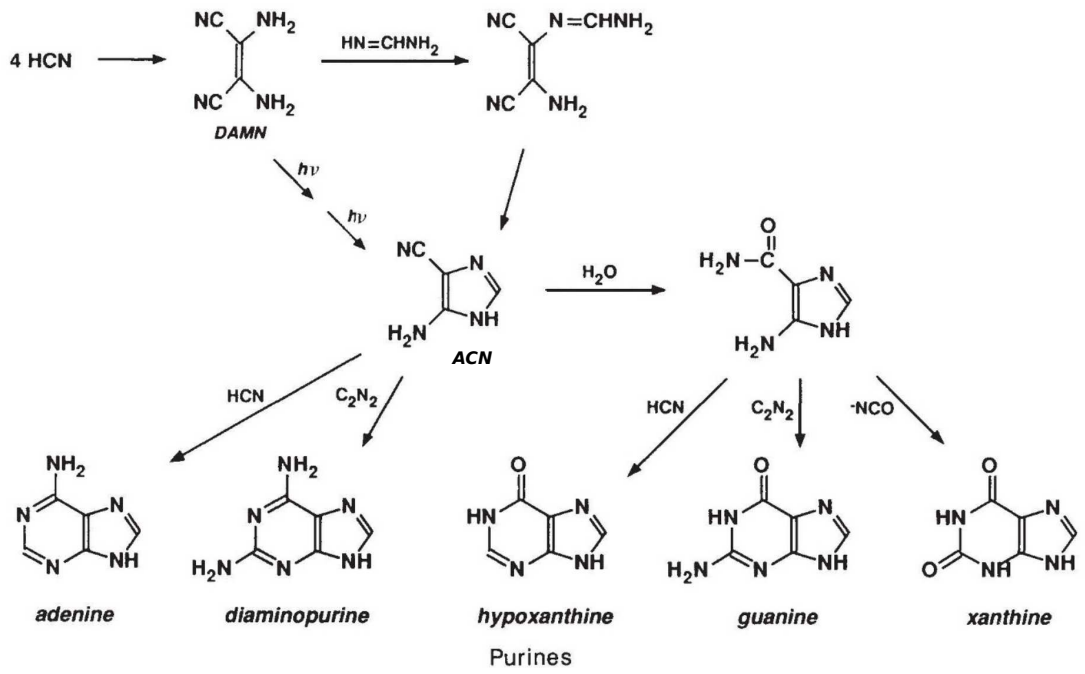

Figure 2.2: Prebiotic synthesis of purines by self condensation of HCN according to [Joyce, 1989].

In [Ferus et al., 2015] another mechanism for the prebiotic production of nucleobases from formamide is proposed. The reaction pathway shown in figure 2.3 starts with the initial reaction of formamide with a cyanide radical ($\mathrm{CN}\bullet$) leading to the production of DAMN through several intermediates. In this suggested pathway the DAMN now undergoes a photoisomerisation reaction converting it to 2,3-diaminofumaronitrile (DAFN). This can then either directly react with another $\mathrm{CN}\bullet$ radical which leads to the formation of cytosine and uracil trough a number of intermediates, or it can undergo another photoisomerisation reaction converting the DAFN to 4-amino-5-cyanoimidazole (AICN) which then reacts with a $\mathrm{CN}\bullet$ radical leading to the formation of adenine and guanine [Ferus et al., 2015].

While this experiment was first conducted using laser induced dielectric breakdown at the Prague Asterix Laser System (PALS) as energy source and pure formamide as atmosphere, the reaction was later discovered to occur equally well in a Miller like experiment, with electric discharges and a reducing atmosphere [Ferus et al., 2017].

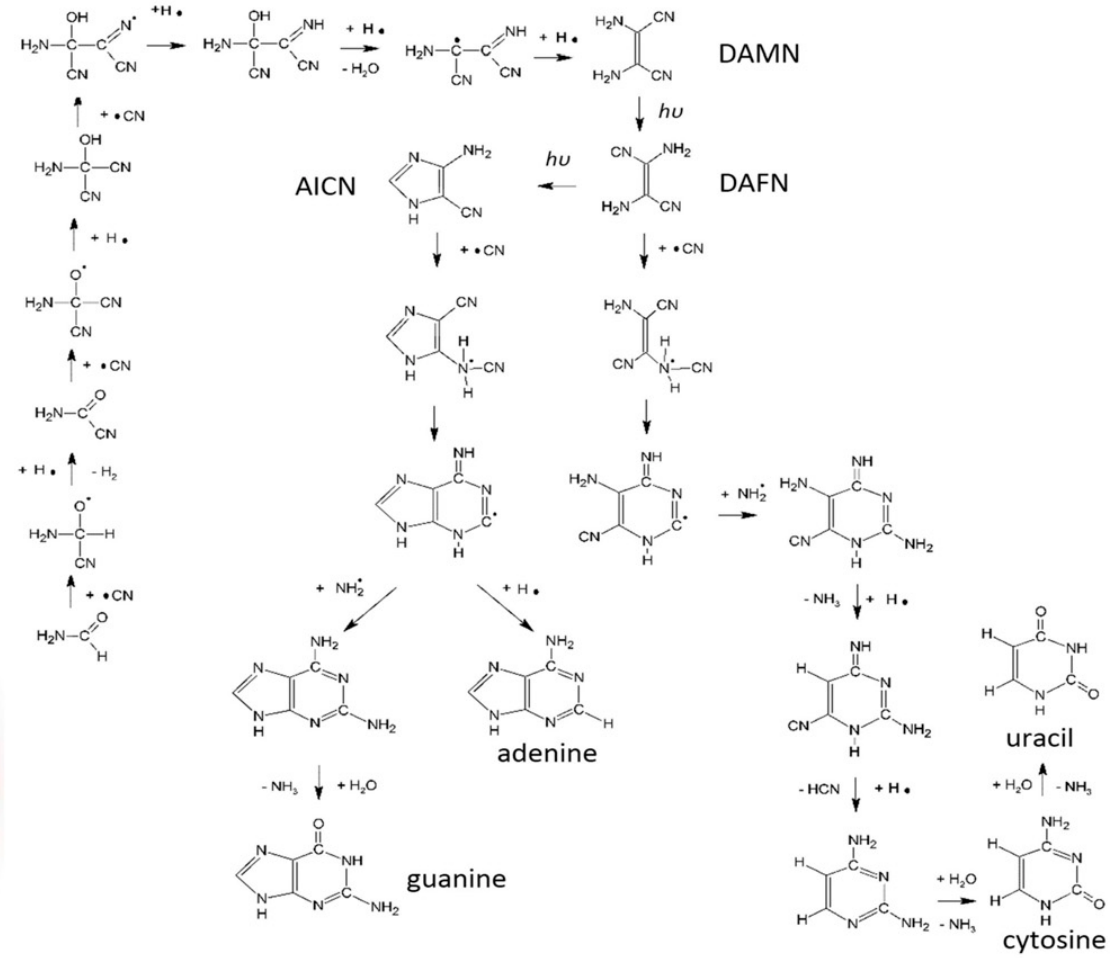

Figure 2.3: Reaction pathway for the synthesis of nucleobases from formamide [Ferus et al., 2015].

Chapter 3

3 The Coupled Gas Chromatography–Mass Spectrometry

Coupled gas chromatography–mass spectrometry (GC-MS) is a universally used analytical routine method. It combines the high separation performance of gas chromatography with the extremely specific data of mass spectrometry, allowing for direct determination of substances in a sample with very high specificity. Source for the general information of this chapter is, if not stated otherwise, the "Handbook of GC/MS" [Hübschmann, 2015].

3.1 Fundamentals

3.1.1 Gas Chromatography

During a GC-MS analysis the gas chromatography provides the needed separation between the substances, as well as additional information in the form of retention times.

The separation power of any form of chromatography is based on multiple repetitions of a separation process. For gas chromatography this separation process is the continuous dynamic partition of the components between two phases, the so called mobile and stationary phase.

To better understand this concept one can have a look at a model system consisting of a series of separating funnels. Each funnel contains a given amount of substance, either liquid or solid, which is called the stationary phase. The sample, consisting of two substances A and B, is placed in the first funnel and dissolved in a second phase, which is called mobile phase. After mixing and subsequent phase separation the mobile phase can be transferred to the next separating funnel and fresh mobile phase is added to the first funnel. The process is then repeated over and over again. Depending on the affinity of a substance for the stationary phase, be it due to solution or adsorption,

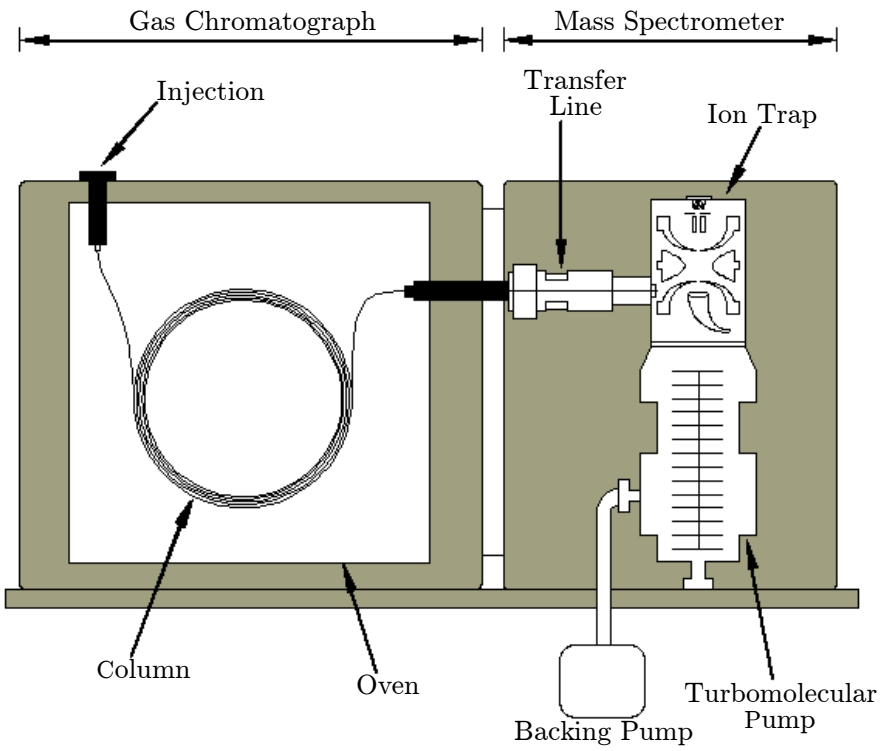

Figure 3.1: Schematic drawing of a coupled gas chromatography–mass spectrometry setup, with the gas chromatograph on the left and the mass spectrometer on the right [Gruber, 2010]

it advances with a characteristic speed in the row of funnels. The two substances A and B in the sample are thus separated after a certain number of separating steps as it is illustrated in figure 3.2.

In the case of gas chromatography there are of course no discrete separating steps with separating funnels, but the separation process happens continuously between the specially coated inside of a fused silica column and the flow of gas which is pushed through this column. The coating acts as the stationary phase and the gas acts as the mobile phase in this case. The whole setup additionally consists of an oven, to precisely control the temperature, and an injection system for the sample (see figure 3.1). Performance of a gas chromatography setup is strongly dependent on the interoperation of these components.

At the end of the chromatographic column a detector is situated. For regular GC setups this can be any kind of detector which is able to measure the incoming substances differing from the carrier gas. Flame ionisation detectors (FID), photo ionisation detectors (PID), flamephotometric detectors (FPD) or electron capture detectors (ECD) are examples for the more regularly used ones, but a large variety of different types of detectors exist, some being used universally and some to detect specific compounds.

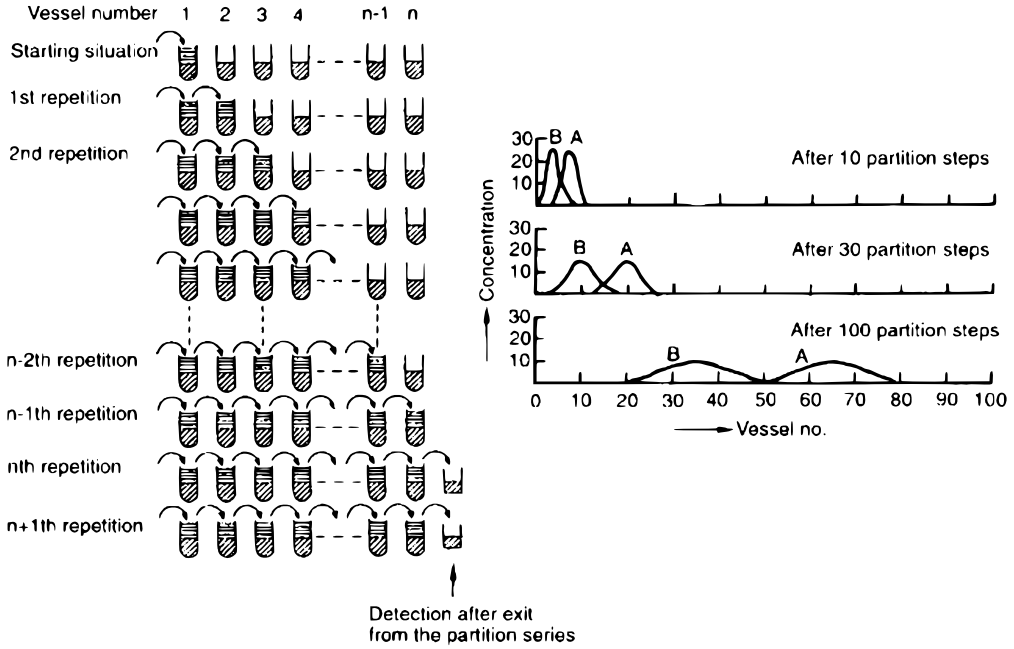

Figure 3.2: *Left:* Schematic of the partition series *Right:* Partition of the substances A and B after 10, 30 and 100 partition steps [Hübschmann, 2015, p. 137-138].

When a mass spectrometer is used as a detector the whole setup is called coupled Gas Chromatography-Mass Spectrometry (GC-MS).

3.1.2 Mass Spectrometry

According to the International Union of Pure and Applied Chemistry (IUPAC) "Gold Book" a mass spectrometer is an instrument in which beams of ions are separated (analysed) according to the quotient mass/charge (m/z), and in which the deflection and intensity of the beams are recorded directly on photographic plate or film [Todd, 1991, Nič et al., 2009]. The mass spectrometers used in GC-MS today have long abandoned the use of photographic plate or film but instead use electronic detectors with digital interfaces.

Mass spectrometers can be built in many different configurations. While in all of them the substance is ionised, the subsequent mass selection can be handled quite differently. Sector field mass analysers use the m/z dependent path an ion travels in static magnetic and electric fields. Time of flight instruments use the difference in velocity between different mass ions of the same kinetic energy. Quadrupole mass filters use a radio frequency quadrupole field which destabilises the path of all ions passing through it, except for the ones with a certain m/z. Ion traps, which are quite often used in GC-MS applications, trap the ions and eject them sequentially depending on their mass to charge ratios.

3.1.3 Chromatographic Resolution

One key feature of coupled gas chromatography-mass spectrometry is the separation of substances in a sample prior to the mass spectral analysis. This separation is essential and thus the overall performance of a GC-MS setup is strongly dependent on the chromatographic resolution of the GC part.

To understand the origin of this chromatographic resolution one can look at the so called theory of plates, developed by MARTIN and SYNGE in 1941 [Martin and Synge, 1941]. Using this theory mathematical relationships for sharpness of the separation and resolving power can be derived from the chromatogram. For this theory one assumes the division of the chromatography column into theoretical plates, sections in the flow direction with a fixed separation capacity. The length of these theoretical sections is called the height equivalent to a theoretical plate (HETP) and is calculated for a given substance i from the length of the chromatographic column L and the number of theoretical plates N_i:

$$\mathrm{HETP_i} = \frac{L}{N_\mathrm{i}} \tag{3.1}$$

The number of theoretical plates can then be calculated from the variance σ_i of a peak, which can be simplified by assuming a Gaussian peak geometry to

$$N_\mathrm{i} = \frac{L^2}{\sigma_\mathrm{i}^2} = 16 \cdot \left(\frac{t_\mathrm{R,i}}{W_\mathrm{i}}\right)^2 = 8 \cdot \ln 2 \cdot \left(\frac{t_\mathrm{R,i}}{W_\mathrm{h,i}}\right)^2 \tag{3.2}$$

where $t_\mathrm{R,i}$ is the retention time, eg., the time of the peak maximum, W_i is the peak width and $W_\mathrm{h,i}$ is the peak width at half height (see figure 3.3) [Swadesh, 2000]. In consequence a chromatographic column is more effective for a given substance, the more theoretical plates it has.

The separation process in the individual theoretical plates can be described by introducing the capacity factor k'_i and the selectivity factor $\alpha_\mathrm{i,j}$. The k'_i value represents the molar ratio of a particular substance i in the stationary and the mobile phase

$$k'_\mathrm{i} = K_\mathrm{i} \cdot \frac{V_\mathrm{s}}{V_\mathrm{m}} \tag{3.3}$$

with V_s and V_m the volume of the phases and K_i the partition coefficient. This can then be expressed in terms of retention times by using the chromatographic dead time t_0, which is the time the carrier gas needs to flow through the column after the injection of the sample, to:

$$k'_\mathrm{i} = \frac{t_\mathrm{R,i} - t_0}{t_0} \tag{3.4}$$

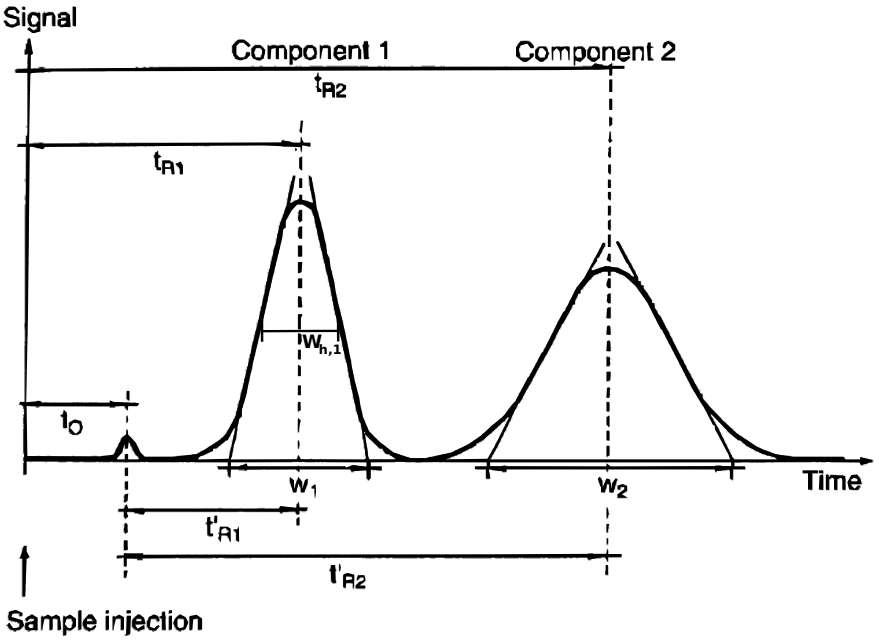

Figure 3.3: Chromatogram peaks and their parameters [Hübschmann, 2015, p. 140].

The selectivity factor $\alpha_{\mathrm{i,j}}$ reflects the difference in affinity of the mobile phase for two substances i and j is defined as:

$$\alpha_{\mathrm{i,j}} = \frac{k'_{\mathrm{j}}}{k'_{\mathrm{i}}}$$

The separation quality of two neighbouring peaks i and j (with $\mathrm{i} < \mathrm{j}$) can now be assessed using the resolution $R_{\mathrm{i,j}}$:

$$R_{\mathrm{i,j}} = 2 \cdot \frac{t_{\mathrm{R,j}} - t_{\mathrm{R,i}}}{W_{\mathrm{i}} + W_{\mathrm{j}}} = 1.198 \cdot \frac{t_{\mathrm{R,j}} - t_{\mathrm{R,i}}}{W_{\mathrm{h,i}} + W_{\mathrm{h,j}}} \tag{3.5}$$

Using definitions for the capacity factor k'_{i}, the selectivity factor $\alpha_{\mathrm{i,j}}$ and the number of theoretical plates N_{i} one can rewrite this equation to

$$R_{\mathrm{i,j}} = \frac{1}{4}\left(\alpha_{i,j} - 1\right) \cdot \frac{k'_{\mathrm{i}}}{1 + k'_{\mathrm{i}}} \cdot \sqrt{N_{\mathrm{i}}} \tag{3.6}$$

and better understand the impact of the measurement parameters on the chromatographic resolution [Schomburg, 1987].

The resolution is directly proportional to $(\alpha_{\mathrm{i,j}} - 1)$, the so called selectivity term, which is dominated by the selectivity factor. This selectivity of a gas chromatographic system is dependent on the polarity of the stationary phase and can thus be changed by switching to an other column. Another way to change the selectivity factor is by changing the column temperature during separation. An increase in temperature generally decreases the selectivity; difficult separations are better carried out at lower temperatures. This

makes the temperature profile a powerful tool for complicated GC-MS analysis.

The second term $\frac{k'_i}{1+k'_i}$ is called retardation term and reflects the dependence of separation on the residence time of a component in the stationary phase. The capacity factor k'_i is thereby mostly influenced by the film thickness of the column, which is especially true for very volatile substances for which a strong increase in resolution can be achieved by choosing a column with adequate thickness of the stationary phase.

The last term $\sqrt{N_i}$, called the dispersion term, depends on the number of theoretical plates N_i, which is directly proportional to the length of the chromatographic column. This leads to a quick effect of diminishing returns when increasing the column length as chromatographic performance is only proportional to the square root of the column length. For an increase in resolution by a factor of 1.4, column cost is doubled while sample throughput is halved.

3.2 Retention Indices

As described in section 3.1.3 the resolution and especially the retention time at which peaks occur is dependent on a plethora of different variables. Only chromatographic setups which are exactly the same will measure the same retention times for the same substances, a situation only worsened by column ageing and matrix effects. When doing GC-MS analysis for samples with known composition, this is not a big issue, as one can simply measure the expected substances in an artificial standard solution and thus know the retention time for the substances in the specific setup used.

When analysing a mixture with lots of unknown substances in it, like it is the case for the primordial broth produced in the Miller-Urey experiment, the identification of the substances based on their retention time becomes difficult, as the measured retention times can not be compared to a library of known retention times. This can be tackled by the use of retention indices (RI), which are relative to an injected standard. A measured substance is included into an retention index system with one standard eluting prior to the substance and one standard eluting later from the column. Small changes in the retention times then affect both the measured substance and both standards and accordingly the calculated retention time remains the same.

Probably the most often used Systems of retention indices are the Kovats RI and the modified Kovats RI. Both are based on a series of n-alkanes. The RI of an alkane is fixed to the number of carbon atoms it has multiplied by 100. While the Kovats index was first developed for isothermal operation of the GC oven, Van den Dool and Kratz later introduced the modified Kovats index for the use with linear temperature programs

[Kováts, 1958, Van den Dool and Kratz, 1963]. The RI values for a substance in both systems can be calculated as follows:

$$\text{Kovats index } \mathrm{RI_K} = 100 \cdot c + 100 \frac{\log\left(t_{\mathrm{R,x}}\right) - \log\left(t_{\mathrm{R,c}}\right)}{\log\left(t_{\mathrm{R,c+1}}\right) - \log\left(t_{\mathrm{R,c}}\right)} \tag{3.7}$$

$$\text{Modified Kovats index } \mathrm{RI_{mod}} = 100 \cdot c + 100 \frac{t_{\mathrm{R,x}} - t_{\mathrm{R,c}}}{t_{\mathrm{R,c+1}} - t_{\mathrm{R,c}}} \tag{3.8}$$

In these formulae c is the number of carbon atoms in the alkane eluted prior to the substance x and $t_{\mathrm{R,x}}$ is the retention time of substance x. Libraries with the modified Kovats index RI values for a large variety of substances are available and can be used for the identification of unknown chromatogram peaks based on their retention time.

3.3 Derivatisation

As gas chromatography works with a gaseous mobile phase, the analytes in the sample need to be volatile enough to be evaporated within the temperature range of the system, thermally stable enough to survive the heating and non reactive enough to not irreversibly alter the stationary phase in the column. These qualities are often not given for polar substances which thus must undergo a process called chemical derivatisation in order to make them suitable for GC-MS analysis.

During chemical derivatisation molecules are altered in order to increase volatility and thermal stability while decreasing reactivity [Knapp, 1979, Ciucanu et al., 1988]. For this process the sample is adequately prepared, often by freeze drying, and then treated with different chemicals to substitute polar or reactive groups.

One of the most used derivatisation methods for simple organic compounds is a combination of methoximation (MeOX) and trimethylsilylation (TMS). During methoximation carbonyl groups are converted to methoxime groups by an oxime-forming reagent such as O-methylhydroxylamine hydrochloride [Yi et al., 2014, Khakimov et al., 2013]:

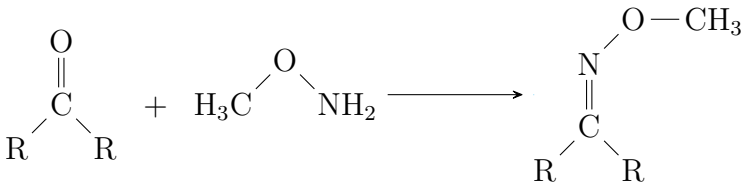

(3.9)

Trimethylsilylation then replaces active hydrogen atoms with trimethylsilyl groups by chemicals like N-Methyl-N-(trimethylsilyl)trifluoroacetamide (MSTFA) or N,O-

Bis(trimethylsilyl)trifluoroacetamide (BSTFA) [Yi et al., 2014, Kataoka, 1996]:

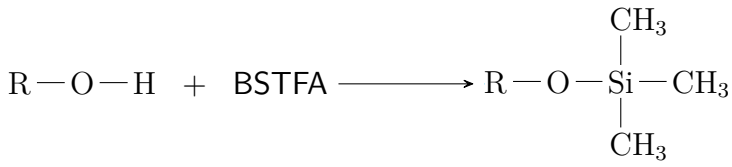

(3.10)

3.3.1 SeaMet Derivatisation

A good example for a modern, optimised derivatisation is SeaMet, a marine metabolomics method that enables metabolite detection in seawater using GC-MS [Sogin et al., 2019]. SeaMet was developed by the Max Planck Institute for Marine Microbiology in Bremen to overcome the limitations of other derivatisation methods which struggle with the presence of salt in samples. In a standard two step MeOX-TMS derivatisation water stored in salt crystals can hamper the derivatisation reactions.

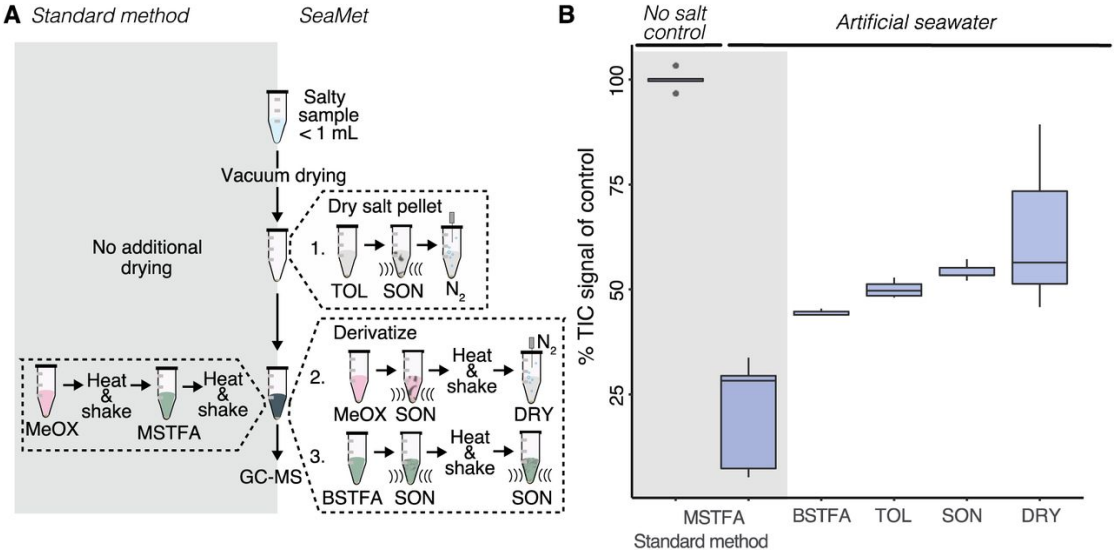

Figure 3.4: Comparison of the SeaMet metabolomics method to a standard two step derivatisation method [Sogin et al., 2019]. *Left:* Comparison of the processing steps of the standard method and the SeaMet methods. *Right*: Effects of the individual processing steps on the total ion count (TIC) signals.

SeaMet introduces additional steps to minimise this effect (see figure 3.4). For the adaptation to the presence of salt in the samples the most commonly used trimethylsilylation reagent, MSTFA, was replaced with BSTFA which is less susceptible to inhibition to water. An additional drying step using toluene (TOL) was introduced to remove water from the samples azeotropically. Ultrasonication (SON) was used to break up salt crystals, releasing the water and sample molecules stored in them. Additionally the MeOX derivatisation agent was evaporated after its use (DRY). These optimisation steps lead to signal improvements and thus allow the GC-MS analysis of metabolome

samples containing salt (see figure 3.4). The SeaMet metabolomics method illustrates the improvements possible in GC-MS analysis, when the analytical method is optimised for the analysed samples.

3.4 Quantitation in GC-MS Measurements

Measuring quantities of substances with high accuracy, while taking uncertainty into account, is called quantitation or quantitative analysis; a job GC-MS analysis can excel at, but only if the needed steps are executed with great care.

When working with GC-MS measurements, it is advisable to keep the limitations the setup provides in mind. These limitations can be expressed in terms of the limit of detection (LOD) and the limit of quantitation (LOQ). To get these limits a series of blank samples not containing any analytes while having the same properties otherwise is measured, and the mean blank signal as well as the standard deviation (SD) are calculated. The LOD is then defined as the mean blank signal plus 2 or 3 SDs. At the mean blank signal plus 10 SD, the LOQ is set. This reflects a higher concentration than the LOD in order to ensure that a value at the LOQ is "real" and not just a random fluctuation [Armbruster et al., 1994]. Both of these statistical quantities can be expressed either in terms of signal or in terms of concentration for a given substance, if a calibration function for this substance has been established.

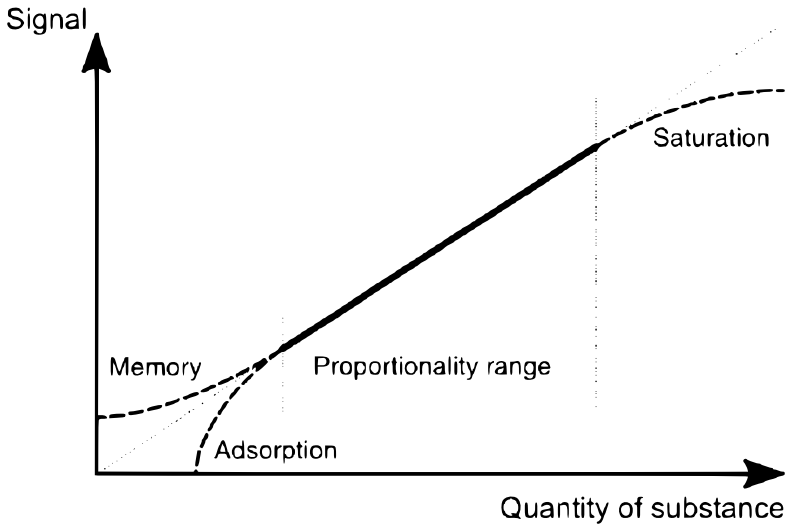

Figure 3.5: Variation of the signal intensity with the quantity of a substance [Hübschmann, 2015, p. 400].

The calibration function for a given substance links the quantity or concentration of a substance to the signal measured. Different approaches exist for acquiring this calibration function:

One Point Calibration is the simplest way to determine a calibration function. For this calibration a simple linear function $S(x) = a \cdot x$ is assumed, where S is the signal produced by the amount of substance x. The proportionality factor a is then the slope of a line drawn through the origin and one measurement of a known quantity of substance.

Multipoint Calibration is done by measuring a number of different dilutions of a standard solution. A linear function $S(x) = a \cdot x + b$ is assumed and the parameters a and b are in this case determined by regression calculation. This sort of calibration function is only valid for quantitation within the working range given by the lowest and highest measured standard dilution. No extrapolation is allowed.

Hyperbolic Calibration is a variation of the multipoint calibration. Instead of a linear function a Padé approximant of a hyperbolic function in the form of $S(x) = \frac{x+a}{b \cdot x+c}$ is used. The parameters a, b and c are determined by fit.

Each calibration method has advantages and disadvantages, which have to be kept in mind when choosing a calibration method for a quantitative analysis. While multipoint calibration with a linear calibration function provides accurate quantitation over a wide range (proportionality range, see figure 3.5) it produces worse results for the non linear range closer to the LOQ, where memory and adsorption effect can produce a large deviation from the linear behavior. In this range hyperbolic calibration and actually one point calibration are more suitable [Whiting et al., 2001].

Another choice one has to make when doing a quantitative GC-MS analysis is the method of normalisation. As GC-MS setups are complex systems, the substance to signal ratios do not have to be the same for every run. This makes measurements only comparable when they are done directly after another. To cope with this problem normalisation methods like internal standardisation or total sum normalisation are used. Internal standards are substances which are added in known quantity to every sample. For further calculations the ratio S_{IS} between peak area values of the substance being analysed A_x and the peak area of the internal standard A_{IS} are used. In this way changes in the system are compensated for. Total sum normalisation (TSN) works in a similar way, but instead of adding substances to the samples and using them for normalisation, the samples remain unaltered and the sum of all chromatogram peaks $\sum A_i$ is used for normalisation. The normalised signals of both normalisation methods can thus be written as:

$$S_{IS} = \frac{A_x}{A_{IS}} \text{ and } S_{TSN} = \frac{A_x}{\sum A_i} \tag{3.11}$$

Again both methods have advantages and disadvantages. For TSN no addition of

a standard to the samples is needed, which results in higher sample throughput and less risk to chemically alter the samples, but is only applicable when changes in the samples are minor. Internal standardisation works well for different samples, but errors in standard addition or standard choice can strongly influence the results, while being very hard to detect as errors [Noonan et al., 2018].

Chapter 4

4 Materials and Methods

4.1 Chemicals and Equipment

The following tables show the used chemicals (table 4.2), consumables (table 4.3) and equipment (table 4.1) used during the practical part of this master thesis.

Name	Model or description	Producer
Heated stirring plate	RCT	Janke & Kunkel GmbH & Co. KG
Heating mantle	G2, 220 V, 700 W	Heraeus
Vacuum pump	RS 5	Vacuumbrand GmbH & Co. KG
GC-MS	Polaris GC	Thermo Fischer Scientific
Centrifuge	4K15 (Rotor 12169-H)	Sigma GmbH
Laboratory dishwasher	G 7883	Miele Professional
Thermomixer	Thermomixer comfort	Eppendorf
Autoclave	V-55	Systec
Heating block with magnet stirrer	Reaci-Therm III Heating/Stirring Module	Thermo Fisher Scientific
Freeze dryer	Alpha 1-4 LDplus	Martin Christ Gefriertrocknungsanlagen GmbH
Glass apparatus	various, also customized	Lenz Laborglas GmbH
Power supply	HNC 20000-1	Heinzinger electronic
Pump, cooling system	MS with M6 Water bath	Lauda Dr. R. Wobser GmbH & Co. KG
Digital manometer	DVR 1	Vacuubrand Inc.
Ultrasound cleaner	Sonorex RK	Bandelin

Table 4.1: Equipment and Instruments.

Name	Molecular Formula	Cas-Nr.	Producer
Acetone	C_3H_6O	67-64-1	Applichem
Alanine	$C_3H_7NO_2$	56-41-7	Sigma-Alderich
Asparagine	$C_4H_8N_2O_3$	70-47-3	Alfa Aesar
Boric Acid	H_3BO_3	10043-35-3	Sigma-Aldrich
BSTFA	$C_8H_{18}F_3NOSi_2$	25561-30-2	Macherey-Nagel
Chloroform	$CHCl_3$	67-66-3	VWR
Cysteine	$C_3H_7NO_2S$	52-90-4	Merck
Ethanol (technical)	C_2H_5OH	64-17-5	VWR
Glycine	$C_2H_5NO_2$	56-40-6	Merck
Glycolic acid	$C_2H_4O_3$	79-14-1	Fluka
Hydrochloric acid (37%)	HCL	7647-01-0	Merck
Methane (gaseous)	CH_4	74-82-8	Linde AG
Methane/Nitrogen mix (50% CH_4, 50% N_2, gaseous)	CH_4N	-	Linde AG
Methanol	CH_3OH	67-56-1	VWR
Methoxyamine HCl	CH_3ONH_2HCL	593-56-6	Sigma-Aldrich
Montmorillonite	$(Na, Ca)_{0,3}(Al, Mg)_2 Si_4O_{10}(OH)_2 \cdot nH_2O$	1318-93-0	Sigma-Aldrich
MSTFA	$C_6H_{12}F_3NOSi$	24589-78-4	Macherey-Nagel
Nitrogen (gaseous)	N_2	7727-37-9	Linde
Potassium hydroxide	KOH	1310-58-3	Carl Roth
Pyridine	C_5H_5N	110-86-1	VWR
Ribitol	$C_5H_{12}O_5$	488-81-3	Sigma-Aldrich

Table 4.2: Chemicals used.

Name	Description	Producer
Autosampling vials	with glass inlay and membrane cap	VWR
Electrodes	WP 3,20x175mm	TIG Electrodes Plansee
PTFE-based grease	Triboflon III	Merkel
Reactivials®	V-shaped 2ml, screw cap	Supelco
Clear vials	7ml, screw cap	Supelco
Test tubes	15ml, screw cap	Sarstedt
Test tubes	50ml, screw cap	Sarstedt
Safe-Lock Tubes	2.0ml, clear	Eppendorf
Silicon oil	M 200	Carl Roth

Table 4.3: Consumables.

4.2 Experimental Setup

The experimental apparatus used for this work differs from the one used by Stanley Miller but is closely related to the setup used for my bachelor thesis [Mense, 2017]. All experiments were conducted between December 2018 and Oktober 2019 at the Center of Biotechnology in Bielefeld, where the apparatus was set up in a fume hood.

4.2.1 Apparatus Construction

Limitations in the available glassware caused some changes in the construction of the apparatus in comparison to the original Miller setup. The glassware at hand for the construction of the apparatus consisted mostly of standard parts connected with ground glass joints. In previous attempts to conduct the Miller-Urey-Experiment in Bielefeld, closed loop setups like used by Miller proved to be quite challenging to construct from our supplies. For this reason an open setup (figure 4.1) is used in all experiments conducted for this work, which was already tested during my bachelor thesis, with some changes in gas supply and exhaust system.

The experimental setup can be segmented into four functional parts

1. gas supply
2. electrical power supply and grounding
3. main reaction chamber
4. cooling and exhaust

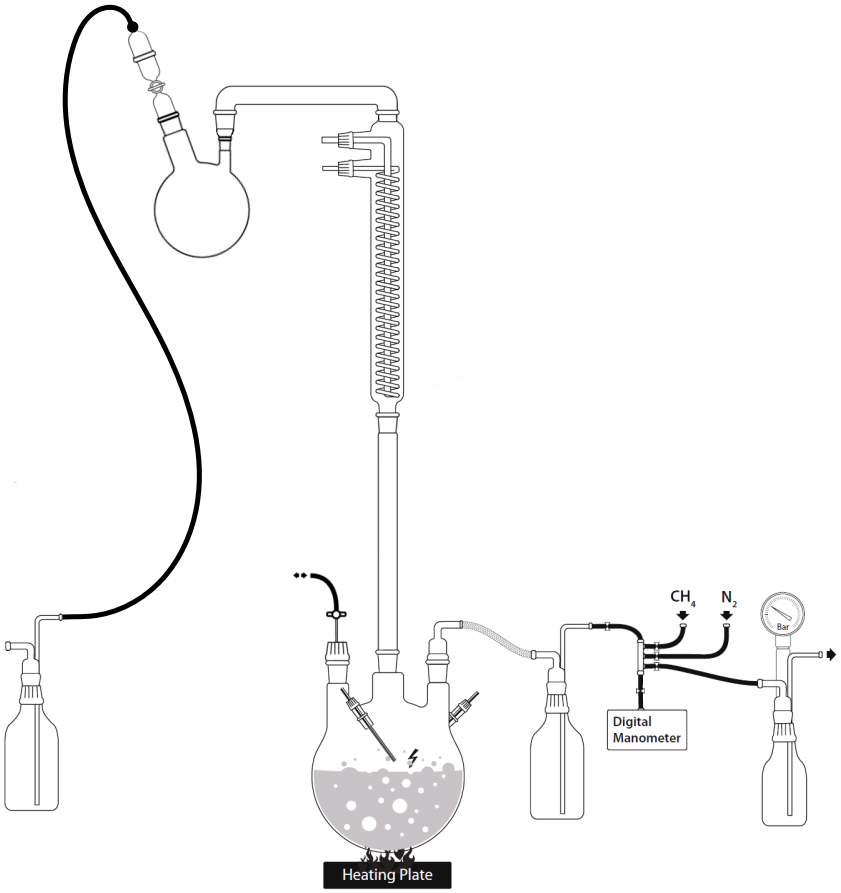

Figure 4.1: The current version of the experimental setup. Gas is fed into the apparatus by the gas supply system on the right, flows through the main reaction vessel and is cooled subsequently by the cooling and exhaust system above and left of the main reaction flask. In this schematic methane (CH_4) is shown as working atmosphere, but a variety of different gas mixtures can be used instead.

Gas from the gas bottles is fed into the gas supply system using two pressure regulators, regulating both the pressure and the flow of the gas. During the experimental run both the pressure and the flow adjustments were used to set the regulator to the lowest possible gas flow. The gas is then transported to the apparatus by pneumatic lines made from PTFE, where the gas flow can be switched on and off by an additional set of valves. An arrangement of two washing flasks is used to protect the gas supply system from contamination (see fig. 4.1, right) and the vacuum pump from condensation. One digital and one analogue manometer are used to observe the pressure in the apparatus.

The power for the experiment is supplied by a high voltage (HV) laboratory power supply and a custom made integrator circuit. The integrator protects the HV supply from the high current associated with the electrical discharges. As the integrator circuit consists

of resistors and capacitors a characteristic charging time of $\tau = RC = 25\,\mathrm{M\Omega} \cdot 2\,\mathrm{nF} = 0.05\,\mathrm{s}$ can be calculated, with $\frac{1}{\tau}$ being the maximal theoretical sparking frequency. The frequency of discharges can be controlled by limiting the HV supplies current. During the experimental runs the current was adjusted to keep the sparking frequency between 1.5 Hz and 2.5 Hz. To reduce the risk of electric shocks the high voltage power supply and the support stands share a common ground.

The main reaction vessel is made from a custom made 4000 ml flask. Three NS 29 ground glass joints on top of the vessel are used to connect it to the gas supply, the cooling and exhaust system and the sample device, while the electrodes are fitted into two additional NS 14 ground glass joints. The whole vessel is placed in a heating mantle to boil the water.

A glass tube connects the reaction vessel with the cooler, which is connected via a glass bridge to another two-necked flask. A NS 29 stopcock is connected to this flask and serves as exit valve of the apparatus. Using a flexible hose it is connected to a washing flask filled with silicon oil serving both as a bubble counter and an airlock to protect the apparatus from contamination.

4.3 Methods and Protocols

4.3.1 Cleaning Protocol

Before every experimental run the apparatus is cleaned meticulously. First all alkaline resistant parts are cleaned in the laboratory washer for two washing cycles of which at least one heats up to 93°C for more than 10 minutes. In the first cycle laboratory dishwasher detergent was used, the second cycle was done without any detergent to prevent contamination of the apparatus with detergent. Subsequently the parts are treated with potassium hydroxide in a 0.5 mol/l concentration over night. The parts are then rinsed with demineralised water and placed on aluminium foil to dry. All parts which were not alkaline resistant enough to be cleaned in the KOH bath, like electrodes and gaskets, are cleaned by submersion in acetone and ethanol. When sufficiently dried the apparatus is assembled under a fume hood wearing gloves.

After assembly the apparatus is heated and evacuated until no visible water is left in the apparatus. All needed fluids are then filled into the reaction vessel and the apparatus is sealed again. It is then evacuated and subsequently filled with nitrogen. This is repeated 5 times, so that no oxygen should remain in the apparatus. The apparatus is then evacuated and filled with the gas used in the experimental run.

4.3.2 Sampling

Sampling is done via a sampling device consisting of a 0.1 ml pipette, silicon hose and a Luer-Lock 3 way stopcock. Each time a sample was taken the voltage supply was shut off, the electrodes were earthed and a syringe was screwed to the Luer-Lock port of the stopcock. The stopcock was then opened, a 30 ml sample was drawn with the syringe and transferred to a labelled Sarstedt 50 ml test tube. Sampling was done after 1 hour and 72 hours of running with at least 3 samples taken each time. After sampling the samples were stored in a -80°C freezer.

A 30ml sample size was chosen as it should be sufficient to detect even less abundant organic molecules.

experimental run	number of samples	number of runs [n]	1 hour	72 hours
N	3	3	Nna1/2/3	Nne1/2/3
M	3	3	Mna1/2/3	Mne1/2/3
C	3	3	Cna1/2/3	Cne1/2/3
MT	3	1	MTa1/2/3	MTe1/2/3
CT	3	1	CTa1/2/3	CTe1/2/3
Blank	3	3	-	Bne1/2/3

Table 4.4: List of samples taken with the used abbreviations for the experimental run and their respective label coding .

4.3.3 Freeze Drying

All samples were frozen using a -80°C freezer. The samples were uncapped and then placed in a Christ Alpha 1-4 LS plus laboratory freeze dryer and dried at a temperature of -44°C and a pressure of 0.07 mbar until no signs of ice were visible anymore.

After drying the sample tubes were capped again and stored dark and at room temperature until derivatisation on the next day.

4.3.4 Derivatisation

For the sample preparation prior to GC-MS analysis two different methods were used. The first was based on an established derivatisation protocol for metabolom samples, the second was based on [Sogin et al., 2019], a new derivatisation protocol for the measurement of metabolites in seawater. The main difference between the standard method and the new method is the usage of Eppendorf tubes instead of Reactivials to increase sample throughput and the change form MSTFA to BSTFA as derivatisation agents.

Standard Method

For the first method the dried samples were resuspended in 1 ml of 10 μmol/l ribitol in 80% methanol. The solution was then transferred to Eppendorf tubes and centrifuged for 20 minutes at 14000 rpm. From each Eppendorf tube 750 μl of the supernatant were then transferred to a Reactivial and placed in a preheated to 37°C Reacti-Therm heating and stirring module. In the Reacti-Therm module the methanol from the solution was evaporated using a constant flow of nitrogen gas. While the samples dried a solution of 20 mg MeOX in 1 ml Pyridine was prepared in a Supleco vial. 50 μl of the MeOX solution and a micro stir bar were added to the dried samples and placed in the Reacti-Therm module. After 90 minutes 50 μl premixed MSTFA solution were added to the Reactivials and incubated for 30 minutes more. The samples were then centrifuged for 5 min at 4000 rpm and the supernatant was transferred to glass vials. After derivatisation the reusable micro stir bars and Reactivials are first cleaned in an ultrasound cleaner with water and methanol and then washed in two baths of analytical grade methanol.

New Method

For the second method the dried samples were resuspended in 1 ml of 80% methanol, with 20 μmol/l methionine and cysteine added as internal standard. The solution was centrifuged like for the standard method. From each Eppendorf tube 750 μl of the supernatant were then transferred to a fresh Eppendorf tube instead of Reactivials. The Eppendorf tubes were placed in a preheated 37°C Reacti-Therm module and dried under a constant flow of nitrogen gas. Again, a solution of 20 mg MeOX in 1 ml Pyridine was prepared in a Supleco vial. When completely dried 50 μl of MeOX solution were added to the dried samples and the tubes were placed in an Eppendorf Thermomixer, set to 37°C and 1200 rpm mixing. After 90 minutes 50 μl premixed BSTFA solution was added to the Reactivials and incubated for 30 minutes more. The samples were then centrifuged for 15 min at 14000rpm and the supernatant was transferred to glass vials.

4.3.5 GC-MS Analysis

Derivatised samples were analysed using the ITQ 900 GC-MS analyser at the CeBiTec. Two different instrument methods were used for the analysis. The first method was similar to the method I used during my bachelor thesis with the Polaris GC-MS analyser [Mense, 2017]. The second method was derived from the old method in order to increase resolution and simplify identification of substances using retention indices.

The first method uses an oven temperature profile with two ramps. It starts with an initial temperature of 40°C held for 6 minutes constant. After 6 minutes the temperature is increased with a rate of 10 $\frac{^{\circ}\mathrm{C}}{\mathrm{min}}$ for two minutes until a temperature of 60°C is reached, followed by a rate of 12 $\frac{^{\circ}\mathrm{C}}{\mathrm{min}}$ up to a temperature of 320°C. The final temperature is held for one minute.

The new method works with just a single temperature ramp. The initial temperature of 40°C was again held for 6 minutes followed by an temperature ramp with 8 $\frac{^{\circ}\mathrm{C}}{\mathrm{min}}$increasing up to 320°C over 35 minutes. The final temperature was again held for one minute.

Thermo Fisher's Xcalibur software as well as OpenChrom was used for general evaluation of the GC-MS data, peak identification and peak area calculation. Further analysis of the data was done with Python version 3.6.8.

4.3.6 Scanning Electron Microscope Observation of used Glass

To compare the surface properties of fresh and used borosilicate glass a scanning electron microscope (SEM) was used. This type of microscope uses a focused electron beam to scan the surface. The emission of secondary electrons from the surface is then detected to produce the image. As an electron beam is used the samples have to be conductive in order to prevent the accumulation of electrostatic charge on the samples surface. For non conductive samples like glass a thin layer of metal is applied to the surface using the process of sputter deposition. In our case this deposited metallic layer consisted of a roughly 1 nm thick layer of tantalum topped by a 9 nm thick layer of ruthenium. These layers were applied using a custom made sputter chamber situated at the thin films work group of the universities physics department. The argon plasma sources of the sputter chamber were run with a power of 25 Watt leading to deposition times of ~30 s for both the tantalum and ruthenium layer.

After coating the samples, they were placed in the SEM and contacted with electrically conductive tape. Images were taken with a acceleration voltage (electron high tension, EHT) of 10 kV at 50x, 300x, 1000x, 5000x, 20000x and 50000x magnification.

Additionally energy-dispersive X-ray spectroscopy (EDX) was used to determine the composition of the surface layer. In this case an acceleration voltage of 20 kV was used for the electron beam.

Chapter 5
5 Results and Discussion

5.1 Experimental Runs

For this thesis a total of 14 runs were done in the Miller-Urey configuration described in section 4.2.1 and three additional runs were done to observe the dissolution of substances from the glassware, amounting to a total experimental time of 17 weeks.

Miller-Urey Runs

The Miller-Urey runs can be characterised by the used atmosphere and the abundance of montmorillonite clay. For all experimental runs 600ml of autoclaved Milli-Q water was added to the main reaction flask and run preparation was done according to section 4.3.1. The water was then boiled for 72 hours with electric discharges occurring for the same time in all runs except the blank run. For the blank runs a pure atmosphere of nitrogen was used as well as for the N runs. The M and MT runs used a mixture of equal amounts (50/50) of methane and nitrogen. The C and CT runs used a pure methane atmosphere. In the MT and CT runs 5g of montmorillonite clay were added to the Milli-Q water. An overview of these conditions is given in table 5.1.

abbreviation	atmosphere	montmorillonite clay	discharges
N	nitrogen	no	yes
M	nitrogen/methane	no	yes
C	methane	no	yes
MT	nitrogen/methane	yes	yes
CT	methane	yes	yes
Blank	nitrogen	no	no

Table 5.1: Overview of the conditions during the experimental runs with their respective abbreviations.

Dissolution Runs

Additional to the Miller-Urey runs three runs were done to observe the dissolution properties of substances from the glassware. For each of these runs 600ml of autoclaved Milli-Q water was boiled for 72 hours in the apparatus under regular air as an atmosphere. The first dissolution run used a fresh 2L round bottom flask instead of the main reaction vessel. The second and third run used the main reaction vessel. To the aqueous phase of the third run 5g of montmorillonite clay were added prior to autoclave sterilisation.

5.2 Observations

5.2.1 Colour

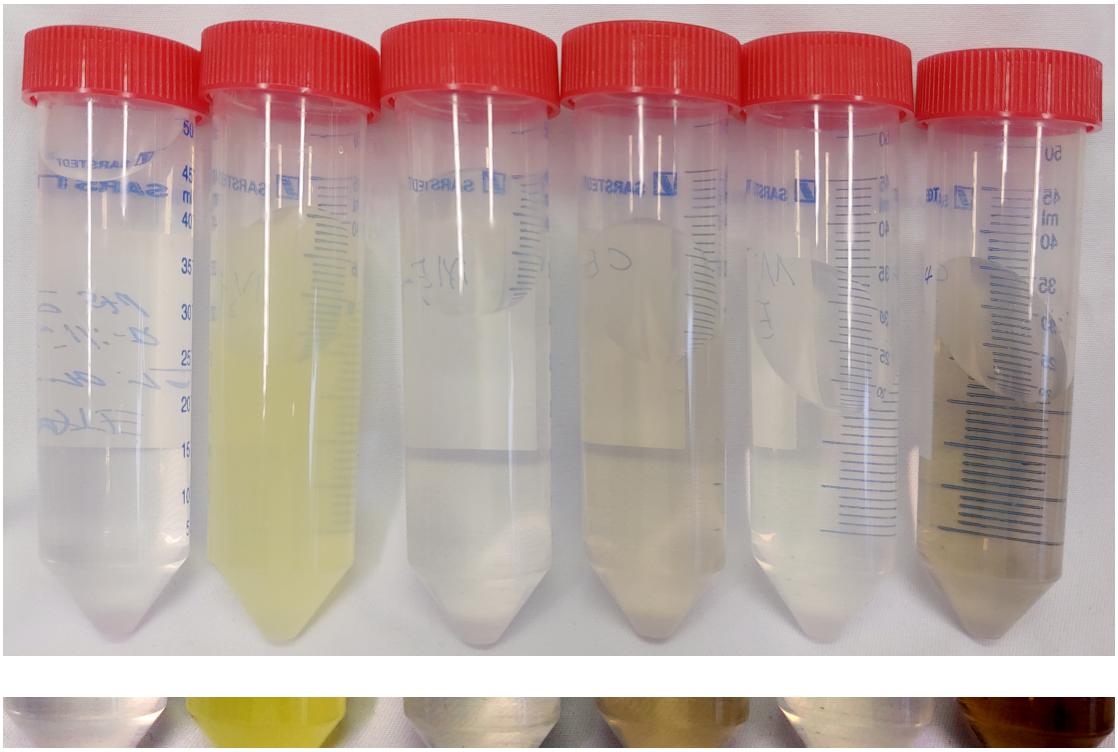

Figure 5.1: *Top:* Typical end samples from each type of run. From left to right: blank (B), pure nitrogen (N), nitrogen methane mix (M), pure methane (C), nitrogen methane mix with clay (MT), pure methane with clay (CT). *Bottom:* Cut from the above image with increased contrast.

During the runs a colour shift of the aqueous phase in the apparatus was clearly visible. The most impressive colour change was observable during the runs with pure nitrogen atmosphere and electric discharges. A bright yellow coating started to form on the tungsten electrodes, with the aqueous phase turning slowly yellow as well. After the

boiling had been stopped a yellow powder fell out of the suspension and acculmulated at the bottom of the flask. This colour change is probably caused by microscopic particles of tungsten trioxide, a bright yellow oxide of tungsten with relatively high density [Nogueira et al., 2004].

Also a clear colour change was observable for the runs using a pure methane atmosphere. The aqueous phase turned to a light brown during the experimental runs. This was more pronounced for the experimental run with clay present.

Only a very slight colour change was observable for the runs with the mixed atmosphere containing both methane and nitrogen. The aqueous phase developed a slightly brownish hue only visible by naked eye in direct comparison with a sample of clean water and with increased contrast when digital imaging is used (see figure 5.1).

No change in colour was observed during blank runs.

5.2.2 Gas and Energy input

Due to the open design of the experimental setup, a continuous flow of gas through the apparatus was necessary to prevent air from entering. The flow of this gas was measured multiple times over the course of an experimental run using the bubbling in the silicon oil filled exhaust washing flask. Bubble frequency was measured by stopping the time required for 100 bubbles to occur. When the gas flow was adjusted by hand over the course of an experimental run an additional measurement was taken. To calculate the volume of gas passing through the apparatus during one run, the measured bubble frequencies were plotted against the time of measurement, linearly interpolated (see figure 5.2). Integration of the interpolated function gave the estimate number of bubbles occuring during one run. The bubbles to millilitres conversion factor ($0.322\,\frac{\mathrm{ml}}{\mathrm{bubble}}$) was determined experimentally by pushing air through the washing flask with a syringe. From the volume the amount of gas N can be estimated using the ideal gas law:

$$N = \frac{P}{RT} \cdot V \tag{5.1}$$

in which R is the universal gas constant, P is the pressure and V is the estimated volume. Over the course of the experiments the temperature of the cooler was monitored showing that gas is at room temperature when passing the bubble counter. Thus values of $P = 101.3\,\mathrm{kPa}$ and $T = 296.2\,\mathrm{K}$ were used.

The number of discharges of the course of an experiment were estimated in the same fashion as the number of bubbles. To estimate the energy input into the system through the discharges the formula

$$E = \frac{1}{2} C U^2 \cdot n_{el} \tag{5.2}$$

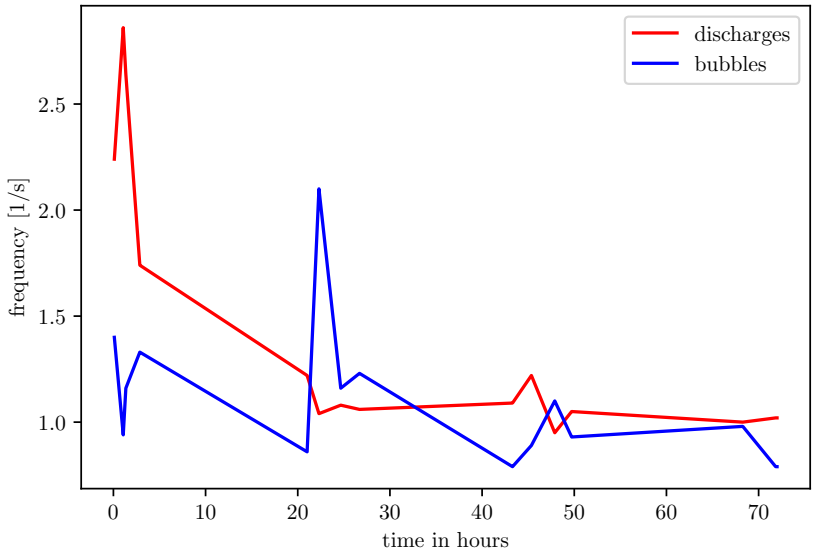

Figure 5.2: Linear interpolation of discharge and bubble frequency over the course of the C2 experimental run. Peaks occur due to the manual adjustments of flow and discharges.

can be used, in which C is the capacity of the integrator circuit, U is the ignition voltage of the arc and n_{el} is the number of discharges. Values of $C = 2\,\mathrm{nF}$ and $U = 10\,\mathrm{kV}$ were used.

From the estimated values the ratio of energy input to molar gas input was calculated. All results can be found in table 5.2.

Run	V [L]	N [mol]	n_{el}	E [kJ]	$\frac{E}{N}\left[\frac{\mathrm{kJ}}{\mathrm{mol}}\right]$
N1	92.6	3.81	325105	32.5	8.5
N2	182.4	7.50	615010	61.5	8.2
N3	174.9	7.19	394619	39.5	5.5
M1	101.8	4.19	542816	54.3	13.0
M2	121.7	5.00	429971	43.0	8.6
M3	74.3	3.05	670543	67.1	21.9
C1	134.6	5.54	392321	39.2	7.1
C2	134.6	5.60	313715	31.4	8.7
C3	101.9	4.19	248153	24.8	5.9
MT	223.9	9.21	705320	70.5	7.7
CT	147.9	6.10	797344	79.7	13.1

Table 5.2: Estimated values for flow volume V, number of moles N in that volume, number of discharges n_{el}, energy input E and energy per mole $\frac{E}{N}$

5.2.3 pH Values

Due to constraints in freezer space the aqueous phase was collected in 1 liter duran laboratory glass bottles after each run and thus mixed with other samples of the same type. pH values of the collected liquids were measured using a pH meter after completion of all runs. While the blank runs were slightly alkaline, the aqueous phases of the other experimental runs were slightly acidic. Measured values can be found in table 5.3.

run	N	M	C	MT	CT	Blank
pH	3.05	3.85	3.56	3.89	3.50	9.00

Table 5.3: Measured pH values of the aqueous phase after the completion of different types of experimental runs.

5.2.4 Scent

During sample processing different odours were perceptible. When fresh, hot samples of the M and MT runs were taken, a distinctive scent like burned electronics or burned hair was noticeable. This scent quickly became a stench when the reaction vessel was opened for cleaning.

A more pleasant odour was perceptible after freeze drying. When handling samples of the C and CT run a sweet scent of caramel character escaped from the beaker. Interestingly it was only perceivable when the samples were dry.

5.3 First GC-MS Analysis

Early GC-MS analysis used the standard derivatisation method and the old temperature profile explained in 4.3.4 and 4.3.5. Chromatograms produced using these method showed major issues with the analytical procedure, exhibiting high noise not suitable for trace analysis (see figure 5.3). The cause of this issue appeared to be samples from the N runs, which degraded the column quickly. Column degradation then caused the high noise, which persisted even for subsequent users. The degraded column had to be replaced, as even removing some length of column from the beginning did not solve the noise problem. To preserve the GC-MS analyser I refrained from other analysis attempts of N run samples.

After the new column had been installed in the GC-MS analyser, the measurements showed another problem. The ribitol added as internal standard during the derivatisation

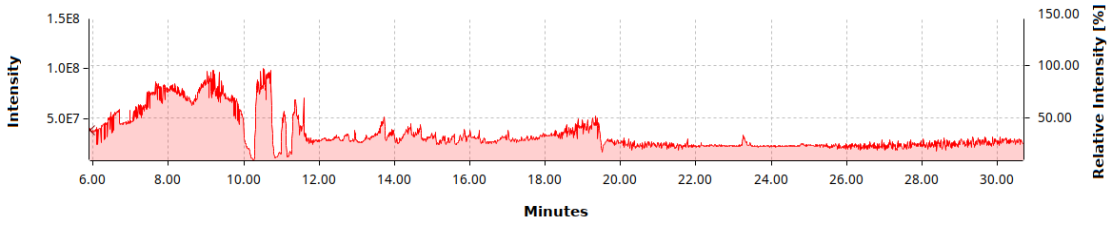

Figure 5.3: Chromatogram of a C2e sample measured after an N1e sample with only few identifiable peaks. The bad signal to noise ratio is clearly visible.

produced no peak in the chromatograms of measured samples, while working fine for technical blanks to which no sample of any type was added. This error occurred even when samples of the blank run were used.

An initial attempt to resolve the issue was done by changing from the old to the new derivatisation method, which involved replacing MSTFA with BSTFA as derivatisation agent and using single-use Safe-Lock tubes instead of reusable glassware. A precise description of the method can be found in section 4.3.4. This was done based on the assumption that residue water stored in the samples caused problems during derivatisation. The new method is a lot less sensitive to this kind of residue water, as it was inspired by the SeaMet method developed for the derivatisation of sea water samples with a lot of water being stored in the salt crystals [Sogin et al., 2019].

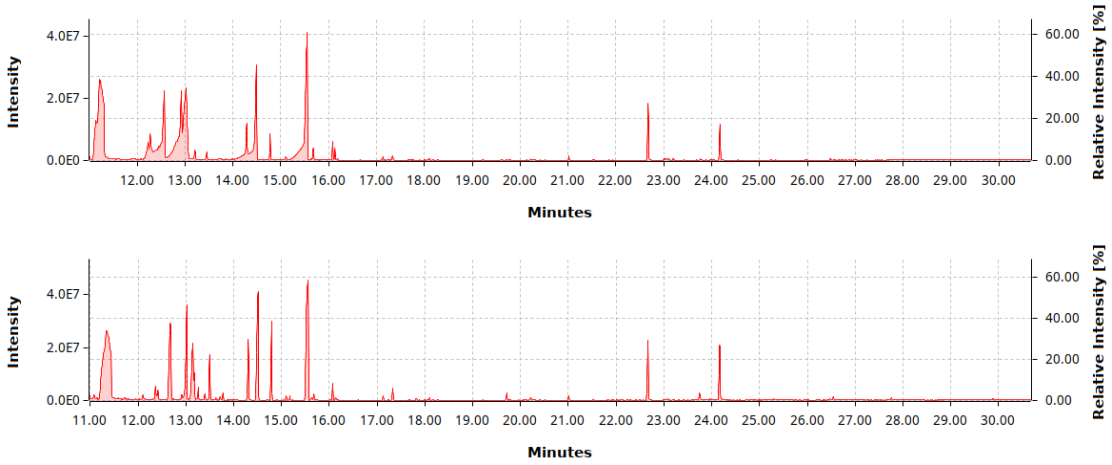

Figure 5.4: *Top:* Chromatogram of a spiked, undiluted blank sample using the old derivatisation method *Bottom:* Chromatogram of the same sample but using the new derivatisation method

To estimate the performance of the new method different dilutions of a blank run sample were spiked with a standard mixture containing glycine, glycolic acid, alanine, hydroxylamine and glyceraldehyde and processed using the new and the old method. The chromatograms produced by the new method showed much narrower peaks, with

a better signal to noise ratio and better peak symmetry. The resolution of the adjacent hydroxylamine peaks at 13 minutes was calculated using equation (3.5). For the old method a resolution of $R = 2.133$ was calculated, while the new method produced a resolution of $R = 4.59$. This amounts to a resolution increase of about 115%.

Additionally to the increase in resolution another interesting observation could be made when looking at the different dilutions of the analysed sample. With increasing sample dilution the missing ribitol peak slowly reappeared while another large peak at ~11.3 minutes disappeared (see fig. 5.5).

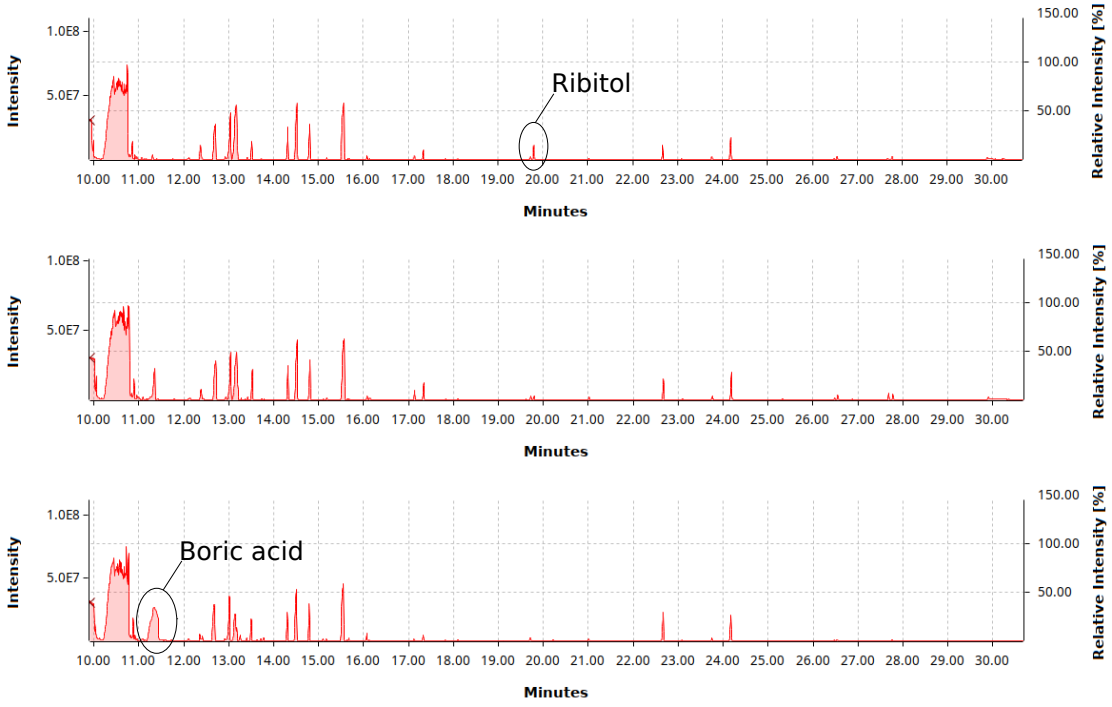

Figure 5.5: Chromatograms of a blank sample at different dilutions. The peaks between boric acid and ribitol can be attributed to the added standard mix. Derivatisation was done with the new method using BSTFA *Top:* 100x dilution *Middle:* 10x dilution *Bottom:* Undiluted

Using the Golm Metabolome Database (GMD) I was able to identify the peak as three times trimethylsilylated derivate of boric acid. As boric acid reacts with OH groups in cis-configuration forming boric acid esters this explains the disappearance of the ribitol [Reichvilser, 2010].

5.4 Boric Acid Characterisation

As the only possible origin of boric acid in the experiment was the borosilicate glassware, dissolution experiments were conducted as discribed in section 5.1. This included

three experimental runs in which water was boiled in the apparatus; one with fresh glassware, one with used glassware and one with used glassware and five grams of montmorillonite clay added to the aqueous phase. A number of samples (5 ml) were taken over the course of a run for time resolved concentration measurements and processed for GC-MS analysis. During GC-MS analysis the new derivatisation method and the old temperature profile were used. For quantitation one point calibration was used with a measured boric acid standard (see section 3.4).

According to [Noyes and Whitney, 1897] the time dependent concentration $C(t)$ from dissolution can be described using the function

$$C(t) = (C_0 - C_E) \cdot e^{-k \cdot t} + C_E \tag{5.3}$$

using the starting concentration C_0, the end concentration C_E and the dissolution rate constant k. This function was fitted to the measured concentrations using the Orthogonal Distance Regression (ODR) SciPy package [Boggs and Rogers, 1990, Boggs et al., 1992]. As visible in figure 5.6, the function describes the measured concentrations quite well, with concentration equilibrium reached within the 72 hours of the dissolution runs.

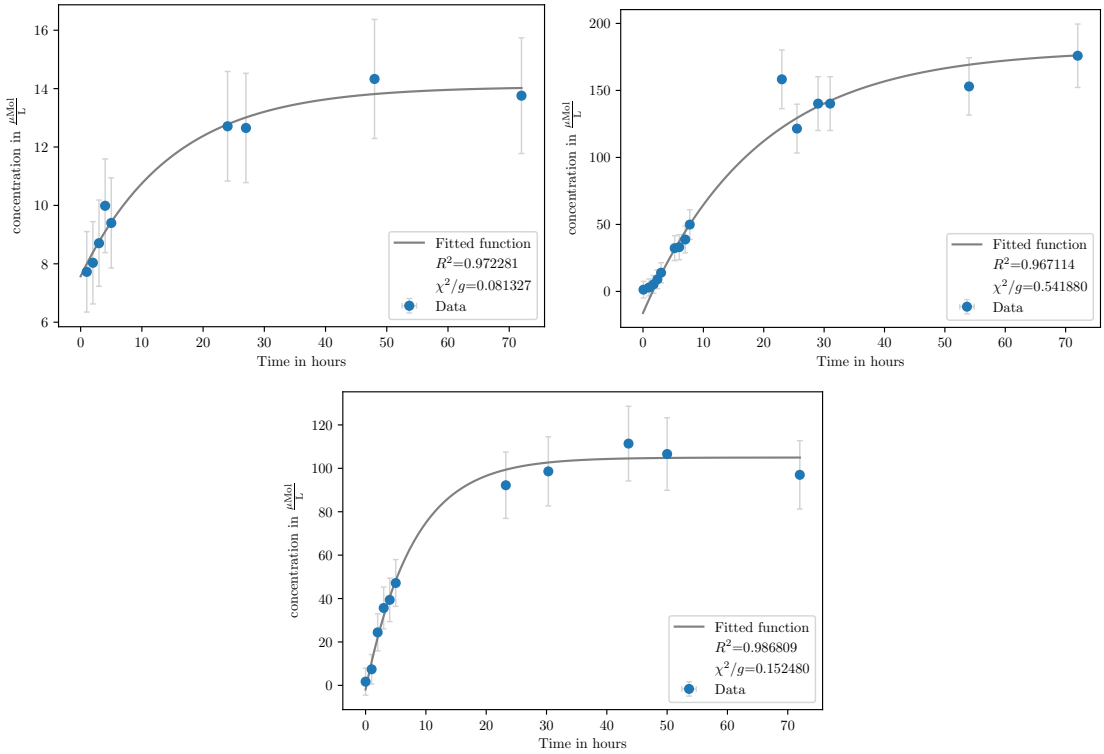

Figure 5.6: Dissolution curves of boric acid from borosilicate glass. *Top Left:* Fresh glassware. *Top Right:* Used, cleaned glassware. *Bottom:* Used, cleaned glassware with clay added to the aqueous phase.

Fit results for C_E and dissolution rate constant k can be found in table 5.4 together with their respective errors. For fitting a simple 10 percent error was assumed as the standard deviation.

glassware	$C_E \left[\frac{\mu\text{mol}}{\text{L}}\right]$	$\Delta C_E \left[\frac{\mu\text{mol}}{\text{L}}\right]$	$k \left[\frac{1}{\text{h}}\right]$	$\Delta k \left[\frac{1}{\text{h}}\right]$
fresh	14.1	0.62	0.067	0.014
used	180.5	39.6	0.53	0.009
used + clay	105.0	7.9	0.13	0.019

Table 5.4: Results for end concentration C_E and dissolution rate constant k together with their respective standard errors from the fit of function 5.3

5.5 SEM Analysis

Due to the significantly higher concentration of boric acid in samples produced with the used glassware the surface of both new and used glassware was inspected using a scanning electron microscope. While the fresh glassware showed no signs of structure

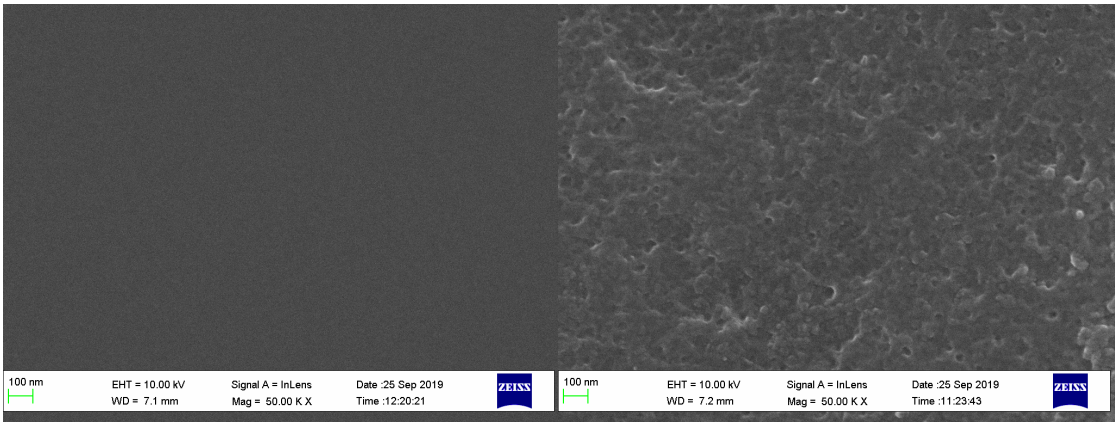

Figure 5.7: SEM images of the surface of fresh and used glassware *Left:* Fresh glassware *Right:* Used glassware

and appeared to be perfectly smooth, the rugged structure of the used glassware's surface was clearly visible even with magnifications lower than 50000x. Even with the naked eye the surface difference was perceivable after the coating with ruthenium. The fresh glassware had a mirror like finish, while the used glassware appeared much more dull.

Energy-dispersive X-ray spectroscopy (EDX) showed little difference between the two glass samples. Boron and Oxygen were invisible to the EDX analysis due to their low atomic numbers.

Element	Fresh glass	Used glass
Silicon	80.089	79.711
Aluminium	6.495	6.956
Ruthenium	5.400	4.561
Sodium	4.894	6.574
Potassium	1.612	1.335
Tantalum	1.509	0.863

Table 5.5: Surface composition in atom percent measured with EDX. Ruthenium and Tantalum traces are measured due to the conductive coating.

5.6 Final GC-MS Measurements

After boric acid had been identified as the cause of the missing ribitol peak, GC-MS analysis was done using both new methods for derivatisation and temperature profile. To evaluate the effect of these changes the resolution of the hydroxylamine double peak, now at ~16 minutes, has been calculated using equation (3.5). The calculated resolution of $R = 6.868$ for the combination of both new methods equates to an increase of 50% compared to just using the new derivatisation and to an increase of 222% compared to the combination of both old methods.

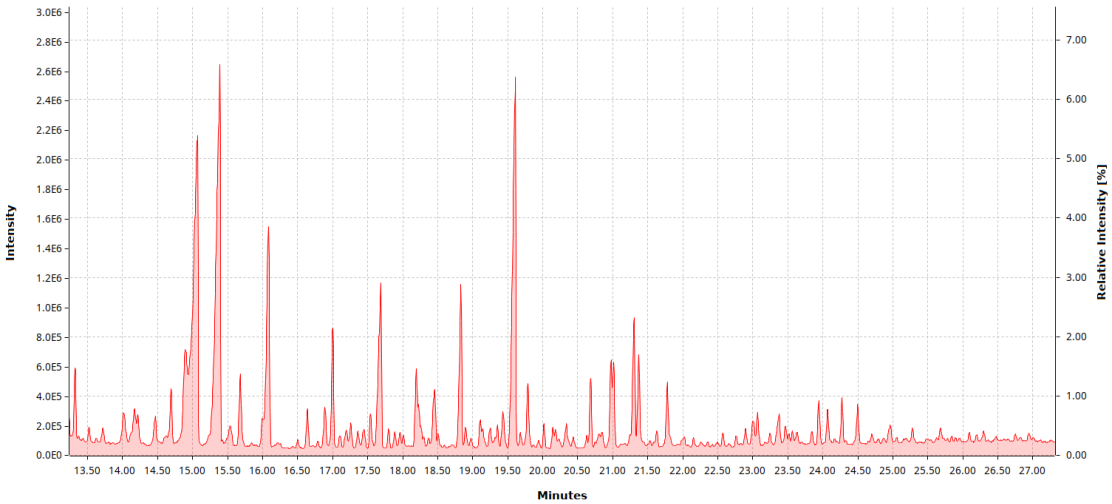

Figure 5.8: Chromatogram cutout of the MTE sample showing the increased resolution and good identifiable peaks under utilisation of both new methods.

5.6.1 Peak Identification

To identify the substances in the GC-MS data a combination of calculated retention times and mass spectra was used. The expected retention time of 2594 substances was

calculated from the retention indices provided with the Golm Metabolome Database [Hummel et al., 2010]. For this a linear function was assumed as conversion function from retention indices and fitted to the measured values for the boric acid and ribitol peaks, giving:

$$t_{\mathrm{R,i}}\left(\mathrm{RI}_{\mathrm{mod,i}}\right) = 0.02187\,\mathrm{min} \cdot \mathrm{RI}_{\mathrm{mod,i}} - 8.31\,\mathrm{min} \tag{5.4}$$

A peak is assumed to have been identified if the database comparison with the NIST-DB identifier gives a good match with a probability factor above 20%[1] and, in addition, the retention time calculated for the substance from the retention index lies around the peak in a 30-second window. In this way 21 different substances were identified in the chromatograms and can be found in table 5.7, together with the retention time of the corresponding peak and the m/z ratio used for quantitation (quantitation mass).

[1] The probability factor given by the NIST-DB identifier should not be interpreted as an absolute probability of identification. Due to the variations present in mass spectra even in measurements of pure standard solutions the factor rarely has values above 40% for identified peaks.

substance	retention time [min]	quantitation mass [m/z]	found in
Boric acid	12.90	263	MA,ME,CA,CE, ETA,MTE,CTE, Blank
Glyoxylic acid	13.20	160	ME, CE, MTE, CTE
Lactic acid	14.90	190	MA, ME, CA, CE, ETA, MTE, CTE, Blank
Glycolic acid	15.39	177	ME, CE, MTE, CTE
Hydroxylamine	16.07	133	ME, ETA, MTE, CTE
Oxalic acid	16.63	190	ME, CE, MTE, CTE
3-Hydroxy-propanoic acid	17.00	177	ME, CE, MTE, CTE
Glyceraldehyde	18.83	163	ME, CE, MTE, CTE
1,3-Dihydroxyacetone	19.60	163	ME, CE, MTE, CTE
Ethanolamine	19.79	174	ME, MTE, (CE, CTE)
Glycerol	20.01	205	all runs
Glycine	20.69	174	ME, MTE
Succinic acid	21.01	247	ME, CE, MTE, CTE
Glyceric acid	21.30	292	ME, CE, MTE, CTE
Lactic acid dimer	21.50	117	ME, CE, MTE, CTE
Malic acid	22.36	233	ME, CE, MTE, CTE
2,4-dihydroxy-Butanoic acid	23.08	219	ME, CE, MTE, CTE
β-Alanine	23.39	248	ME, MTE
Erythrose	23.96	205	ME, MTE, CTE
Threonic acid	25.75	292	ME, MTE, CTE
Asparagine	26.78	188	ME, MTE

Table 5.7: List of identified substances with their respective retention times, the m/z value used for quantitation and the runs they were found in.

5.6.2 Qualitative Results

For a general overview over the data, the cumulative number profile and the inverse cumulative area profile were generated from the chromatograms of the end samples using a Python script. Inverse cumulative plotting works similar to cumulative plotting, but instead adding up the individual measurements they are subtracted from the total sum of all measurements. This type of plotting was chosen for the measured peak areas to emphasise the contribution of later occurring peaks, which in a regular cumulative plot is not noticeable. As visible from the generated chromatogram profiles in figure

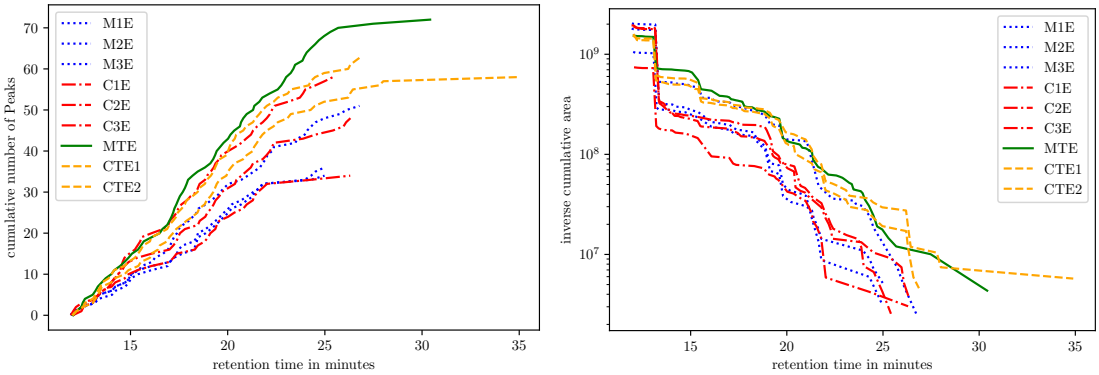

Figure 5.9: Profiles generated from the chromatograms of the endsamples *Left:* cumulative number profile *Right:* Inverse cumulative area profile

5.9, the samples with added clay MTE and CTE have more peaks with a larger area at nearly all retention times. Especially at longer retention time this effect is pronounced. For the M (mixed nitrogen/methane atmosphere) and C (pure methane atmosphere) runs no clear difference can be made out, since different chromatograms from the same run types vary a lot.

The 21 identified substances were grouped according to the number of incorporated carbon atoms, and the sum of peak areas was calculated for each group and run. The results of these calculations were averaged over the run types and show a clear hierarchy of the experimental runs (see table 5.8). For all number of carbon atoms the MT run produces the peaks with the largest total area, followed by the CT run and the M runs. The C runs with pure methane as an atmosphere produce the lowest total peak area for all number of carbon atoms.

For all measured samples, the peak area of identified peaks was determined using Thermo Fisher's Xcalibur and the respective quantitation mass [m/z]. For M and C runs the mean and the uncorrected sample standard deviation were calculated from the three different runs of the same type. For the MT, CT and Blank (B) runs as well as technical blank (BB) the standard deviation could not be calculated this way,

run type	2·C $[\cdot 10^5]$	3·C $[\cdot 10^5]$	4·C $[\cdot 10^4]$
MT	19.41	12.45	2.33
CT	12.28	7.41	1.58
M	9.10	6.98	1.09
C	4.63	2.82	0.32

Table 5.8: Sum of all peak areas for identified substances with the same number of carbon atoms, averaged by the type of run.

as only a single run was done for each, and thus it was approximated by the average relative standard deviation of the M and C runs. Standard deviations approximated in this way are marked with orange colour. Results were scaled to improve readability and comparability, plotted using Python and can be found in completion in Appendix B. Samples taken after one hour of the experimental run are marked with an A and and samples taken after 72 hours are marked with E as last letter in the abbreviations. No results are given for the CTA sample as it was lost due to a processing error.

Boric Acid

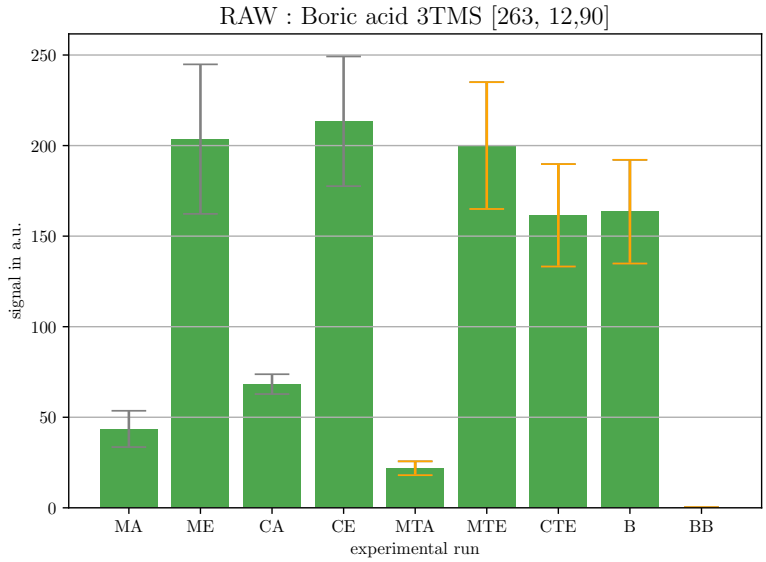

Figure 5.10: Measurements of boric acid in the different experimental runs

Boric Acid is the largest peak found in all GC-MS measurements of all samples as long as they have been boiled in the apparatus for an extended period of time. It is noteworthy that for all samples taken at the same time the measured peak areas are roughly the same (see figure 5.10).

Hydroxylamine

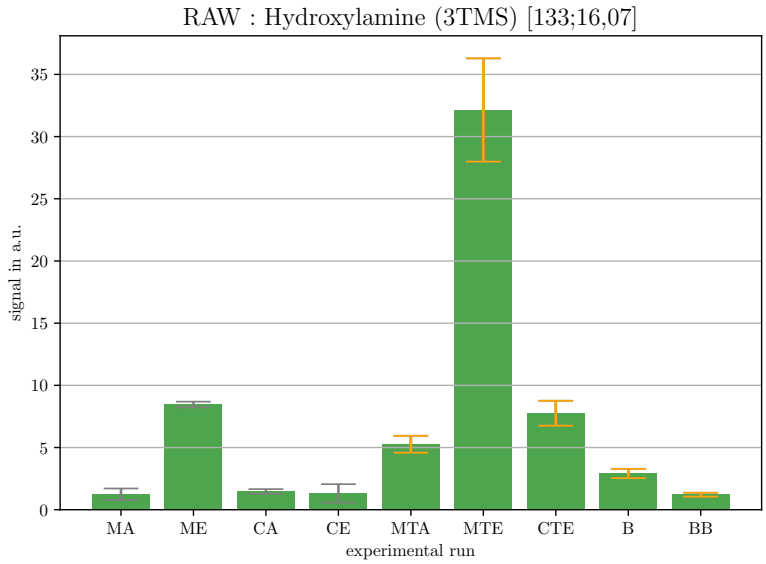

Figure 5.11: Measurements of hydroxylamine in the different experimental runs

Hydroxylamine is an indicator for the abundance of nitrogen in the atmosphere of the Miller-Urey experiment, but is also introduced in the analytical process as the measurements of the technical blank (BB) show. The highest quantity of hydroxylamine can be found in the MTE sample, while ME, MTA and CTE samples show an increased level of hydroxylamine as well (see figure 5.11).

Amino Acids and Corresponding Hydroxy Acids

Glycine, β-alanine and asparagine were identified in the end samples of both runs utilising the mixed atmosphere of methane and nitrogen. For β-alanine and glycine higher peaks were found in the MT run with clay added to the aqueous phase. For asparagine the opposite was true. The glycine peak was the largest amino acid peak found, followed by β-alanine and asparagine (see figure 5.12).

Glycolic acid and 3-hydroxypropionic acid are the corresponding hydroxy acids to glycine and β-alanine in the Strecker synthesis. Both were found at an increased level in all of the end samples from the M, C, MT and CT experimental runs. For both hydroxy acids the MT and CT runs showed a higher production than the M and C runs (see figure 5.13).

The ratios between the amino acids and their corresponding hydroxy acids were calculated and can be found in table 5.9

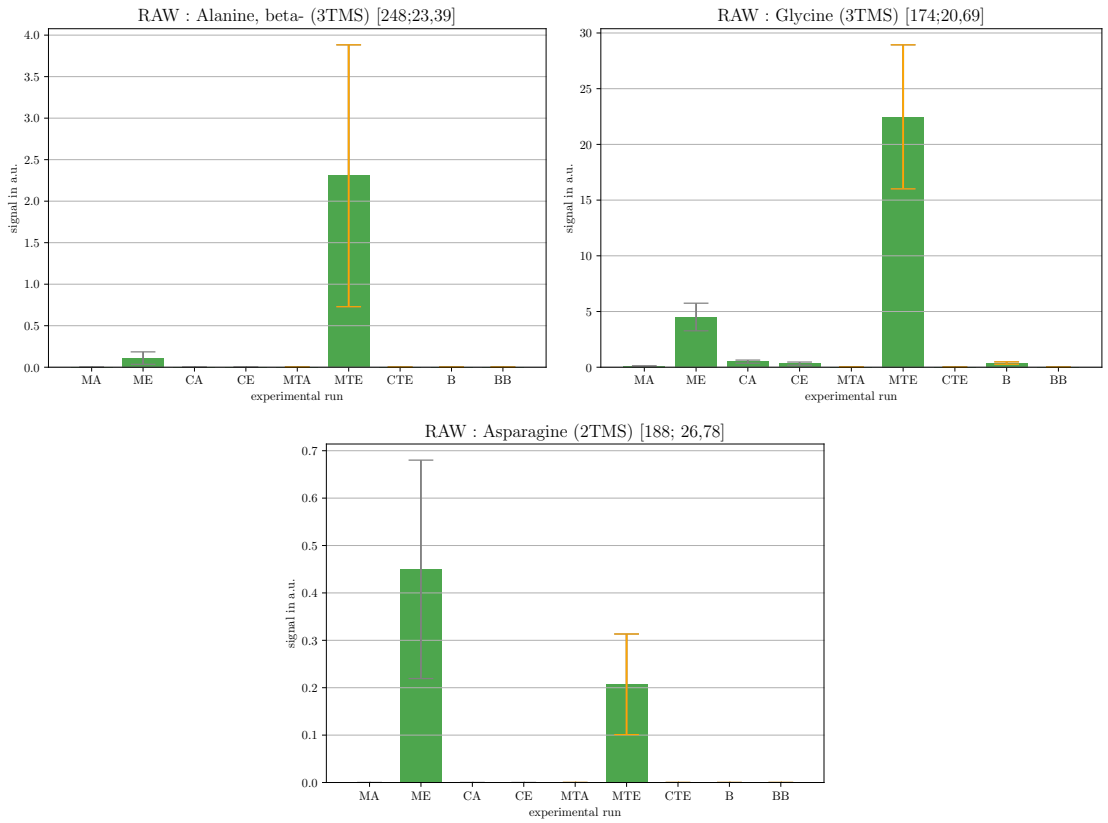

Figure 5.12: Measurements of the three amino acids found in the different experimental runs

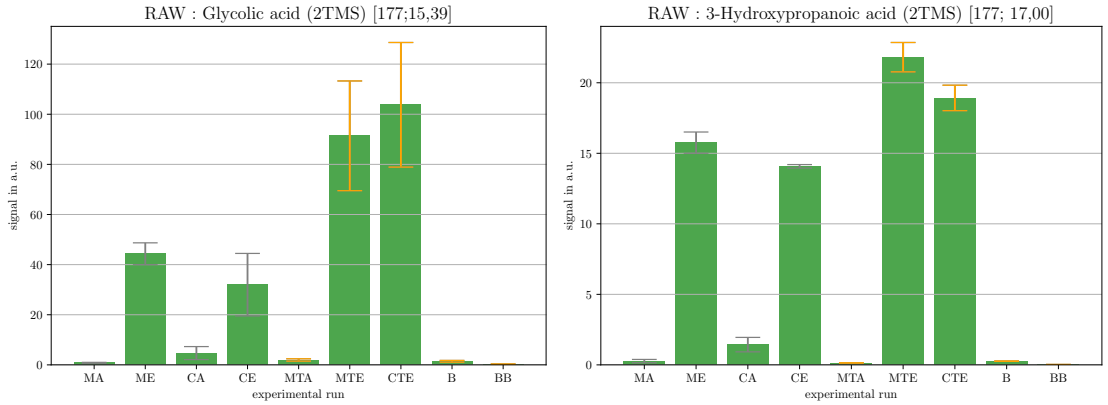

Figure 5.13: Measurements of glycolic acid and 3-hydroxypropionic acid found in the different experimental runs

experimental run	$\frac{[\text{Glycine}]}{[\text{Glycolic acid}]}$	$\frac{[\beta-\text{Alanine}]}{[3-\text{hydroxypropionic acid}]}$
M	0.102	$6.97 \cdot 10^{-3}$
MT	0.246	0.106

Table 5.9: Calculated ratios of glycine and β-Alanine and their corresponding hydroxy acids.

Sugars

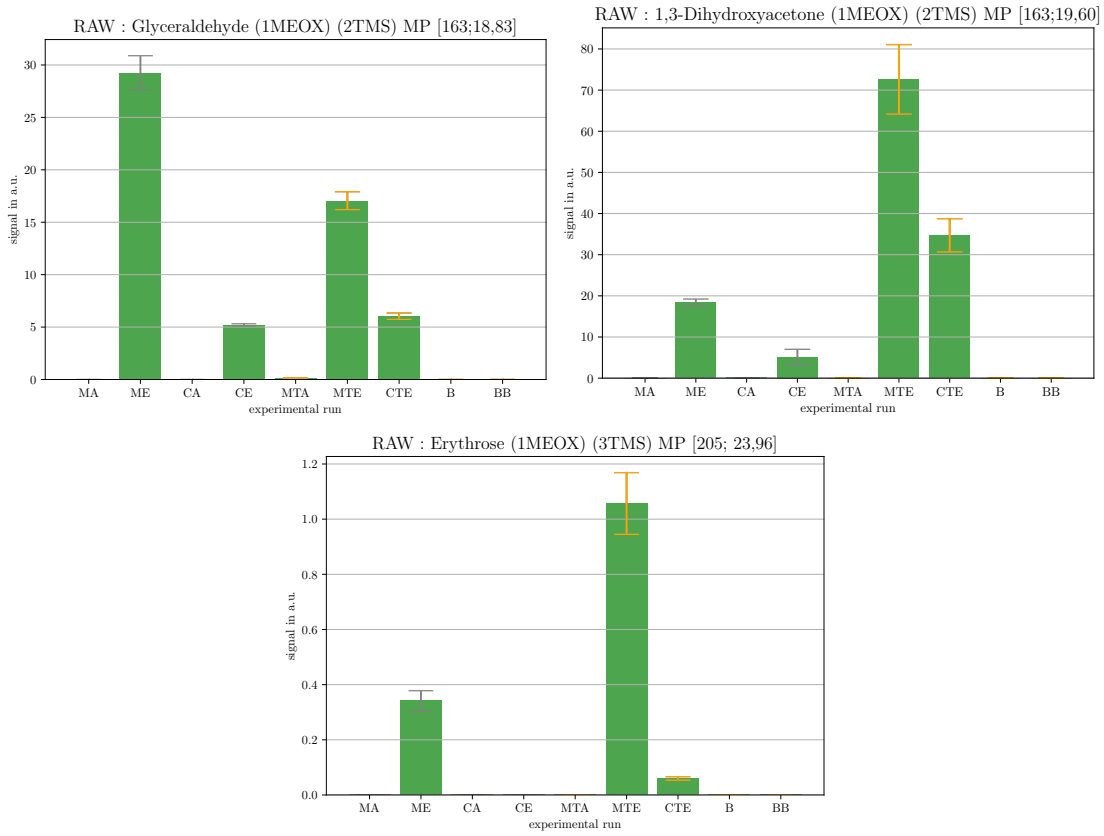

Figure 5.14: Measurements of the three sugars found in the different experimental runs

The sugars glyceraldehyde and 1,3-dihydroxyacetone have been identified in end samples from all M, C, MT and CT experimental runs, while erythrose was only identified in the ME, MTE and CTE samples but not in the CE samples (see figure 5.14). Erythrose and dihydroxyacetone show the highest concentration in the MTE sample, while glyceraldehyde is most abundant in the ME samples. Least (or none in the case of erythrose) of the sugars is found in the CE samples. Only for dihydroxyacetone a higher concentration can be found for the CTE run when compared to the ME run.

5.6.3 Quantitation

One of the key assumptions for the quantitative analysis of the measured data is that all of the end samples contain the same amount of boric acid, which can be used as an internal standard. Two arguments can be made for this assumption. On the one hand the measured data show similar peak areas for all of the end samples, as it can be seen in figure 5.10. On the other hand the dissolution curves measured in 5.4 show that saturation is reached within the run time of our experiments.

Additionally, the measured data were normalised with both the internal standard method using boric acid (Bor) and the total sum normalisation (TSN) as described in 3.4 and compared to the results without any normalisation applied (RAW). Direct comparison of the three normalisation methods can be seen in figure 5.15 for glyceraldehyde. All normalised measurements can be found in Appendix B as well. From this comparison

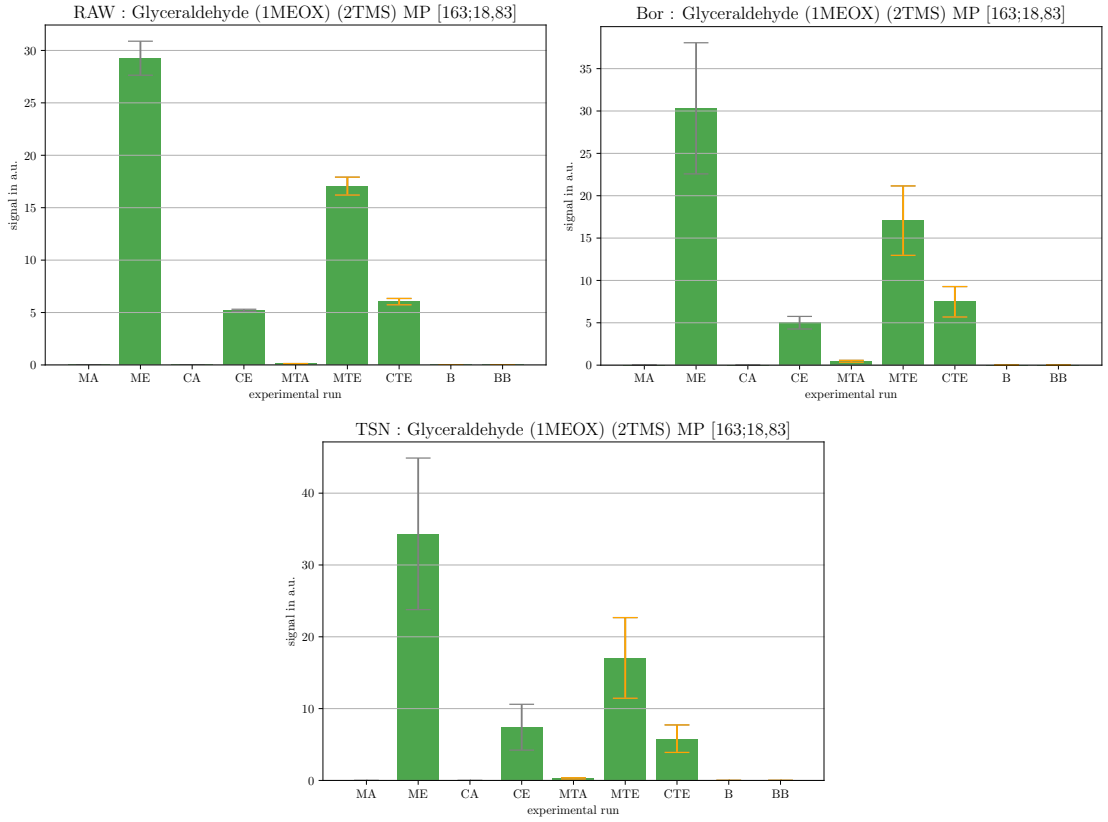

Figure 5.15: Measurements of glyceraldehyde with the three different normalisation methods *Top Left:* Without normalisation (RAW) *Top Right:* Internal standard normalisation (Bor) *Bottom:* Total sum normalisation (TSN)

it becomes clear that the impact of normalisation on the overall statement of the measurements is small. The signal values stay roughly the same when taking standard deviation into consideration and no drastic change in the hierarchy of the experimental

runs can be observed.

To quantify this observation the standard deviation introduced by the different normalisation methods was compared to the standard deviation produced by the different runs of the experiment using a Python script. Using the calculated and estimated standard deviations for the measurements without any normalisation, as discussed in section 5.6.2, the standard deviation introduced by normalisation can be estimated to be roughly 50% of the standard deviation introduced by differences between the individual runs. The normalisation error is thus well within the margin of measurement error. Together with the previous observations this built the confidence to use boric acid as internal standard during quantitation.

substance	weighed portion [mg]	final concentration $\left[\frac{mmol}{L}\right]$
Lactic acid	4.84	5.4
Glycolic acid	42.2	55.5
Hydroxylamine	26.5	38.1
Oxalic acid	8.7	6.9
Glyceraldehyde	7.5	8.3
1,3-Dihydroxyaceton	32.2	35.7
Ethanolamine	7.5	12.3
Glycine	6.8	9.1
Succinic acid	10.2	8.6
β-Alanine	1.5	1.7
Asparagine	2.4	1.8

Table 5.10: Composition of the standard mix used for quantitation. All substances are added to 10ml of Milli-Q water and mixed.

For calibration a standard mix was made by dissolving the substances listed in table 5.10 in 10 millilitres of Milli-Q water. From this solution 5 μl, 25 μl, 45 μl and 65 μl were added to freeze dried blank samples and processed like the other samples. For later fitting and calculation of χ^2 values it was required to estimate the standard deviation of the standard mix measurements. This was done by plotting the calculated (not the estimated) standard deviations from the measurements of the M and C runs against the measured values (see figure 5.16) followed by linear regression. Additionally the concentration error of the measurements was assumed to be 5% of the maximal concentration due to pipette errors.

A linear calibration function in the form of $f(x) = a \cdot x$ was assumed and fitted to the measured data with Python using the Orthogonal Distance Regression (ODR) SciPy package. The goodness of fit was evaluated by calculating χ^2 over the degrees of freedom g. The fitted function was accepted as calibration function if the $\frac{\chi^2}{g}$ was below

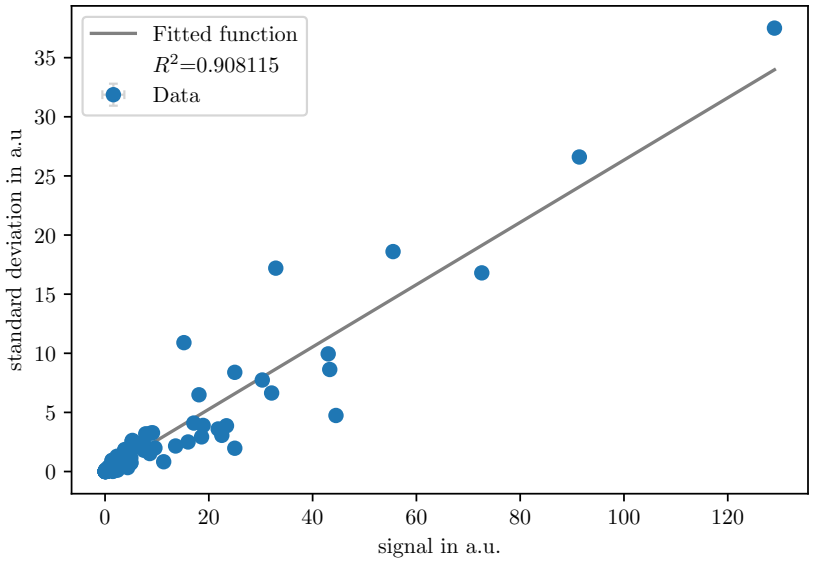

Figure 5.16: Linear regression of standard deviation relative to the measured signal used to estimate the measurement error of single point measurements.

two. Plots done during fitting of the calibration function can be found in Appendix C.

This method allowed for quantitation of lactic acid, hydroxylamine, glyceraldehyde, dihydroxyacetone, ethanolamine, glycine, succinic acid, β-alanine and asparagine, while the quantitation functions for glycolic acid and oxalic acid had to be rejected. The standard error of quantitation was estimated using Gaussian error propagation with the standard error given by the fit routine and the calculated standard deviation from section 5.6.2. Results of Quantitation are shown in table 5.11 and table 5.12.

	ME	CE	MTE	CTE
Lactic acid	138 ± 23	221 ± 114	532 ± 209	1050 ± 414
Hydroxylamine	778 ± 154	125 ± 84	2899 ± 653	867 ± 195
Glyceraldehyde	884 ± 235	146 ± 24	498 ± 125	218 ± 55
1,3-Dihydroxyaceton	583 ± 141	165 ± 88	2272 ± 671	1346 ± 397
Ethanolamine	70 ± 5	1 ± 0.5	156 ± 13	3 ± 0.3
Glycine	81 ± 12	5 ± 2	419 ± 79	0
Succinic acid	83 ± 18	47 ± 10	376 ± 82	59 ± 13
β-Alanine	6 ± 4	0	145 ± 85	0
Asparagine	2597 ± 1585	0	1303 ± 795	0

Table 5.11: Concentration of different substances in the end samples in $\frac{\text{nmol}}{\text{L}}$ as calculated during quantitation.

	MA	CA	MTA	B
Lactic acid	66 ± 31	93 ± 44	288 ± 113	160 ± 63
Hydroxylamine	194 ± 36	153 ± 15	1702 ± 383	321 ± 72
Glyceraldehyde	0	0	13 ± 3	0
1,3-Dihydroxyaceton	3 ± 1	4 ± 1	7 ± 2	0
Ethanolamine	0	0	0	1 ± 0.3
Glycine	4 ± 2	11 ± 4	0	9 ± 2
Succinic acid	1 ± 1	0	0	0
β-Alanine	0	0	0	0
Asparagine	0	0	0	0

Table 5.12: Concentration of different substances in the start samples taken after 1 hour of the run and the blank in $\frac{\text{nmol}}{\text{L}}$ as calculated during quantitation.

5.7 Discussion

Experiments utilising a complex apparatus like our Miller-Urey setup always bear some risk of unexpected failure. This was gladly not the case for our experiments and the apparatus worked as well as its limitations allowed during the conducted experiments.

The color and scent described in sections 5.2.1 and 5.2.4 as well as the acidic pH of the end samples described in section 5.2.3 strongly indicate the occurrence of interesting organic chemistry in the experimental runs. The pleasing, caramel like odour noticeable after freeze drying the CE and CTE samples raises questions about its origin. "It might be caused by ethyl maltol, which is an aromatic compound" a companion perfumer suggested after a description of the scent. Descriptions found in literature fit to this suggestion as well [Wiedmer and Buettner, 2019]. Additionally, aqueous solutions of ethyl maltol emit only a very limited scent, while the dry substance smells much stronger. As a sugar alcohol derivative, ethyl maltol might be produced in the experiments as a result of the formose reaction. Even though all of these observations suggest the presence of ethyl maltol, it was not identified in the GC-MS analysis.

As the intermediates of the formose reaction glyceraldehyde, 1,3-dihydroxyacetone and erythrose have been identified in the end samples, it is assumed that the formose reaction occurs during the experimental runs. While I initially expected the formose reaction to be suppressed by the Strecker synthesis in abundance of a nitrogen source as both reaction pathways compete for the available formaldehyde, this was clearly not the case. The formose reaction seems to benefit from the abundance of both nitrogen and montmorillonite clay as a catalyst. While in the ME samples a higher concentration of glyceraldehyde is found than in the MTE samples, a much higher 1,3-dihydroxyacetone concentration was measured in the MTE sample (see table 5.11).

The isomerisation reaction from glyceraldehyde to 1,3-dihydroxyacetone is reported to be catalysed by divalent metals such as calcium [Breslow, 1959], which can be found in montmorillonite clay. Thus the catalytic effect of the montmorillonite clay on the formose reaction can probably be attributed to the catalysis of this isomerisation reaction, shifting the equilibrium more towards 1,3-dihydroxyacetone. Against our expectations the abundance of nitrogen in the used atmosphere did not hamper the production of sugars by the formose reaction. The opposite was the case with roughly six times more glyceraldehyde produced in the M runs than in the C runs. The reason for this might be an increased number of pathways for the production of organic molecules, and thus the raw materials used in the formose reaction, and not any catalytic properties of the nitrogen.

Even though the atmosphere used in the M and MT runs is less reducing than the atmosphere originally used by Miller, with N_2 as nitrogen source instead of ammonia, the amino acids glycine, β-Alanine and asparagine are produced in these runs. During the MT run, utilising clay as a catalyst, significantly more glycine and β-alanine are produced. Using the ratio between the amino acids and their corresponding hydroxy acids found in table 5.9, the selectivity of the catalytic properties can be estimated. As the ratio increases significantly when clay is used in the experiment, the catalytic effect of montmorillonite clay can be assumed to be selective, favouring the production of amino acids over the production of hydroxy acids.

Boric acid was found as the highest peak in all samples. As shown in section 5.4, it leaches out of the borosilicate glass apparatus during the experimental run, with the roughened surface of the repeatedly cleaned glassware increasing the saturation concentration compared to fresh glassware. While the presence of boric acid in the samples was mentioned briefly by *Stanley Miller* in [Miller, 1955] I was unable to find any mentions of this issue in more recent literature about Miller-like experiments. The effect boric acid has on the analysis of our samples and the experiment itself is hard to estimate. It might react to molecules produced during the runs, like it reacted to the ribitol standard during the first GC-MS analysis. This would explain the missing detection of higher sugars, like ribose, which should be produced by the formose reaction in the experiment. Reactions of boric acid with sugars have been suggested as a method to stabilise these sugars during the evolution of life, but they make the GC-MS detection of them quite difficult [Scorei, 2012].

For a proper quantitation a normalisation step is required and thus the presence of boric acid was both, curse and blessing. On one hand boric acid prevents the use of ribitol as internal standard as it was initially planned by reacting with it. On the other hand the boric acid peak showed a very consistent behaviour and could thus be used as a standard for the normalisation step itself. Thus only the thorough understanding of the boric

acid dissolution gained by the additional dissolution runs made the quantitation possible. Quantitation itself was only possible for 8 of the 21 identified substances which an be attributed to two problems. One problem was a lack availability of pure samples for many of the substance. Another problem was the rejection of fitted calibration curves due to high χ^2/g values where the linear model was just not applicable. A change to hyperbolic calibration was considered but discarded as much more measurements of the calibration mix would have been required to reliably restrain the parameters and GC-MS time was limited.

From the concentration results of quantitation found in table 5.11 the total amount of substance produced in the experiment can be calculated. For glycine this equates to a total of $251\,\mathrm{nmol}$ produced during the MTE run, which was already the best run. This is roughly 2500 times less than the $630\,\mu\mathrm{mol}$ produced during the original Miller-Urey experiment. When looking at the percentage yield this verdict becomes even worse. During the original Miller-Urey experiment $59.1\,\mathrm{mmol}$ of carbon in the form of methane were used giving a percentage yield of 2.1% [Miller and Urey, 1959]. During the MTE run $4.6\,\mathrm{mol}$ of methane were pushed through the apparatus giving a percentage yield of 0.000011 %.

The low overall yields in the experiment can be attributed to two factors. The first factor is the usage of a different, more neutral atmosphere, which is already reported to produce slightly lower yields of amino acids [McCollom, 2013]. The second factor which is probably much more significant than the atmosphere is the experimental setup. Even though it was tried to carefully control the gas flow through the apparatus, the flow control given by the pressure regulators was very limited. This resulted in very high volumes pushed through the apparatus. In the MT experiment 223 litres of gas were pushed through the apparatus, replacing the volume of the main reaction flask ~56 times. This might have seriously hampered the occurring reactions. When comparing the individual runs it is obvious that a high energy/mole ratio benefits the production of organic molecules, with the M3 run having the lowest gas flow while showing the highest yields of all three M runs.

Proper measurements of concentrations this low were only allowed by improving the GC-MS analysis, with updated derivatisation and instrument methods leading to a 222% increase in resolution compared to the previously used methods. Only this level of tuning allowed for the identification of 21 different substances during the GC-MS analysis of the produced samples. Many of the identified substances can be categorised as important building blocks of life, like sugars, amino acids and hydroxy acids.

Chapter 6
6 Conclusion and Outlook

In this work a Miller-Urey like experiment was performed using an open setup with three different atmospheres pushed through the main reaction vessel, with the goal of observing the impact of atmosphere and a montmorillonite clay catalyst on the reaction pathways for the production of sugars and amino acids. In total 14 experimental runs were conducted of which three were blank runs, three used a pure nitrogen atmosphere, three used a pure methane atmosphere and three used an equal part mix of methane and nitrogen. Two experiments were run with montmorillonite clay as a catalyst, one with a pure methane and one with a mixed atmosphere. The samples produced in the experimental runs were analysed by using GC-MS, utilising improved methods for derivatisation and temperature programming. Due to the resolution increase caused by the new methods up to 21 different substances could be identified in the samples, including amino acids, hydroxy acids, sugars, carboxylic acids, boric acid and various other organic compounds. Theories about the origin of amino acids, hydroxy acids and sugars by the Strecker synthesis and the formose reaction were discussed in the theoretical part of this work.

Gas Flow

During the experimental runs it became clear that controlling the gas flow through the experiment was more complicated than expected when only using the pressure regulators on the gas bottles. A mass flow regulator was ordered to solve this problem, but due to a lengthy procurement process could not be utilised in the experimental runs done for this thesis. The low yields which are probably caused by the high gas flow through the main reaction vessel made the detection of substances fairly difficult.

Boric Acid

Further the analysis of the samples was complicated by the presence of boric acid. The dissolution of boric acid from the used glassware was measured and showed to converge to a saturation concentration over time. The amount of boric acid leaching from the glassware was drastically increased by cycles of repeated use and aggressive cleaning,

which roughened the surface of the glass. As boric acid can react to many organic molecules featuring cis configured OH groups, this might affect the chemistry in the experiment and possibly mask the production of substances like ribose. As we are certainly not the only ones conducting the experiment in borosilicate glassware, other groups might have the same problem without being aware of it. The boric acid peak can easily vanish in the solvent peaks, if a more aggressive temperature profile is used, as the three times trimethylsilylated derivate of boric acid has a low retention index of only 973.23, which is the fifth lowest reported in the Golm metabolome database.

Amino Acid Production

Even though there were some challenges to overcome, the overall results of the experimental runs can be considered a success, as they allow a deeper insight into the reactions occurring in the Miller-Urey experiment. The production of amino acids during the runs with the mixed atmosphere shows that N_2 alone is a sufficient nitrogen source for the formation of amino acids. Additionally to glycine the more complex amino acids β-alanine and asparagine were detected. When comparing the yields to the original experiment it becomes clear, that our experimental setup works much less efficient than the original experiment. Whether the low yields can be attributed to the atmosphere used or the flaws of the experimental setup, remains unclear.

Sugar Production

The presence of glyceraldehyde, 1,3-dihydroxyacetone and erythrose as intermediates of the formose reaction clearly show the occurrence of this reaction. As the formose reaction allows for the production of ribose, one essential step towards the production of RNA and DNA is taken. In contrast to our expectations the abundance of nitrogen in the used atmosphere did not hamper the production of sugars, with in fact the opposite being the case. Yet even in the runs with the highest yields of glyceraldehyde, 1,3-dihydroxyacetone and erythrose no ribose was detected. An explanation for this lack of ribose might be the formation of complexes with boric acid.

Effect of Montmorillonite Clay

The effect of montmorillonite clay as a catalyst can be estimated, based on the ratios of the substances found. An overall increased production of various substances can be seen when the clay is added to the aqueous phase, showing its property as a general solid acid catalyst. Additionally more specific catalytic behaviour can be observed for the Strecker

synthesis and the formose reaction. In the Strecker synthesis montmorillonite selectively enhances the production of amino acids. In the formose reaction the montmorillonite catalyses the isomerisation reaction from aldoses to ketoses and thus allows for the faster addition of another formaldehyde. This shows once more that the effects of minerals and surfaces play an important role in prebiotic chemistry and must not be neglected when talking about the origin of life.

GC-MS Improvements

For the GC-MS analysis of the samples the modifications to the derivatisation and the instrument method proved to be an effective way of increasing the chromatographic resolution. Only these optimisations to the analytical methodology gave the accuracy to detect the substances in our low yield samples.

Outlook

The experimental setup itself worked as planned, though it suffered from the bad control of gas flow through the apparatus; an issue which should be solved in future runs by using the acquired mass flow controller.

The dissolution of boric acid from the glassware is a problem which has to be addressed for a future implementation of the experiment, although it might be difficult to solve. Fused quartz glassware might be an option as it does not contain boron, but as fused quartz is harder to work with, it is questionable whether a main reaction vessel like the one used in our setup can be acquired. Another option might be a more thorough wash with demineralised water to get rid of as much boric acid in the surface layer of the glass as possible.

Interesting for future experiments would be experimental runs with different atmospheric conditions. The apparatus poses little limitations on the used atmosphere. Less reducing atmospheres with carbon monoxide instead of methane or more reducing atmospheres with ammonia instead of N_2 can easily be injected into the apparatus and thus checked for their plausibility as raw materials for the origin of life. As the open design allows for replenishment of the used gasses the run time of the experiment could be extended to weeks or months, giving the substances more time to react and possibly form other interesting molecules.

A

Appendix A

Relevant Molecules

Table A.1: Molecules found in the analytical runs with the retention times in minutes and quantitation masses (m/z) in the second analytical run

Substance name	Structural formula	retention time	m/z
Boric acid	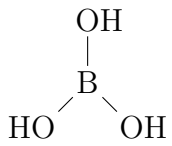	12.90	263
Glyoxylic acid	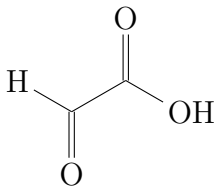	13.20	160
Lactic acid	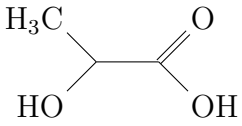	14.90	190
Glycolic acid	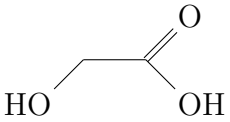	15.39	177
Hydroxylamine	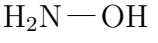	16.07	133
Oxalic acid	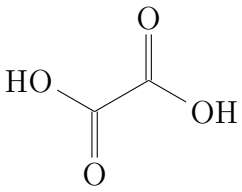	16.63	190

Substance name	Structural formula	retention time	m/z
3-hydroxy-propanic acid	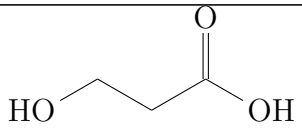	13.74	219
Glyceraldehyde	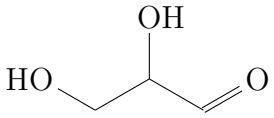	18.83	163
1,3-Dihydroxyacetone	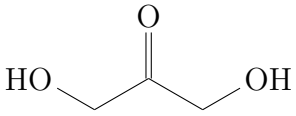	19.60	163
Ethanolamine	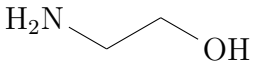	19.79	174
Glycerol	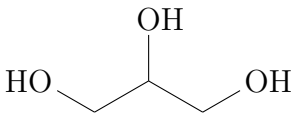	20.01	205
Glycine	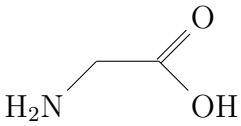	15.80	174
Succinic acid	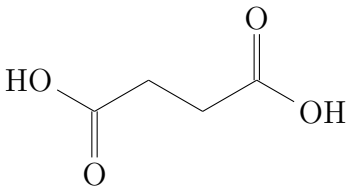	21.01	247
Glyceric acid	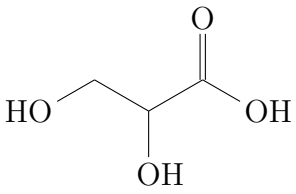	21.30	292
Lactic acid dimer	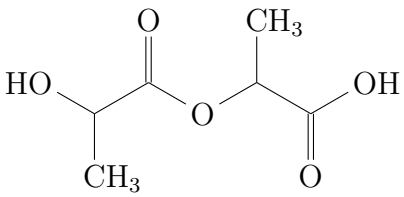	21.50	117

Substance name	Structural formula	retention time	m/z
Malic acid	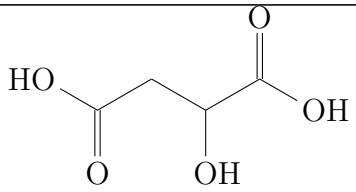	22.36	233
2,4-dihydroxy-Butanoic acid	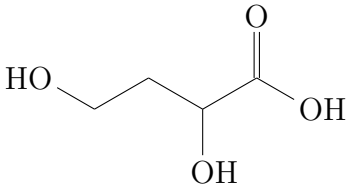	23.08	219
β-Alanine	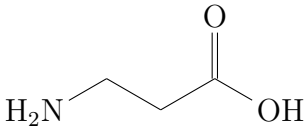	23.39	248
Erythrose	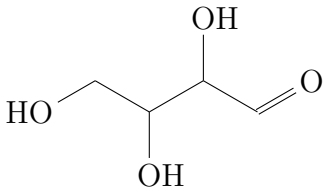	23.96	205
Threonic acid	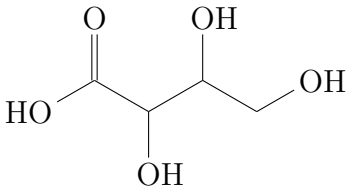	25.75	292
Asparagine	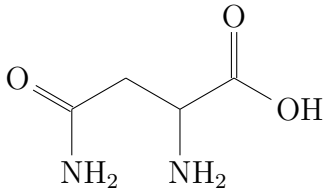	26.78	188

Table A.2: Other relevant molecules and their structural formulas

Substance name	Structural formula
Aldehydes	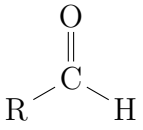

Table A.2: Other relevant molecules and their structural formulas

Substance name	Structural formula
Formaldehyde	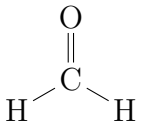
Hydrogen cyanide	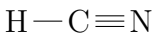
Ammonia	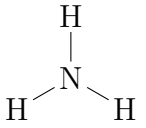
Ribose	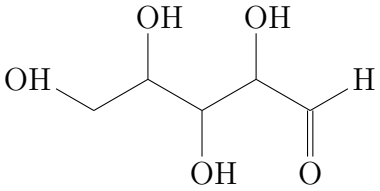
Deoxyribose	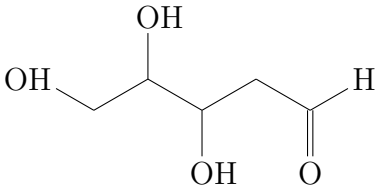
Adenine	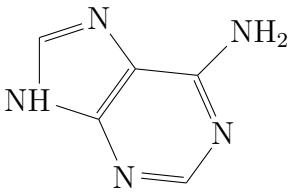
Guanine	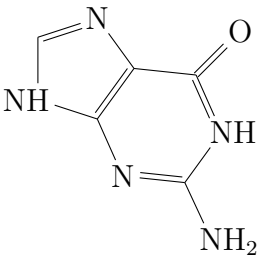

Table A.2: Other relevant molecules and their structural formulas

Substance name	Structural formula
Cytosine	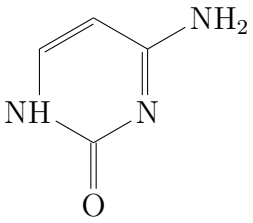
Uracil	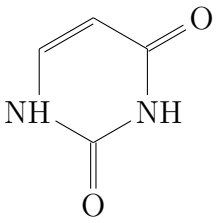
Amino acids	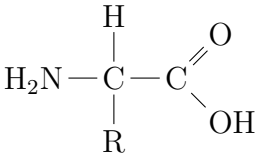
α-Hydroxy acids	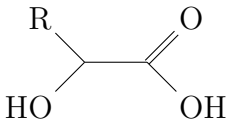

B Appendix B

Qualitative Results

This appendix contains the unnormalised results (RAW), the normalised results using boric acid as internal standard (Bor) and the normalised results using the total sum normalisation method (TSN). Plots show the mean signal in arbitrary units for the different types of samples. Grey error bars represent the uncorrected sample standard deviation of three individual measurements. The standard deviation represented by the orange error bars was approximated by the average relative standard deviation of the M and C runs.

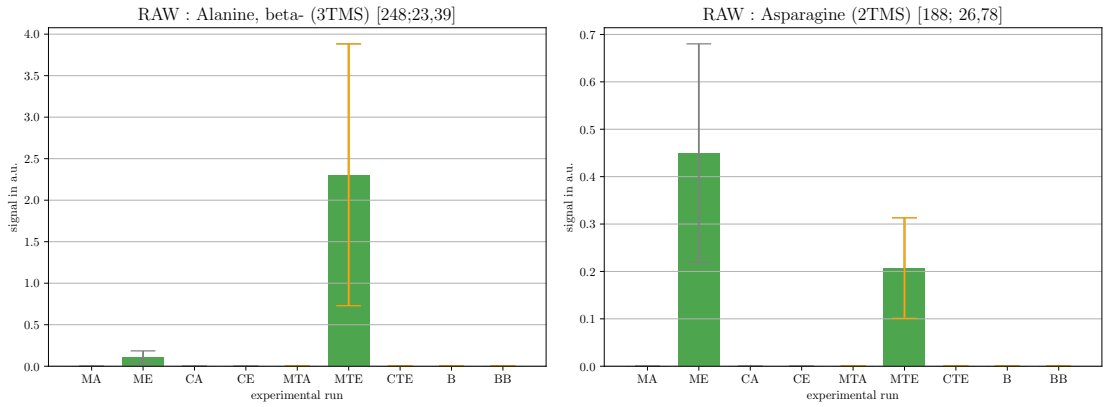

Figure B.1: Unnormalised relative concentrations of various substances in the experimental runs

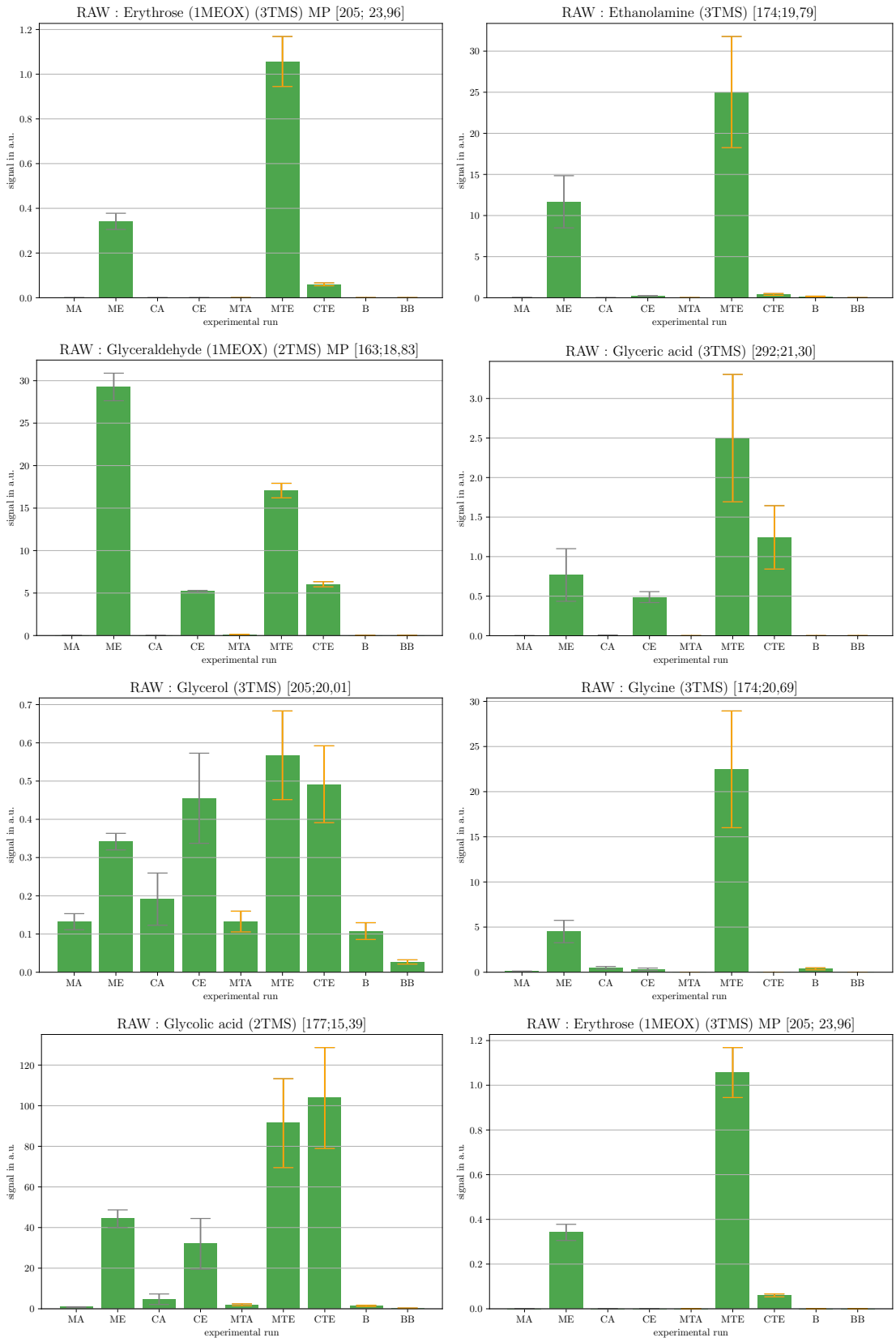

Figure B.2: Unnormalised relative concentrations of various substances in the experimental runs

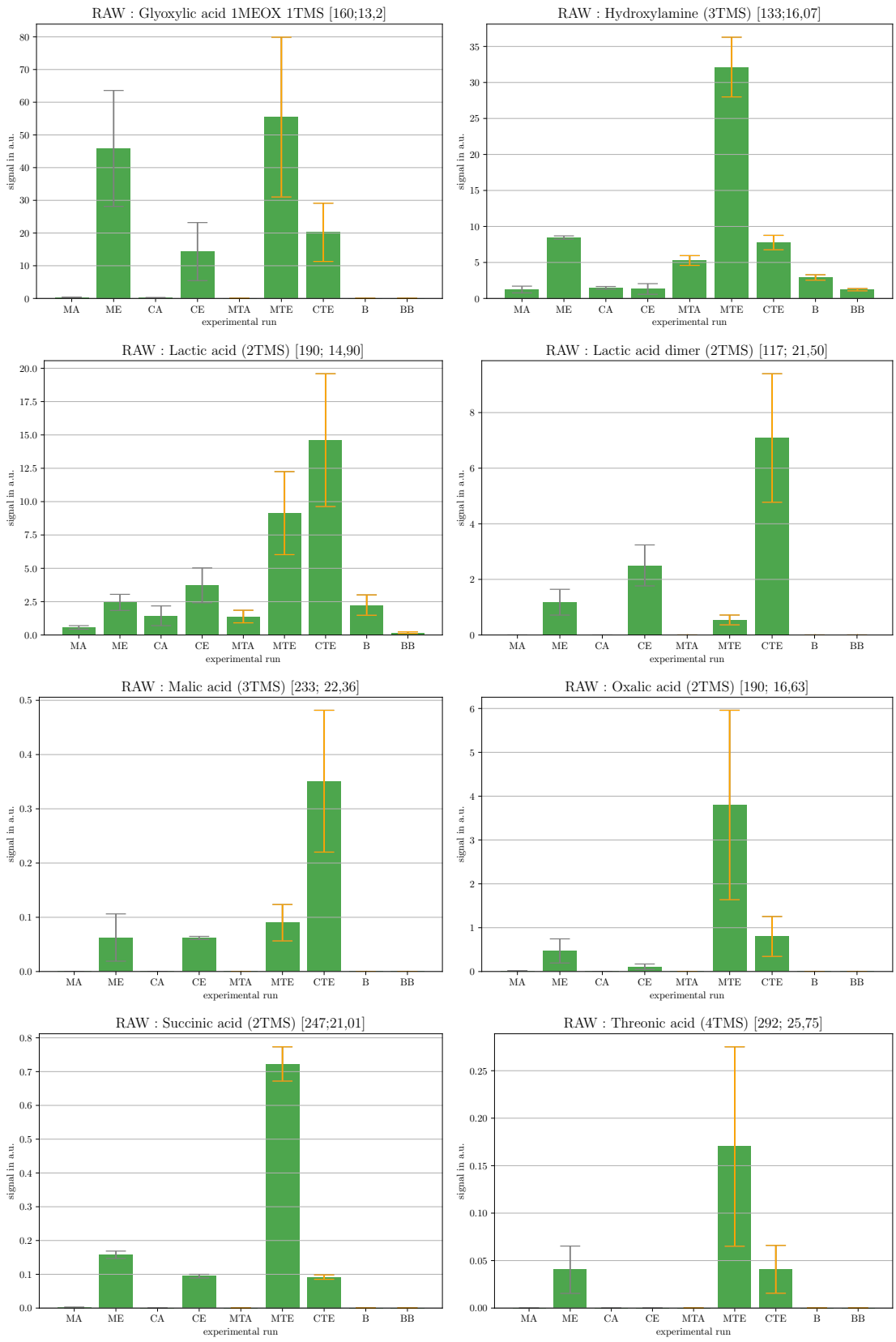

Figure B.3: Unnormalised relative concentrations of various substances in the experimental runs

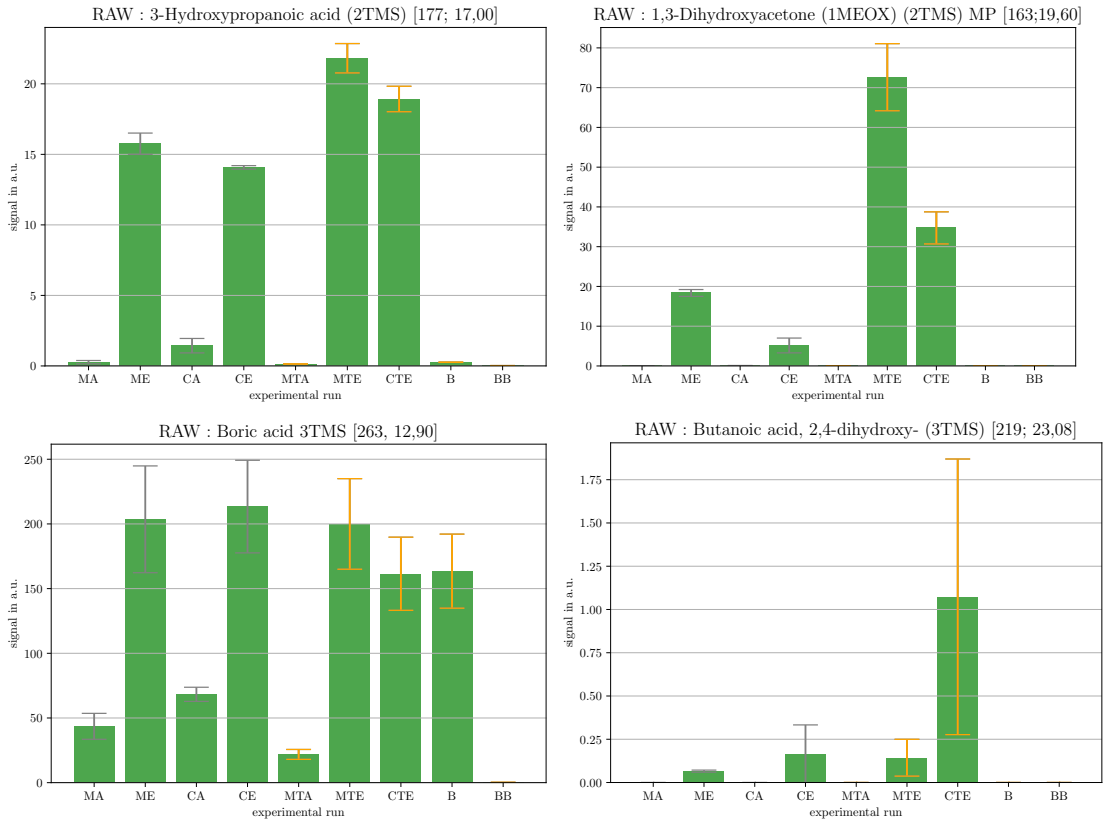

Figure B.4: Unnormalised relative concentrations of various substances in the experimental runs

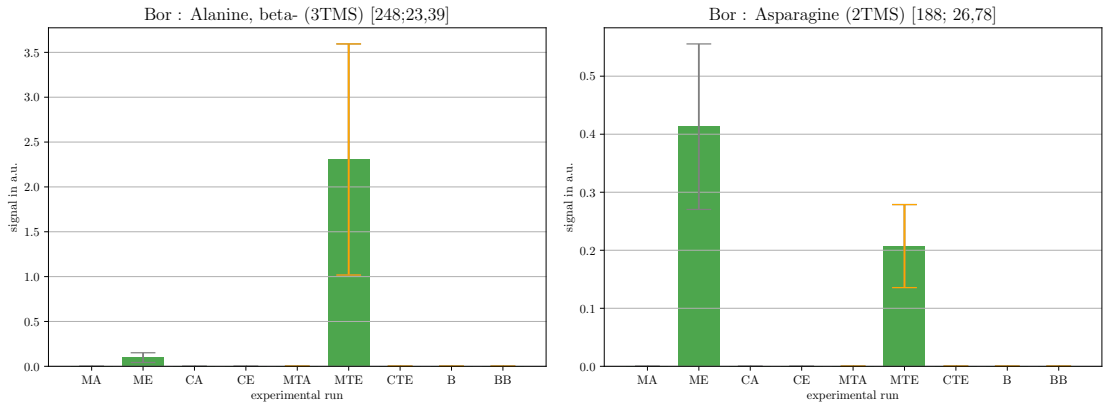

Figure B.5: Bor normalised relative concentrations of various substances in the experimental runs

Figure B.6: Bor normalised relative concentrations of various substances in the experimental runs

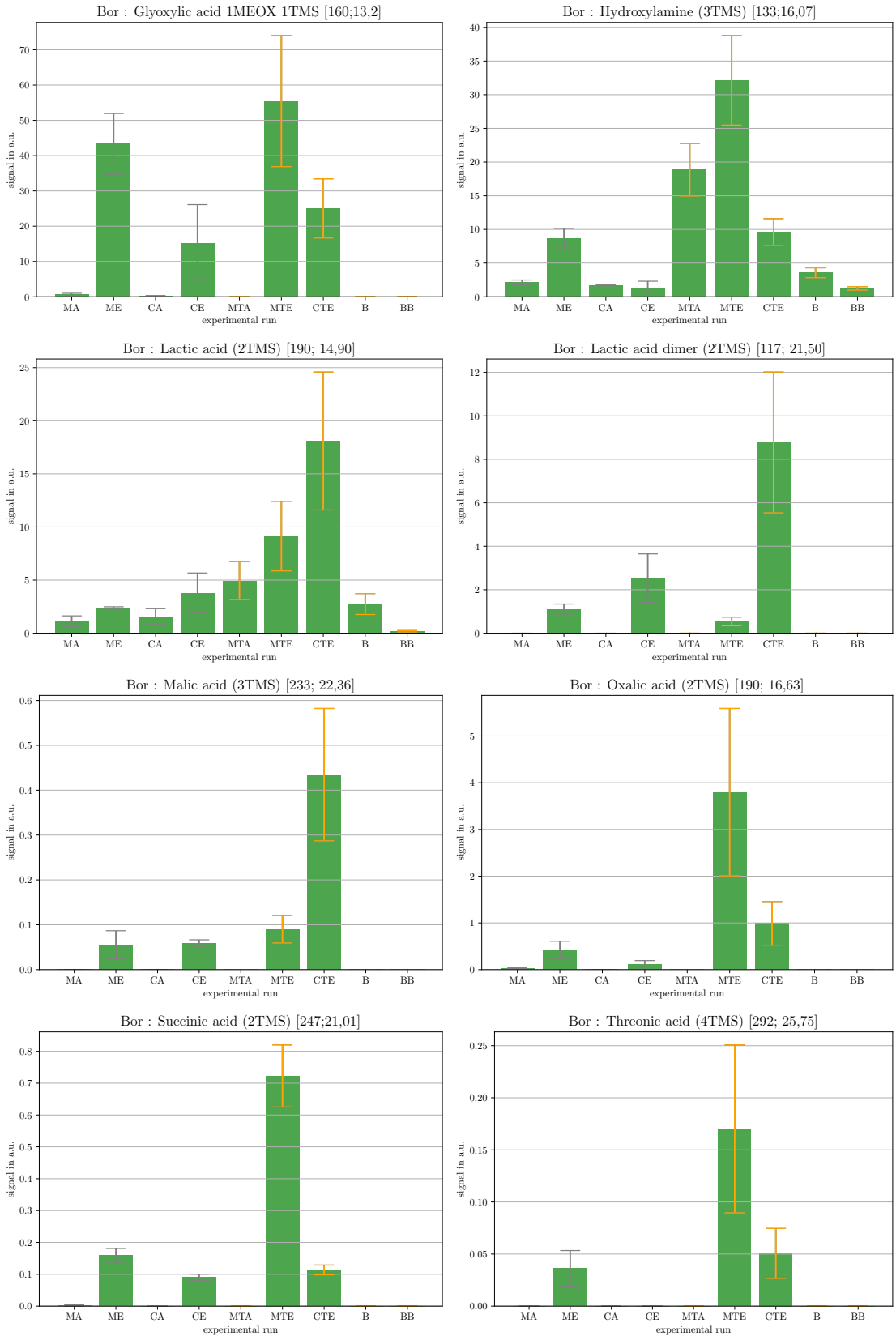

Figure B.7: Bor normalised relative concentrations of various substances in the experimental runs

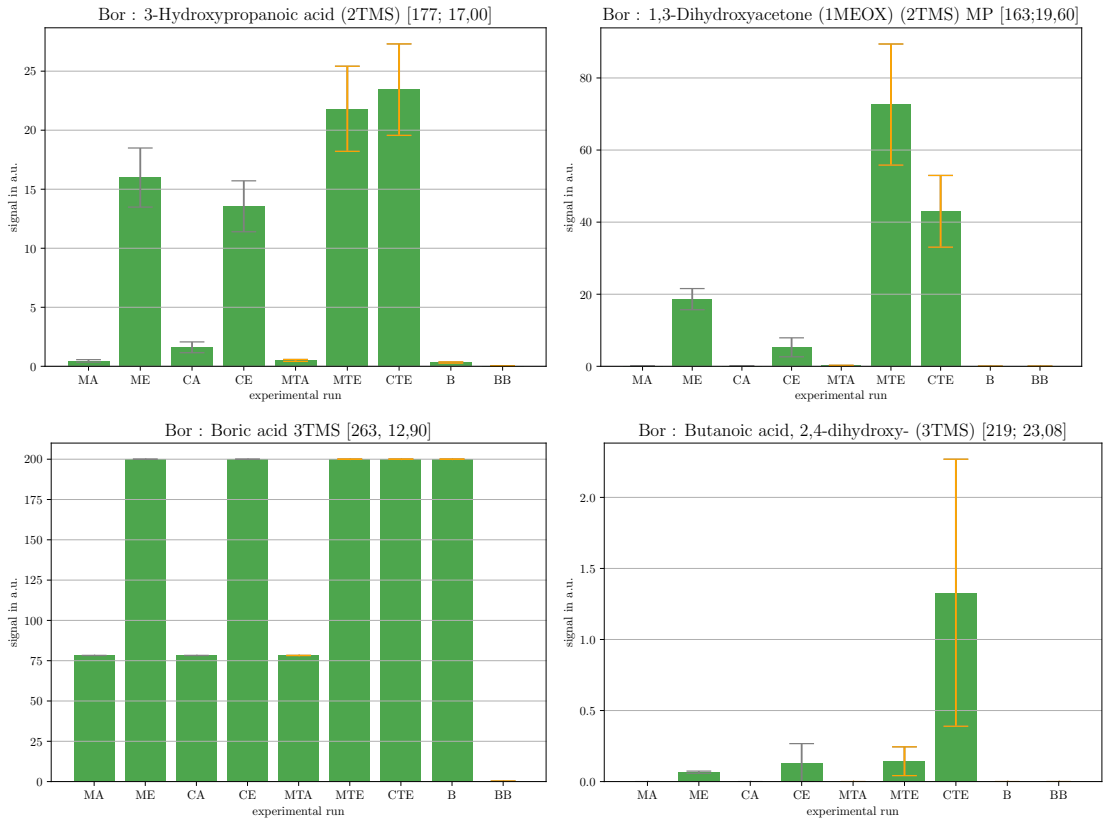

Figure B.8: Bor normalised relative concentrations of various substances in the experimental runs

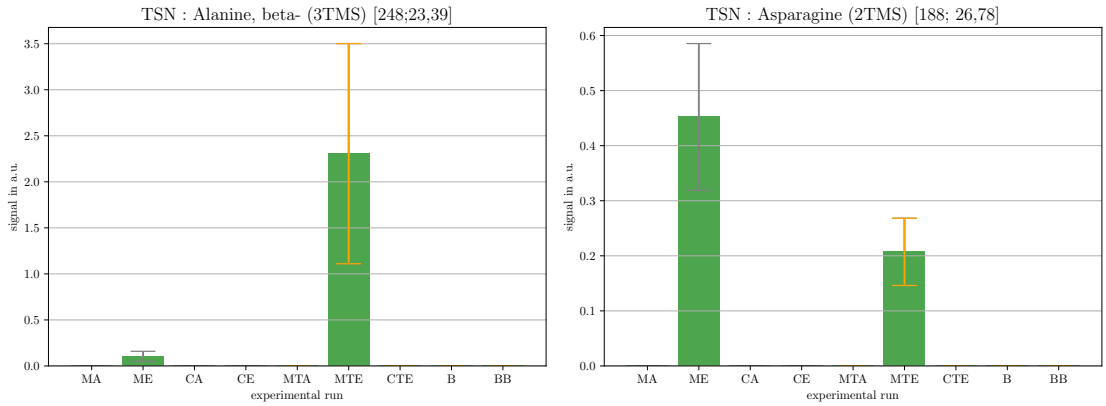

Figure B.9: TSN normalised relative concentrations of various substances in the experimental runs

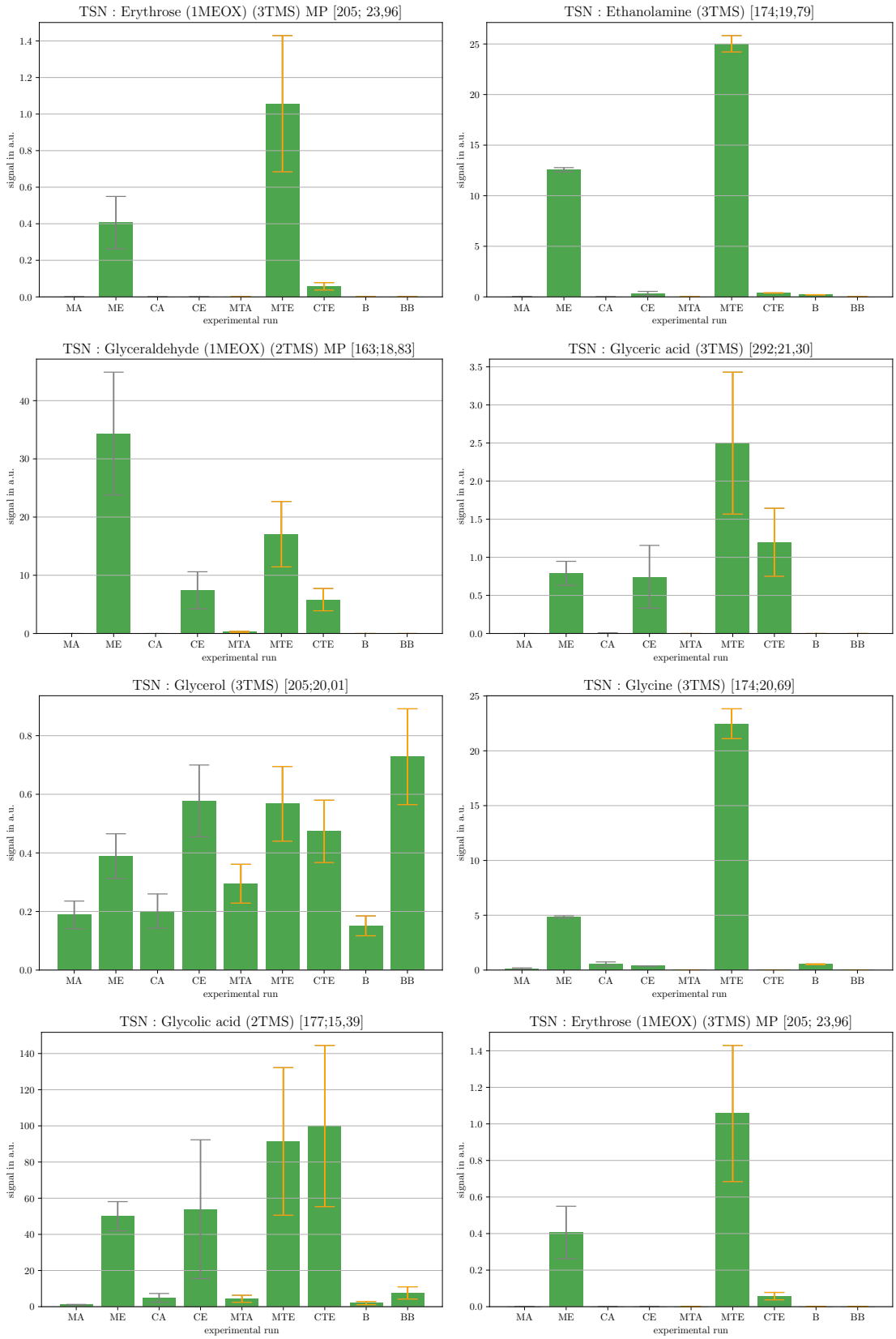

Figure B.10: TSN normalised relative concentrations of various substances in the experimental runs

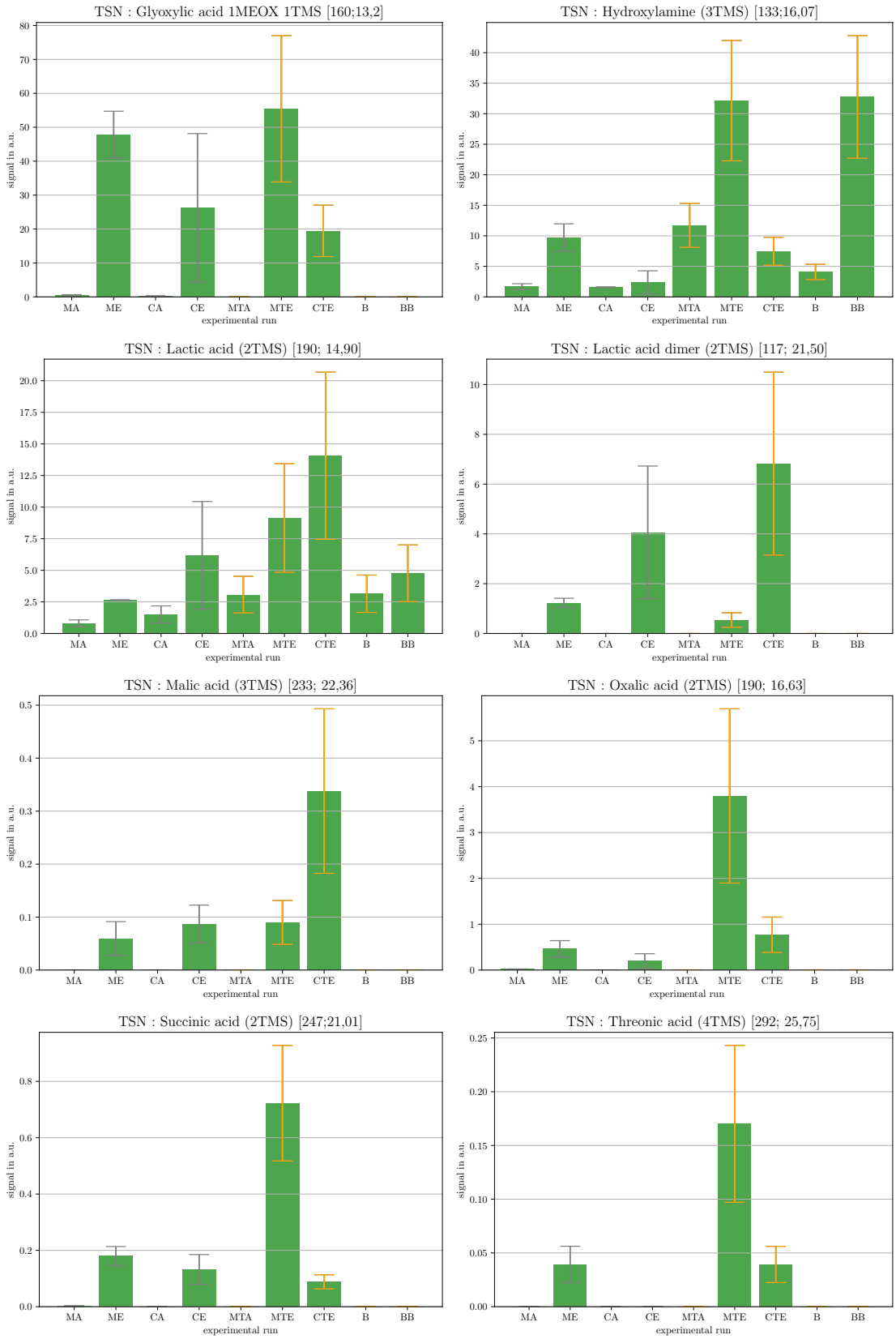

Figure B.11: TSN normalised relative concentrations of various substances in the experimental runs

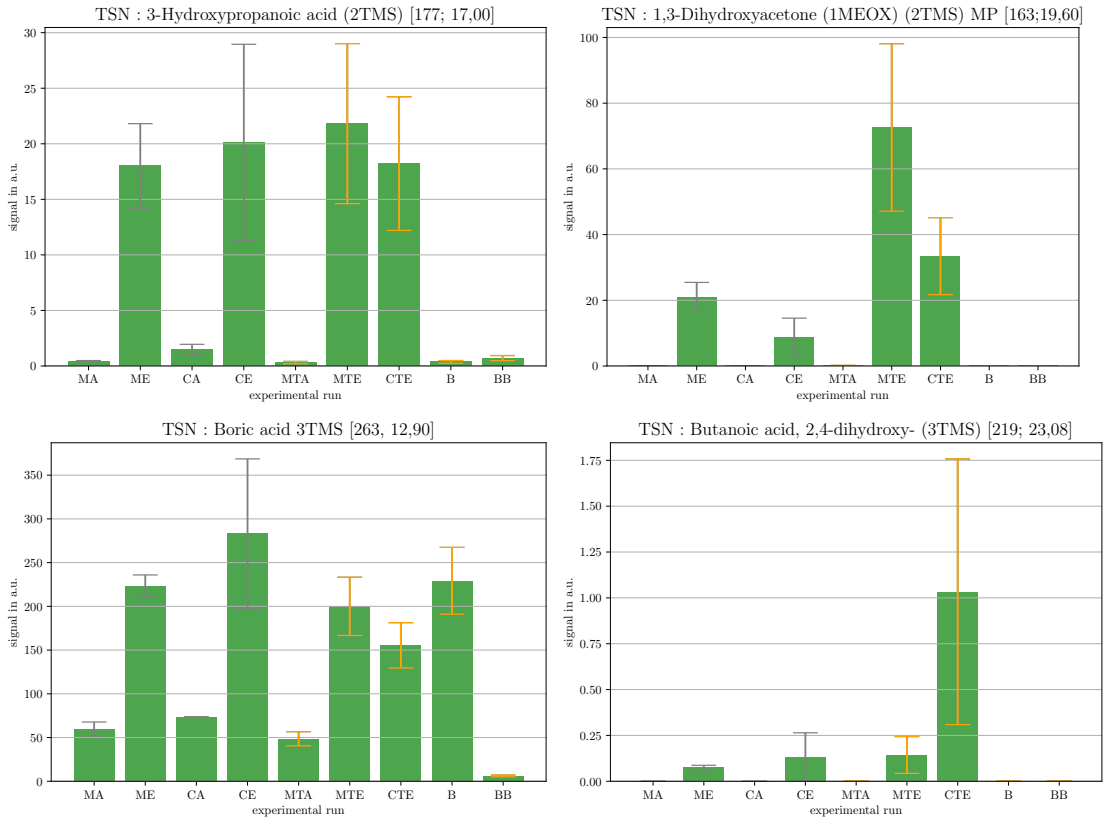

Figure B.12: TSN normalised relative concentrations of various substances in the experimental runs

C Appendix C

Quantitation

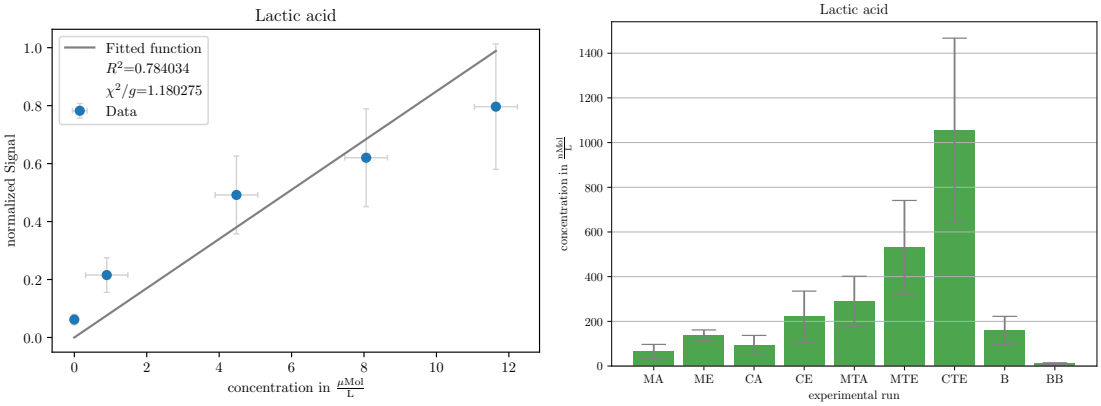

Figure C.1: Quantitation results for lactic acid *Left:* Quantitation function *Right:* Calculated concentrations

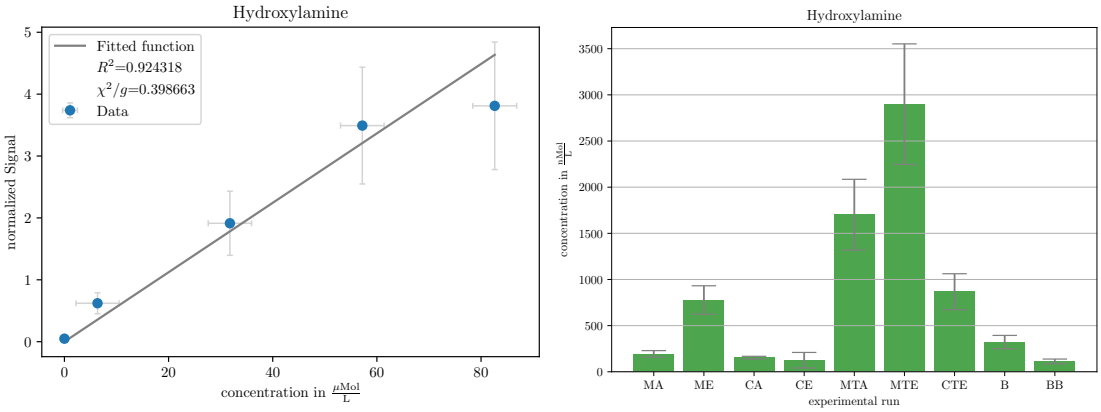

Figure C.2: Quantitation results for hydroxylamine *Left:* Quantitation function *Right:* calculated concentrations

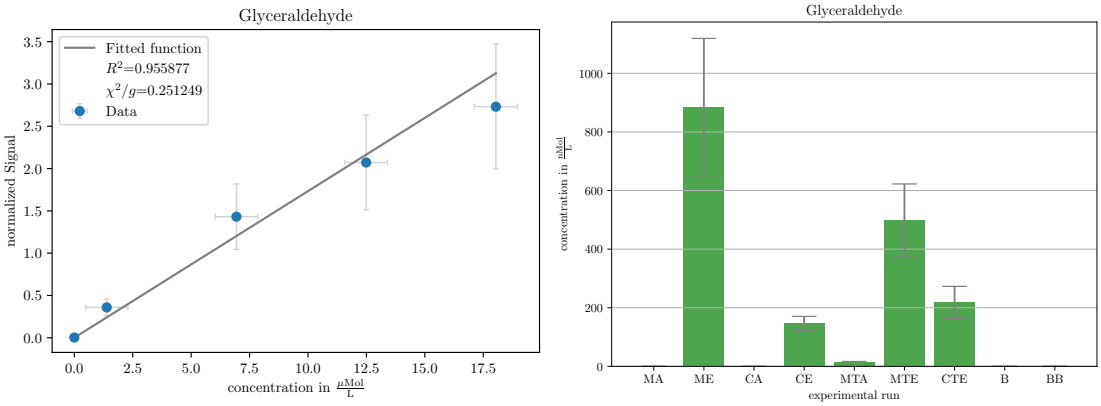

Figure C.3: Quantitation results for glyceraldehyde *Left:* Quantitation function *Right:* Calculated concentrations

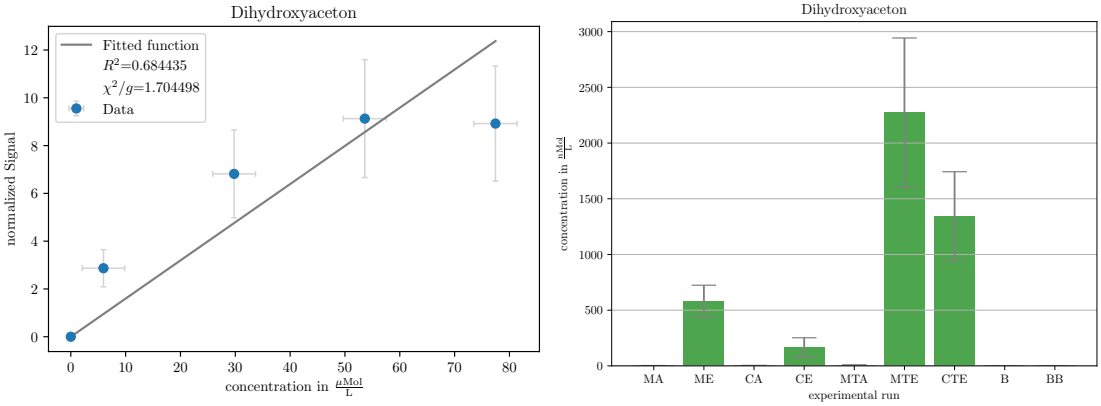

Figure C.4: Quantitation results for dihydroxyacetone *Left:* Quantitation function *Right:* Calculated concentrations

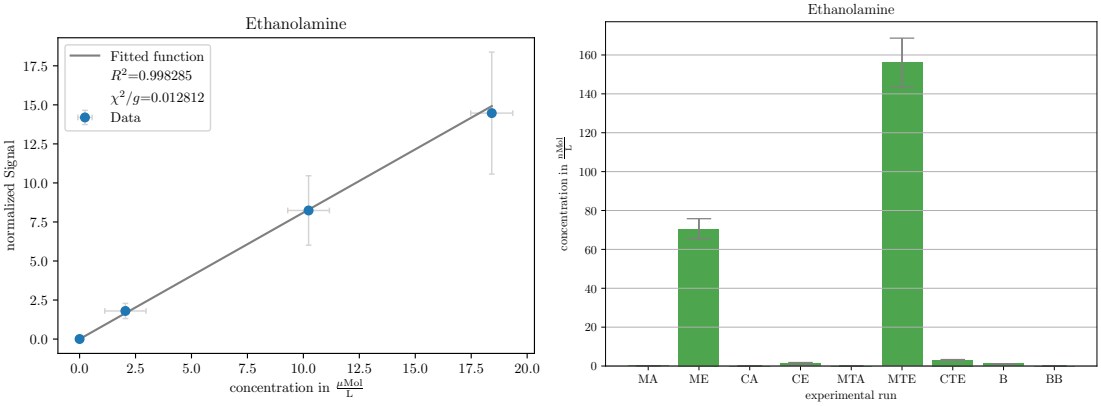

Figure C.5: Quantitation results for ethanolamine *Left:* Quantitation function *Right:* Calculated concentrations

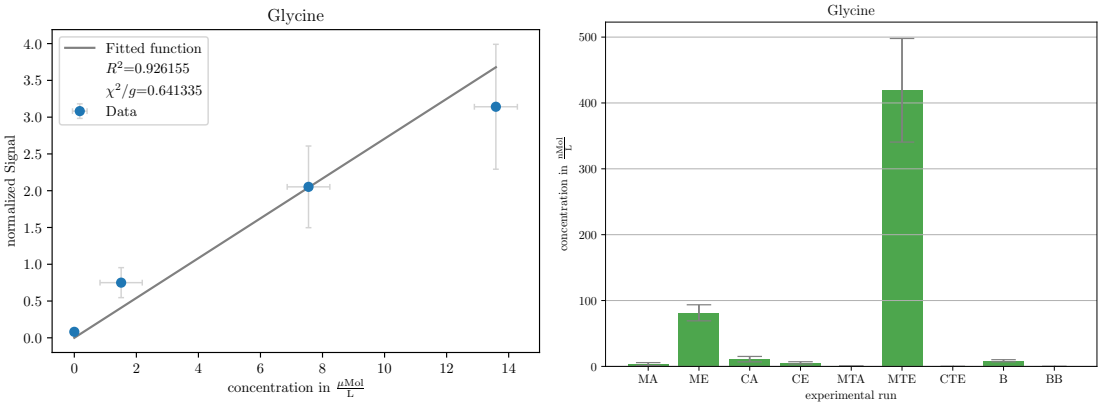

Figure C.6: Quantitation results for glycine *Left:* Quantitation function *Right:* Calculated concentrations

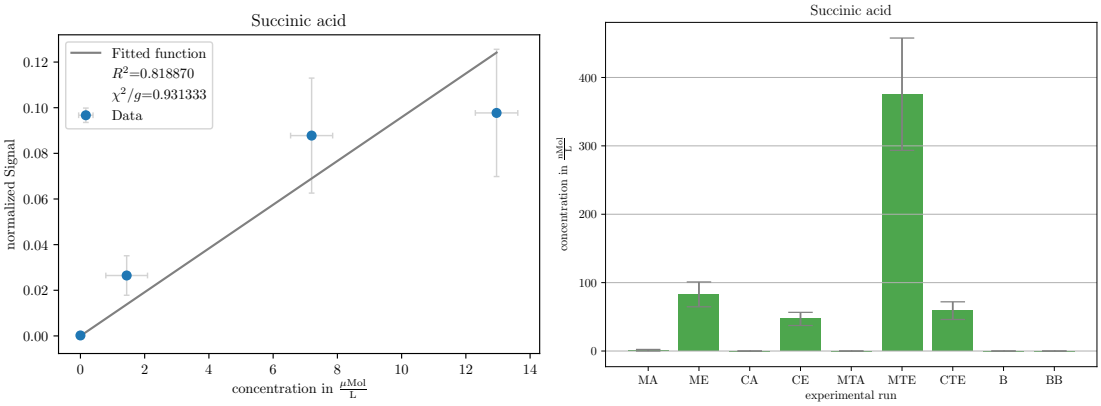

Figure C.7: Quantitation results for succinic acid *Left:* Quantitation function *Right:* Calculated concentrations

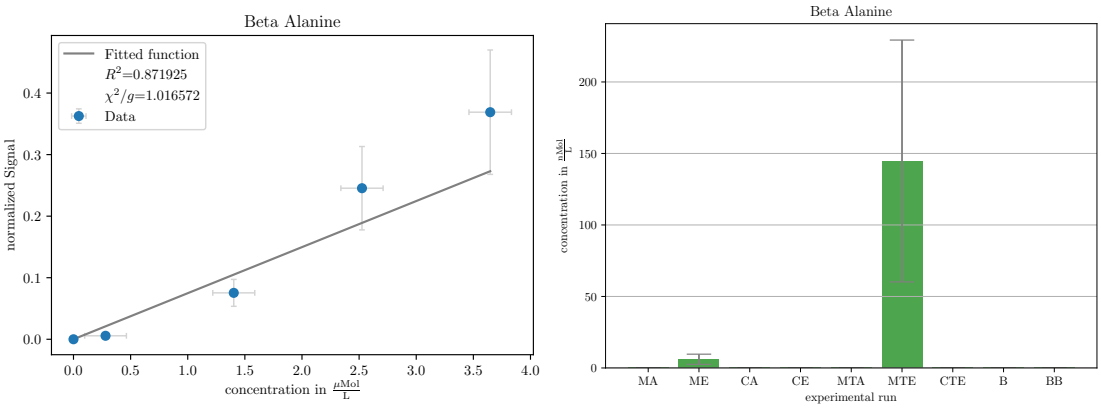

Figure C.8: Quantitation results for β-alanine *Left:* Quantitation function *Right:* Calculated concentrations

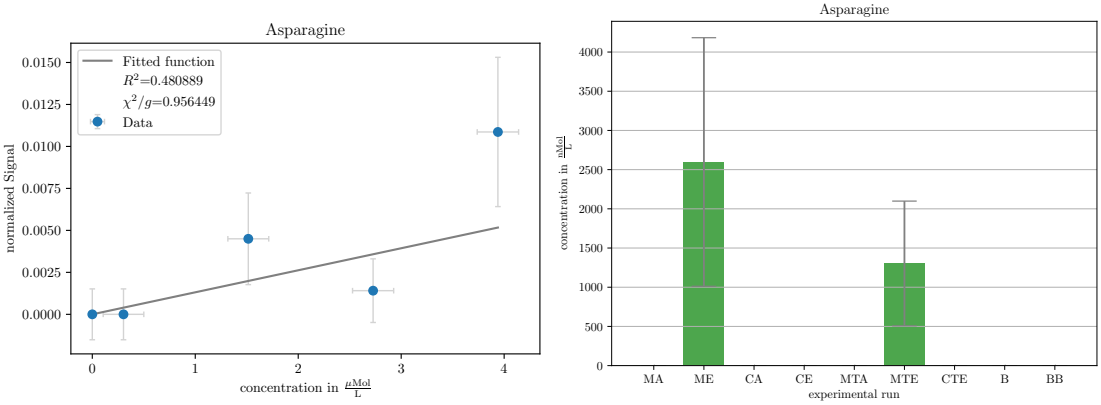

Figure C.9: Quantitation results for asparagine *Left:* Quantitation function *Right:* Calculated concentrations

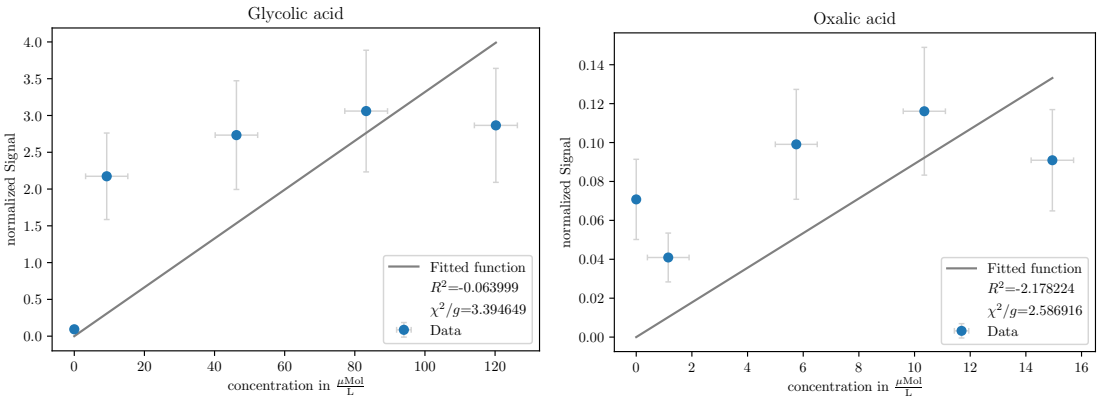

Figure C.10: Rejected quantitation functions of glycolic acid and oxylic acid, showing a χ^2/g value above 2.

Bibliography

[Altwegg et al., 2016] Altwegg, K., Balsiger, H., Bar-Nun, A., Berthelier, J.-J., Bieler, A., Bochsler, P., Briois, C., Calmonte, U., Combi, M. R., Cottin, H., Keyser, J. D., Dhooghe, F., Fiethe, B., Fuselier, S. A., Gasc, S., Gombosi, T. I., Hansen, K. C., Haessig, M., Jäckel, A., Kopp, E., Korth, A., Roy, L. L., Mall, U., Marty, B., Mousis, O., Owen, T., Rème, H., Rubin, M., Sémon, T., Tzou, C.-Y., Waite, J. H., and Wurz, P. (2016). Prebiotic chemicals—amino acid and phosphorus—in the coma of comet 67p/churyumov-gerasimenko. *Science Advances*, 2(5):e1600285.

[Armbruster et al., 1994] Armbruster, D. A., Tillman, M. D., and Hubbs, L. M. (1994). Limit of detection (lqd)/limit of quantitation (loq): comparison of the empirical and the statistical methods exemplified with gc-ms assays of abused drugs. *Clinical Chemistry*, 40(7):1233–1238.

[Arrhenius, 1908] Arrhenius, S. (1908). *Worlds in the making: the evolution of the universe*. Harper & brothers.

[Aubrey et al., 2009] Aubrey, A., Cleaves, H., and Bada, J. L. (2009). The role of submarine hydrothermal systems in the synthesis of amino acids. *Origins of Life and Evolution of Biospheres*, 39(2):91–108.

[Bernal, 1949] Bernal, J. D. (1949). The physical basis of life. *Proceedings of the Physical Society. Section A*, 62(9):537.

[Boggs et al., 1992] Boggs, P. T., Boggs, P. T., Rogers, J. E., and Schnabel, R. B. (1992). User's reference guide for odrpack version 2.01: Software for weighted orthogonal distance regression.

[Boggs and Rogers, 1990] Boggs, P. T. and Rogers, J. E. (1990). Orthogonal distance regression. *Contemporary Mathematics*, 112:183–194.

[Breslow, 1959] Breslow, R. (1959). On the mechanism of the formose reaction. *Tetrahedron Letters*, 1(21):22–26.

[Bullard et al., 2007] Bullard, T., Freudenthal, J., Avagyan, S., and Kahr, B. (2007). Test of cairns-smith's 'crystals-as-genes' hypothesis. *Faraday Discussions*, 136:231.

[Cairns-Smith, 1966] Cairns-Smith, A. (1966). The origin of life and the nature of the primitive gene. *Journal of Theoretical Biology*, 10(1):53–88.

[Chen and Walde, 2010] Chen, I. A. and Walde, P. (2010). From self-assembled vesicles to protocells. *Cold Spring Harbor Perspectives in Biology*, 2(7):a002170–a002170.

[Chyba and Sagan, 1997] Chyba, C. and Sagan, C. (1997). Comets as a source of prebiotic organic molecules for the early earth. In *Comets and the Origin and Evolution of Life*, pages 147–173. Springer.

[Ciucanu et al., 1988] Ciucanu, I., Pop, D., and Timoceanu, V. (1988). Derivatization of prostaglandis and related compounds to (methoxime) alkyl ester alkyl ether derivatives for gas chromatographic analysis. *Journal of Chromatography A*, 436:219–228.

[de Marcellus et al., 2011] de Marcellus, P., Meinert, C., Nuevo, M., Filippi, J.-J., Danger, G., Deboffle, D., Nahon, L., d'Hendecourt, L. L. S., and Meierhenrich, U. J. (2011). NON-RACEMIC AMINO ACID PRODUCTION BY ULTRAVIOLET IRRADIATION OF ACHIRAL INTERSTELLAR ICE ANALOGS WITH CIRCULARLY POLARIZED LIGHT. *The Astrophysical Journal*, 727(2):L27.

[Dyson, 1985] Dyson, F. J. (1985). *Origins of life*. Cambridge University Press, Cambridge.

[Eigen, 1971] Eigen, M. (1971). Selforganization of matter and the evolution of biological macromolecules. *Naturwissenschaften*, 58(10):465–523.

[Eigen and Schuster, 1982] Eigen, M. and Schuster, P. (1982). Stages of emerging life - five principles of early organization. *Journal of molecular evolution*, 19(1):47–61.

[Ferus et al., 2015] Ferus, M., Nesvorný, D., Šponer, J., Kubelík, P., Michalčíková, R., Shestivská, V., Šponer, J. E., and Civiš, S. (2015). High-energy chemistry of formamide: A unified mechanism of nucleobase formation. *Proceedings of the National Academy of Sciences*, 112(3):657–662.

[Ferus et al., 2017] Ferus, M., Pietrucci, F., Saitta, A. M., Knížek, A., Kubelík, P., Ivanek, O., Shestivska, V., and Civiš, S. (2017). Formation of nucleobases in a miller–urey reducing atmosphere. *Proceedings of the National Academy of Sciences*, 114(17):4306–4311.

[Furukawa et al., 2019] Furukawa, Y., Chikaraishi, Y., Ohkouchi, N., Ogawa, N. O., Glavin, D. P., Dworkin, J. P., Abe, C., and Nakamura, T. (2019). Extraterrestrial ribose and other sugars in primitive meteorites. *Proceedings of the National Academy of Sciences*, page 201907169.

[Gargaud et al., 2011] Gargaud, M., Amils, R., Quintanilla, J. C., Cleaves, H. J., Irvine, W. M., Pinti, D. L., and Viso, M., editors (2011). *Encyclopedia of Astrobiology*. Springer Berlin Heidelberg.

[Gishlick, 2002] Gishlick, A. D. (2002). Icons of evolution? why much of what jonathan wells writes about evolution is wrong. *The Quarterly Review of Biology*.

[Gruber, 2010] Gruber, L. (2010). Gc-ms-kopplung mit ionenfallen-ms. https://commons.wikimedia.org/wiki/File:GC-MS-Kopplung_mit_Ionenfallen-MS.png. Accessed: 2019-11-06.

[Haldane, 1929] Haldane, J. (1929). The origin of life, rationalist annual (reprinted in haldane, jbs, science and life, with an introduction by maynard smith, j (1968)).

[Hazen and Sverjensky, 2010] Hazen, R. M. and Sverjensky, D. A. (2010). Mineral surfaces, geochemical complexities, and the origins of life. *Cold Spring Harbor Perspectives in Biology*, 2(5):a002162–a002162.

[Hübschmann, 2015] Hübschmann, H.-J. (2015). *Handbook of GC-MS: fundamentals and applications*. John Wiley & Sons.

[Hummel et al., 2010] Hummel, J., Strehmel, N., Selbig, J., Walther, D., and Kopka, J. (2010). Decision tree supported substructure prediction of metabolites from GC-MS profiles. *Metabolomics*, 6(2):322–333.

[Iglesias-Groth et al., 2010] Iglesias-Groth, S., Cataldo, F., Ursini, O., and Manchado, A. (2010). Amino acids in comets and meteorites: stability under gamma radiation and preservation of the enantiomeric excess. *Monthly Notices of the Royal Astronomical Society*, pages no–no.

[Jia et al., 2019] Jia, T. Z., Chandru, K., Hongo, Y., Afrin, R., Usui, T., Myojo, K., and Cleaves, H. J. (2019). Membraneless polyester microdroplets as primordial compartments at the origins of life. *Proceedings of the National Academy of Sciences*, 116(32):15830–15835.

[Joyce, 1989] Joyce, G. F. (1989). Rna evolution and the origins of life. *Nature*, 338(6212):217.

[Kamminga, 1982] Kamminga, H. (1982). Life from space — a history of panspermia. *Vistas in Astronomy*, 26:67–86.

[Kasting, 1993] Kasting, J. F. (1993). Earth's early atmosphere. *Science*, 259(5097):920–926.

[Kataoka, 1996] Kataoka, H. (1996). Derivatization reactions for the determination of amines by gas chromatography and their applications in environmental analysis. *Journal of Chromatography A*, 733(1-2):19–34.

[Khakimov et al., 2013] Khakimov, B., Motawia, M. S., Bak, S., and Engelsen, S. B. (2013). The use of trimethylsilyl cyanide derivatization for robust and broad-spectrum high-throughput gas chromatography–mass spectrometry based metabolomics. *Analytical and bioanalytical chemistry*, 405(28):9193–9205.

[Knapp, 1979] Knapp, D. R. (1979). *Handbook of analytical derivatization reactions*. John Wiley & Sons.

[Kováts, 1958] Kováts, E. (1958). Gas-chromatographische charakterisierung organischer verbindungen. teil 1: Retentionsindices aliphatischer halogenide, alkohole, aldehyde und ketone. *Helvetica Chimica Acta*, 41(7):1915–1932.

[LaRowe and Regnier, 2008] LaRowe, D. E. and Regnier, P. (2008). Thermodynamic potential for the abiotic synthesis of adenine, cytosine, guanine, thymine, uracil, ribose, and deoxyribose in hydrothermal systems. *Origins of Life and Evolution of Biospheres*, 38(5):383.

[Lazcano, 2010] Lazcano, A. (2010). Historical development of origins research. *Cold Spring Harbor Perspectives in Biology*, 2(11):a002089–a002089.

[Lazcano, 2011] Lazcano, A. (2011). Origin of life. In Gargaud, M., Amils, R., Quintanilla, J. C., Cleaves, H. J. J., Irvine, W. M., Pinti, D. L., and Viso, M., editors, *Encyclopedia of Astrobiology*, pages 1183–1190. Springer Berlin Heidelberg, Berlin, Heidelberg.

[Martin and Synge, 1941] Martin, A. J. P. and Synge, R. L. M. (1941). A new form of chromatogram employing two liquid phases. *Biochemical Journal*, 35(12):1358–1368.

[Martin et al., 2014] Martin, W. F., Sousa, F. L., and Lane, N. (2014). Energy at life's origin. *Science*, 344(6188):1092–1093.

[McCollom, 2013] McCollom, T. M. (2013). Miller-urey and beyond: What have we learned about prebiotic organic synthesis reactions in the past 60 years? *Annual Review of Earth and Planetary Sciences*, 41(1):207–229.

[Mense, 2017] Mense, T. H. (2017). Montmorillonite clay in the miller experiment. Bachelor's thesis, Bielefeld University.

[Miller, 1955] Miller, S. L. (1955). Production of some organic compounds under possible primitive earth conditions1. *Journal of the American Chemical Society*, 77(9):2351–2361.

[Miller et al., 1953] Miller, S. L. et al. (1953). A production of amino acids under possible primitive earth conditions. *Science*, 117(3046):528–529.

[Miller and Orgel, 1974] Miller, S. L. and Orgel, L. E. (1974). *The Origin of Life on the Earth*. Prentice-Hall.

[Miller et al., 1997] Miller, S. L., Schopf, J. W., and Lazcano, A. (1997). Oparin's "origin of life": Sixty years later. *Journal of Molecular Evolution*, 44(4):351–353.

[Miller and Urey, 1959] Miller, S. L. and Urey, H. C. (1959). Organic compound synthesis on the primitive earth. *Science*, 130(3370):245–251.

[Miller and Van Trump, 1981] Miller, S. L. and Van Trump, J. E. (1981). The strecker synthesis in the primitive ocean. In *Origin of life*, pages 135–141. Springer.

[Nič et al., 2009] Nič, M., Jirát, J., Košata, B., Jenkins, A., and McNaught, A., editors (2009). *IUPAC Compendium of Chemical Terminology*. IUPAC.

[Nogueira et al., 2004] Nogueira, H. I., Cavaleiro, A. M., Rocha, J., Trindade, T., and de Jesus, J. D. P. (2004). Synthesis and characterization of tungsten trioxide powders prepared from tungstic acids. *Materials Research Bulletin*, 39(4-5):683–693.

[Noonan et al., 2018] Noonan, M. J., Tinnesand, H. V., and Buesching, C. D. (2018). Normalizing gas-chromatography-mass spectrometry data: Method choice can alter biological inference. *BioEssays*, 40(6):1700210.

[Noyes and Whitney, 1897] Noyes, A. A. and Whitney, W. R. (1897). The rate of solution of solid substances in their own solutions. *Journal of the American Chemical Society*, 19(12):930–934.

[Oparin, 1924] Oparin, A. I. (1924). The origin of life. *Izd. Moskovskii Rabochii*. translation from the original "Proiskhozhdenie zhizni" by Ann Synge.

[Oparin, 1968] Oparin, A. I. (1968). *Genesis and evolutionary development of life*. Acad. Pr., New York [u.a.].

[Oparin et al., 1957] Oparin, A. I. et al. (1957). The origin of life on the earth. *The origin of life on the earth.*, (3rd Ed).

[Pross, 2004] Pross, A. (2004). Causation and the origin of life. metabolism or replication first? *Origins of Life and Evolution of the Biosphere*, 34(3):307–321.

[Reichvilser, 2010] Reichvilser, M. (2010). *Borsäure- und Boronsäureester von Kohlenhydraten*. PhD thesis.

[Richter, 1865] Richter, H. E. (1865). Zur darwin'schen lehre. *Schmidt's Jahrbuch der gesammten Medicin*, 126:243–249.

[Richter, 1870] Richter, H. E. (1870). Bericht uber medicinische meteorologic und klimatologie. *Schmidt's Jahrbuch der gesammten Medicin*, 148:57–140.

[Robertson and Joyce, 2014] Robertson, M. P. and Joyce, G. F. (2014). Highly efficient self-replicating rna enzymes. *Chemistry & biology*, 21(2):238–245.

[Sagan, 1980] Sagan, C. (1980). *Cosmos*. Random House.

[Schomburg, 1987] Schomburg, G. (1987). *Gaschromatographie*. VCH, Weinheim [u.a.], 2., bearb. und erw. aufl. edition.

[Scorei, 2012] Scorei, R. (2012). Is boron a prebiotic element? a mini-review of the essentiality of boron for the appearance of life on earth. *Origins of Life and Evolution of Biospheres*, 42(1):3–17.

[Sogin et al., 2019] Sogin, E. M., Puskas, E., Dubilier, N., and Liebeke, M. (2019). Marine metabolomics: a method for the non-targeted measurement of metabolites in seawater by gas-chromatography mass spectrometry.

[Swadesh, 2000] Swadesh, J. K. (2000). *HPLC: practical and industrial applications*. CRC press.

[Szostak et al., 2016] Szostak, N., Wasik, S., and Blazewicz, J. (2016). Hypercycle. *PLoS computational biology*, 12(4):e1004853.

[Todd, 1991] Todd, J. F. J. (1991). Recommendations for nomenclature and symbolism for mass spectroscopy (including an appendix of terms used in vacuum technology). (recommendations 1991). *Pure and Applied Chemistry*, 63(10):1541–1566.

[Urey, 1952] Urey, H. C. (1952). The planets: their origin and development.

[Vaidya et al., 2012] Vaidya, N., Manapat, M. L., Chen, I. A., Xulvi-Brunet, R., Hayden, E. J., and Lehman, N. (2012). Spontaneous network formation among cooperative rna replicators. *Nature*, 491(7422):72.

[Van den Dool and Kratz, 1963] Van den Dool, H. and Kratz, P. D. (1963). A generalization of the retention index system including linear temperature programmed gas-liquid partition chromatography. Technical report.

[van Helmont and Knorr von Rosenroth, 1683] van Helmont, J. B. and Knorr von Rosenroth, C. (1683). *Aufgang der Artzney-Kunst: das ist, noch nie erhörte Brund-Lehren von der Natur, zu einer neuen Beförderung der Artzney-Sachen, sowol die Kranckheiten zu vertreiben als ein langes Leben zu erlangen*. Sulzbach.

[Whiting et al., 2001] Whiting, T. C., Liu, R. H., Chang, W.-T., and Bodapati, M. R. (2001). Isotopic analogues as internal standards for quantitative analyses of drugs and metabolites by gc-ms–nonlinear calibration approaches. *Journal of analytical toxicology*, 25(3):179–189.

[Wickramasinghe, 1974] Wickramasinghe, N. C. (1974). Formaldehyde polymers in interstellar space. *Nature*, 252(5483):462–463.

[Wiedmer and Buettner, 2019] Wiedmer, C. and Buettner, A. (2019). Identification and characterisation of odorants in a squishy toy using gas chromatography-mass spectrometry/olfactometry after thermal extraction. *Analytical and bioanalytical chemistry*, pages 1–5.

[Yi et al., 2014] Yi, L., Shi, S., Yi, Z., He, R., Lu, H., and Liang, Y. (2014). MeOx-TMS derivatization for GC-MS metabolic profiling of urine and application in the discrimination between normal c57bl/6j and type 2 diabetic KK-ay mice. *Analytical Methods*, 6(12):4380–4387.

[Zahnle and Grinspoon, 1990] Zahnle, K. and Grinspoon, D. (1990). Comet dust as a source of amino acids at the cretaceous/tertiary boundary. *Nature*, 348(6297):157–160.